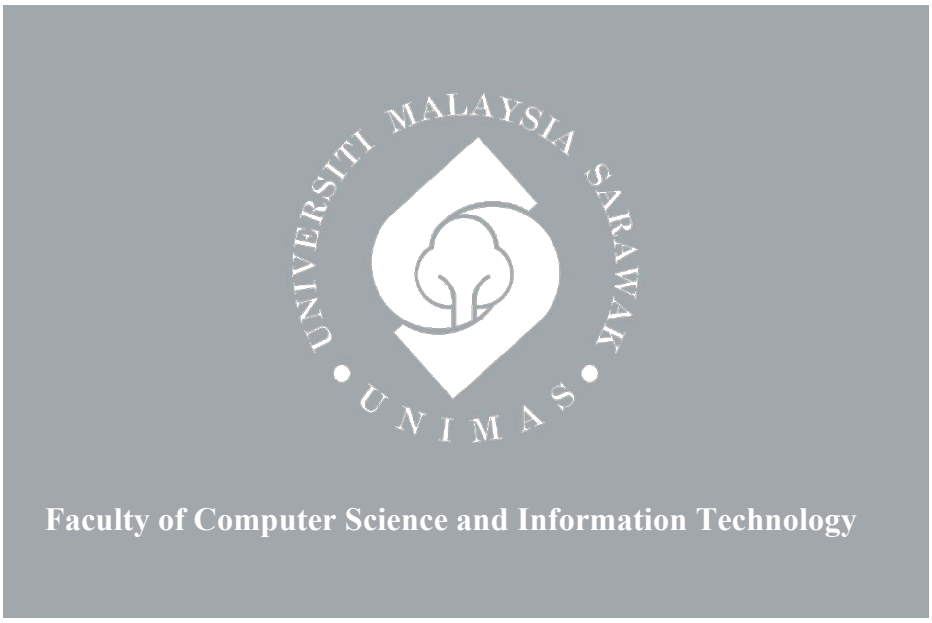

Computational Modeling of SEIPR Model for the Transmission Dynamics of Hand, Foot and Mouth Disease in Sarawak

Chan Sze Jan

Master of Science
2019

Computational Modeling of SEIPR Model for the Transmission Dynamics of Hand, Foot and Mouth Disease in Sarawak

Chan Sze Jan

A thesis submitted

In fulfillment of the requirements for the degree of Master of Science

(Computational Modeling)

Faculty of Computer Science and Information Technology
UNIVERSITI MALAYSIA SARAWAK
2019

DECLARATION

I declare that the work in this thesis was carried out in accordance with the regulations of Universiti Malaysia Sarawak. It is original and is the result of my work, unless otherwise indicated or acknowledged as referenced work. This thesis has not been accepted for any degree and is not concurrently submitted in candidature for any other degree.

Name of Student: Chan Sze Jan

Student ID No: 15020290

Degree: Master of Science

Faculty: Faculty of Computer Science and Information Technology

Thesis Title: Computational Modeling of SEIPR Model for the Transmission Dynamics of Hand, Foot and Mouth Disease in Sarawak

Signature of Student :

Date :

ACKNOWLEDGEMENT

This thesis is written based on the research done in the study area of computational modeling. It would not be able for the research to be completed without the support of the following people. Thus, without further ado, I want to offer my thanks.

First, I would like to express my deep gratitude to my supervisor Associate Professor Dr. Jane Labadin for her patient supervision, enthusiastic encouragement, useful critiques and valuable suggestions of this research work. With your guidance and continuous feedback, I am able to develop ideas and complete my work.

I would also like to thank to my co-supervisor Dr. Yuwana Podin for her advices and assistance especially in clinical parts which give me confidents in finding the relevant facts in order to complete the research.

Next, I would like to offer my thanks to the examiners for my viva voce examination, Associate Professor Dr. Nor Azah Binti Samat and Dr Tiong Wei King for stating clearly the mistakes, giving the useful comments and ideas for every aspects of my thesis, helping me to improve my thesis writing performance of my research study.

Furthermore, I want to thank the examiners for my proposal defense, Dr. Shapiee Abdul Rahman and Dr. Sze San Nah for giving the useful criticism and ideas for my research study.

My special thanks are also extended to technical staffs especially from the Faculty of Computer Science and Information Technology for helping me in handling the technical software problems and also, the support staffs from Centre for Academic Information Services for helping me to obtain the useful information for research purpose.

I am grateful for the financial aid I got through the research grant (RACE/b(2)/1246/2015(02)) from the university.

I am thankful to the Sarawak Health Department and Department of Statistics Malaysia for providing the real clinical data and statistic of the population.

I also thank to all my relatives and friends who have always encouraging me and supporting me to attempt this research study.

Finally, I want to express my heartfelt gratitude to my dad, mum and brother, Cas, for always be with me and support me throughout my studies.

ABSTRACT

This thesis aims to develop a suitable model to describe the transmission dynamics of hand, foot and mouth disease (HFMD) specifically in addressing the insight on the ability of the virus to survive in the respiratory secretion and stool of a patient for a period of time in order to predict the periodic cycle of HFMD infectious cases more accurately. This was found necessary since a basic SIR (Susceptible-Infectious-Fully recovered) model only provide a basic framework to discuss the characteristic of HFMD. Biological characteristics, which are incubation period, infectious period and post-infectious virus shedding period are known to be the factors for the virus spreading. Thus, to provide a complete study framework based on the biological factors of HFMD, basic SIR model was extended to become SEIPR (Susceptible-Incubation period-Infectious-Post infectious virus shedding-Fully recovered) model whereby the incubation period and post-infectious period together with the existing infectious period to act as infected compartments were incorporated. The numerical results of the model were compared with the actual 2006 HFMD infectious data. There is no significance difference between the numerical simulation and the actual data by using the SEIPR during the first wave of the outbreak for ten weeks. Then, SEIPR model is being verified by analyzing the HFMD outbreaks from year 2010 to 2014 and the results during the first wave of the outbreaks are well matched with the actual cases. Hence, with the inclusion of the transmission coefficient gained from incubation period patients, which is β_1 and post-infectious patients, which is β_6 together with the transmission coefficient from infectious individual, which is β_5 to susceptible in the improvement SEIPR model, the numerical simulation results reached a consensus that

the incorporated infected compartments are able to predict the HFMD cases during the first wave of the outbreaks for ten weeks. Furthermore, SEIPR model provides two main parameters that have been evaluated include basic reproductive number, R_0 and the threshold value. The values of R_0 calculated are between 1.13 to 1.54, indicating the outbreaks of the disease occurred from year 2010 to 2014. Meanwhile, the threshold value as minimum proportion of the population to create the liability of the disease spreading for each case was found to be in the range 6500 to 9000 people. It is observed that with higher R_0, the transmission coefficient is higher and the threshold value is smaller, which means more people can be infected. Hence, to reduce the number of infected cases, the transmission coefficients need to be reduced, thus, the number of any contact person within the infected region needs to be controlled, so that the impacts of the outbreaks can be reduced.

Keywords: Hand, foot and mouth disease, SIR model, SEIPR model, incubation period, post-infectious virus shedding period.

Model SEIPR bagi Pemodelan Pengiraan untuk Jangkitan Dinamik Tehadap Penyakit Tangan, Kaki dan Mulut di Sarawak

ABSTRAK

Tesis ini menumpu kepada penghasilan satu model yang sesuai untuk menerangkan tentang jangkitan dinamik yang disebabkan oleh penyakit tangan, kaki dan mulut terutamanya melihat kepada keupayaan virus kekal hidup dalam rembesan pernafasan dan najis pesakit dalam tempoh tertentu dan membuat jangkaan keputusan yang lebih tepat dalam pengiraan kitaran berkala jangkitan kes-kes penyakit tangan, kaki dan mulut. Ini adalah diperlukan kerana penggunaan model asas iaitu model SIR (Orang yang belum dijangkiti-orang yang dijangkiti-orang yang sembuh selepas jangkitan) hanya menyediakan rangka kerja yang asas dalam penerangan sifat-sifat penyakit tangan, kaki dan mulut. Sifat-sifat faktor biologi iaitu tempoh pengeraman, tempoh semasa jangkitan dan tempoh selepas jangkitan adalah faktor-faktor penyebaran jangkitan. Dengan itu, model asas SIR telah dikembangkan kepada model SEIPR (Orang yang belum dijangkiti-orang yang dijangkiti tanpa gejala-orang yang dijangkiti dengan gejala-orang selepas dijangkiti tetapi gejala telah hilang-orang yang sembuh selepas jangkitan) supaya satu rangka kerja yang lengkap berdasarkan sifat-sifat faktor biologi penyakit tangan, kaki dan mulut di mana model SEIPR yang baharu dibina ini telah menggabungkan tempoh pengeraman dan tempoh selepas jangkitan bersama dengan tempoh semasa jangkitan untuk bertindak sebagai komponen-komponen jangkitan. Perbandingan di antara keputusan jangkaan dan keputusan sebenar data 2006 penyakit tangan, kaki dan mulut telah dilakukan. Keputusan berangka simulasi dengan data sebenar didapati tiada perbezaan yang ketara semasa gelombang pertama penyebaran wabak penyakit dalam tempoh sepuluh minggu. Kemudian, model SEIPR telah disahkan penggunaannya dengan

menganalisiskan penyebaran penyakit tangan, kaki dan mulut dari tahun 2010 hingga tahun 2014 dan keputusan semasa gelombang pertama penyebaran wabak penyakit adalah sepadan dengan data sebenar. Oleh itu, dengan penambahan pekali penyebaran dari orang yang dijangkiti tanpa gejala iaitu β_1 *dan orang selepas dijangkiti tetapi gejala telah hilang iaitu* β_6 *bersama dengan pekali penyebaran dari orang yang dijangkiti iaitu* β_5 *kepada orang yang belum dijangkiti dalam model SEIPR, keputusan simulasi berangka mencapai persetujuan di mana penggabungan komponen-komponen jangkitan berupaya membuat jangkaan keputusan kes-kes penyakit tangan, kaki dan mulut dalam tempoh sepuluh minggu semasa gelombang pertama penyebaran wabak penyakit. Dua parameter yang telah dinilai termasuk nombor penyebaran asas,* R_0 *dan nilai ambang.* R_0 *yang terhasil didapati berada dalam lingkungan 1.13 hingga 1.54 menunjukkan wabak penyakit tersebar dari tahun 2010 hingga tahun 2014. Pada masa yang sama, nilai ambang setiap kes yang didapati adalah dalam lingkungan 6500 hingga 9000 orang yang diperlukan supaya wabak boleh tersebar. Keputusan menunjukkan dengan* R_0 *yang tinggi, pekali penyebaran adalah tinggi dan nilai ambang adalah kecil, ini bermakna, lebih ramai orang akan dijangkiti. Bagi mengurangkan kes-kes jangkitan, pekali penyebaran hendaklah dikurangkan, jadi, jumlah keupayaan orang berjumpa di kalangan ramai dengan yang dijangkiti hendaklah dikawal supaya impak yang diterima oleh penyebaran wabak boleh dikurangkan.*

Kata kunci*: Penyakit tangan, kaki dan mulut, model SIR, model SEIPR, tempoh pengeraman, tempoh selepas jangkitan.*

TABLE OF CONTENTS

Page

LIST OF TABLES

Page

LIST OF FIGURES

Page

LIST OF ABBREVIATIONS

α_1	transmission coefficient of susceptible individuals getting infected for SIR model (per time)
α_2	the rate at which a recovered individual loses its immunity for SIR model (per time)
α_3	the rate at which an infectious individual fully recovered for SIR model (per time)
β_1	transmission coefficient of susceptible individuals getting infected by incubation period individual for SEIPR model (per time)
β_2	the rate at which an asymptomatic patient developing symptoms for SEIPR model (per time)
β_3	the rate at which an infectious individual clinically recovered for SEIPR model (per time)
β_4	the rate at which a clinically recovered individual fully recovered for SEIPR model (per time)
β_5	transmission coefficient of susceptible individuals getting infected by infectious individual for SEIPR model (per time)
β_6	transmission coefficient of susceptible individuals getting infected by clinically recovered individual for SEIPR model (per time)

β_7	the rate at which a recovered individual loses its immunity for SEIPR model (per time)
k_1	natural birth rate (per time)
k_2	natural death rate (per time)
k_3	death rate which is caused by disease (per time)
E	number of infected individual during incubation period at time t
I	number of infectious individual at time t
N	total population
P	number of clinically recovered individual (post-infectious virus shedding period) at time t
R	number of fully recovered individual at time t
S	number of susceptible at time t

CHAPTER 1

INTRODUCTION

1.1 Motivation

Hand, foot and mouth disease (HFMD) is a common viral illness and mostly caused by viruses that belong to the enteroviruses group. The major causative agents of HFMD are coxsackievirus and human enterovirus 71 (EV-71) (Podin et al., 2006). The viruses are transmitted via fecal-oral route and can also spread through close contact with the patients, virus-contaminated surfaces, fomites and in respiratory droplets (Solomon et al., 2010). HFMD primarily affects infants and young children under age of 10 (Podin et al., 2006; SHD, 2018). Since 1997, the large outbreaks of human enteroviruses associated with hand, foot and mouth disease (HFMD) across the Asia-Pacific started to catch the public attention (McMinn, 2002; Podin et al., 2006). Countries such as Taiwan, China, Singapore, Malaysia, Vietnam, Mongolia and Brunei have created high number of infected cases and complicated death cases (Roy & Halder, 2010). Enterovirus 71 (EV 71) was first identified in California, USA, in 1969, which causes the HFMD with neurological and systemic complications (Solomon et al., 2010).

In Sarawak, series of HFMD outbreaks have occurred since 1997, affecting mostly children. This has raised the awareness of the public due to the fatalities cases reported. HFMD is endemic in Sarawak (SHD, 2018).

Among the HFMD effects, patients may suffer from rapidly progressive cardiorespiratory failure and lead to fatalities (Chan et al., 2000). In 1997, the major HFMD outbreak in Sarawak has raised the alarm as 29 unusual pediatric deaths due to encephalitis and cardiac failure (Chan et al., 2000; Podin et al., 2006). Since then, there were outbreaks reported again in the state in 2000, 2003 (Podin et al., 2006), 2006 (SHD, 2006a), 2010, 2011, 2012, 2013, 2014 and 2015 (SHD, 2006b, 2015). In 2006, 13 deaths were recorded in the state during the HFMD outbreaks (Tiing & Labadin, 2008).

When a cohort of children that have not been exposed to the disease of which these children are then susceptible encounter the viruses when an ill child is introduced into the group, then the viruses can be easily spread among the children (Podin et al., 2006). With this, to control the widespread of the HFMD viruses, childcare centers or kindergartens that have the HFMD cases will be ordered to close temporary. Working parents involved are affected, as they need to take care of their children. Besides, the challenges encountered include the public health interventions to alarm the public to avoid crowded places when there are HFMD outbreaks (Tiing & Labadin, 2008).

Currently, it was reported that vaccine EV71 has started being used for infants and children in China. However, the vaccinated individuals still can be infected by other HFMD viruses besides virus EV71 (Shi et al., 2018; Tan & Cao, 2018). Besides, the vaccinated individuals do not have life long immunity against the virus EV 71. In other countries, there is no vaccine and specific treatment applied to protect against the virus (Ministry of Health, 2014; SHD, 2018). To relieve the symptoms, patients are advised to be aware of hygiene and avoid dehydration. Supportive therapy and the use of medications recommended by health care provider may help to control the fever and pain (X. Li et al., 2014; Lu et al., 2013). Clinical studies where the patients were being monitored and

behaviors of the disease were recorded in order to combat with the HFMD are further discussed in Section 2.2.

1.2 Problem statement

HFMD is transmitted rapidly via fecal-oral route. The exposure to the viruses affects the patients' risk of infection especially children as they do not have immunity to the virus. Comprehensive biological insights regards to the HFMD viruses during incubation period, infectious period and post-infectious virus shedding period have been studied thoroughly. Once a susceptible individual is infected by the HFMD virus, the patient at first is called asymptomatic patient as no symptoms has been shown yet. Asymptomatic patient, which is grouped into the incubation period group contributes as infectious source and start to transmit the disease. Incubation period is reported within a range from 1 day to 2 weeks (CDC, 2015; Ministry of Health, 2014). HFMD is most contagious during the first week of the infectious period when the symptoms are shown. The symptoms of the illness may subside within one week, which the patient then is grouped into post-infectious virus shedding period group. The post-infection virus shedding may serve as reservoirs of the virus and contribute to the epidemic of the HFMD. The post-infectious virus shedding can persist in the stools for up to few weeks (Mandal, 2017; Ministry of Health, 2014; Podin et al., 2006; Teng et al., 2013; Thomas & Weber, 2001). There is a short immunity against HFMD but not a permanent immunity after fully recovery. The patients return to being susceptible to HFMD once they lost their immunity.

Besides, the patient also can get the disease again from different viruses (CDC, 2015; Chuo, 2008; Mandal, 2017).

Many mathematical models aimed to describe the dynamics of the HFMD were developed since the occurrence of the outbreaks. SIR model was first used to predict the real dynamic infectious behaviors in Sarawak but the prediction was only provided a basic framework while discussing the characteristics of HFMD which is merely based on infectious period (Tiing & Labadin, 2008). To date, there have been some other mathematical models being developed to study the characteristics of HFMD. This will be discussed more in Section 1.5. However, the models did not carry out more comprehensive biological factors in order to study the characteristics of HFMD. With this, we aim to formulate a mathematical model, which incorporate all the biological factors above to better comprehend the characteristic of HFMD.

1.3 Objectives

The aims of the study are as follows:

i. To formulate a simple deterministic new model, SEIPR model, by incorporating the virus biological factors namely the incubation, infectious and post-infectious periods.
ii. To analyze the numerical and analytical solutions of the SEIPR model.

1.4 History of mathematical modeling

Mathematical modeling for infectious diseases is a system description by using mathematical concepts and language to provide an insight into a complex interacting process by studying the behaviors of the diseases and to predict the future epidemics, hence help to control the future outbreaks (Giesecke, 2017; Johnston et al., 2007).

Daniel Bernoulli initiated the first mathematical study of diseases in 1760. He created a mathematical method to evaluate the effectiveness of the variolation techniques against smallpox, aiming to influence the public health policy intervention. In 1906, Harmer introduced 'mass action principle' contributed to the estimation of the rate of contact of the infectious individual and susceptible in discrete-time framework. Later, in 1908, Ronald Ros translated the problem to continuous-time framework. Kermack and McKendrick, in 1927, established the threshold theory which suggested epidemic outbreak occur only when the density of the number of susceptible exceed certain critical value. In 1929, Soper who deduced the hidden mechanisms responsible to the often-observed periodic epidemics extended the ideas above (Anderson & May, 1992).

SIR model, the basic epidemic model was initiated in depth studied by Kermack & McKendrick, 1927. The formalism categorizes hosts as susceptible (*S*), individual that has not been exposed to the disease, infected person (*I*) is the individuals at the infectious stage and recovered (*R*) refers to patient that has successfully cleared the infection. From the modeling perspective, the individual is moving from one compartment to another compartment (Keeling & Rohani, 2008).

1.5 Related works

Over the years, HFMD is a worldwide concern disease as the disease can spread rapidly. In Sarawak, it was reported from year 1997 to 2006, the major outbreaks were occurred with every three years cycle (Podin et al., 2006). However, from year 2010 to 2017, HFMD outbreaks have been occurring every year (SHD, 2018). With this, mathematical can be a powerful tool to help to study more comprehensively the behaviors of the HFMD in order to identify the causes, interrupting the spread and help public health personnel in developing possible interventions.

SIR model was first used to predict the real dynamic infectious behaviors in Sarawak and the study suggested that the number of susceptible is the parameter that may control the disease (Tiing & Labadin, 2008). SEIR model in the other hand is a refinement to SIR model which consider the exposed (E) as one of the compartments is introduced. SEIR model had been used to study the characteristic of HFMD theoretically by using the numerical simulation. The study showed that the disease transmission depends on the number of actively infected people at the initial time and the disease incidence transmission rate at a given time (Roy & Halder, 2010).

In (Hii et al., 2011), the authors suggested the weather parameters can be used as risk indicator for the potential HFMD outbreaks. The study showed that a maximum daily temperature above $32°C$ and rainfall up to 75mm increase the HFMD incidence in the subsequent 1 to 2 weeks. Whereas, in 2012, (Roy, 2012) studied the HFMD model theoretically by using the basic SIR model, SLIR and SLIQR model. SLIR model included the latent period (L) which the susceptible individual after contacts with the infected individual do not get the disease immediately and will become infectious after certain time.

On the other hand, SLIQR model added the quarantine compartment (Q) and show that if the probability of the infected individual being quarantine is increased, then the basic reproductive number could be maintained as less than one.

Another SEI_AI_SQR model, which had been formulated by putting pulse vaccination into some fraction of susceptible and being analyzed theoretically with numerical simulation, the result showed that a large pulse vaccination rate will lead to eradicate the disease (Samanta, 2014). Another study, SEIQR model, consists of susceptible (S), exposed (E), infectious and non-hospitalized (I), infectious and hospitalized (Q), and recovered (R) individual is used to investigate the preventive measure in order to control HFMD. It was shown that by reducing the transmission rate and increasing the recovery rate of non-hospitalized infectious individual, the spread of HFMD can be controlled effectively. However, changing the hospitalized infectious individual rate played a small effect in controlling the disease spreading (Y. Li et al., 2014). In another study, periodic transmission rate and 'psychological' effect which being interpreted as people deter from risky behavior or taking precaution once HFMD appears and spreads were considered into the study of the behavior of HFMD by using SEIQR model. Here, by putting the quarantine as a control measurement as part of the compartments (Q) as well, the SEIQR model showed that the quarantine rate together with the infected rate are important elements in controlling the spread of the HFMD (Zhu et al., 2014).

In 2015, effects on hand washing campaign had been added into $SEII_AR$ model. The model was studied theoretically. Compartments were included infected human population (I) and severe human population (I_A). The effectiveness of hand washing parameter was added to reduce the rate of disease transmission and hence concluded that by increasing the effectiveness of hand washing campaign, the infected cases will decrease

(Phutthichayanon & Naowarat, 2015). On another other study, (Lai et al., 2016) studied a dynamic model of HFMD which included a few compartments namely susceptible (*S*), infectious cases before developing disease (*I*), asymptomatic disease with infectiousness (*AS-I*), immunity after infected (*AS-I* (*R*)), infectious cases after developing symptoms (*EV-I*) and symptomatic cases with immunity after recovery (*EV-R*). The study suggested that the isolation strategy against HFMD delayed the epidemic peak. Meanwhile, in 2017, SEIR model again was being studied to predict the infectious cases in Singapore for the year 2015 and 2016 (Wu, 2017).

Another study in 2018, (Chadsuthi & Wichapeng, 2018) extended the existing SEIR model to $SEII_eHRW$ by adding the indirect transmission via free-living virus obtained from infectious individual into mathematical model. Here, *S* is susceptible, *E* is exposed individual, *I* is symptomatic infectious individual, I_e is asymptomatic infectious individual, *H* is hospitalized, *R* recovered and *W* is density of pathogens contain free-living virus in contaminated environment. From their study, the transmission dynamic was contributed by direct transmission from asymptomatic infected individuals, symptomatic infected individual and indirect transmission via free-living virus. In 2018, (Shi et al., 2018) proposed a model named $SVEII_eQRW$, where vaccinated (*V*), quarantine (*Q*) and density of pathogen of the contaminated environment from infectious individuals (*W*) had been included to study the behavior of HFMD. It was noticed that by increasing the rate of virus clearance, vaccinated young children and quarantine infectious individuals, the HFMD could effectively be controlled. Another other theoretically study done by (Tan & Cao, 2018) in which vaccination compartment (*V*) had been added into the mathematical model, called SEIVT. The simulation results showed that the number of infectious is minimal if the vaccination is implemented.

The existing models explained above did not take into account all the biological insights specifically for Sarawak HFMD cases. Therefore, we create a new model, SEIPR model that incorporates the virus biological factors of incubation, infectious and post-infectious periods to provide a better prediction for the occurrence of the HFMD outbreak.

Table 1.1: Summary of mathematical models of HFMD.

No	Source	Study Area	Model Approached	Finding
1	Ting & Labadin, 2008	Sarawak, Malaysia	SIR	Susceptible is parameter that may control the disease.
2	Roy & Halder, 2010	Bangladesh (theoretically study)	SEIR	Transmission depends on number of infectious individuals and transmission rate.
3	Hii et al., 2011	Singapore	Time series Poisson regression models	Daily temperature above 32°*C* and rainfall up to 75mm increase the HFMD incidence.
4	Roy, 2012	Bangladesh (theoretically study)	SLIR, SLIQR	Quarantine period reduces the transmission cases.
5	Samanta, 2014	United Kingdom (theoretically study)	SEI_AI_SQR • Pulse vaccination is vaccinated to some fraction of susceptible.	Large pulse vaccination rate leads to eradicate the disease.

Table 1.1 continued

6	Y. Li et al., 2014	China	SEIQR	Reduce transmission rate and increasing the recovery rate of non-hospitalized infectious individual control the disease spreading.
7	Zhu et al., 2014	China	SEIQR • Psychological effect was put into susceptible compartment.	Quarantine rate and infected rate control the disease spread.
8	Phutthichayanon & Naowarat, 2015	Thailand (theoretically study)	$SEII_AR$ • Hand washing parameter was put to reduce the transmission rate.	Effectiveness of hand washing campaign controls the disease spread.
9	Lai et al., 2016	Taiwan	Compartmental models of S,I,AS-I, AS-I(R), EV-I and EV-R	Isolation strategy delays the epidemic peak.
10	Wu, 2017	Singapore	SEIR	Basic reproductive number obtained can realize real time estimation.
11	Chadsuthi & Wichapeng, 2018	Thailand	$SVEII_eQRW$ • Indirect transmission via free-living virus from infectious individual is added into the model.	Direct transmission and indirect transmission (free-living virus) gained from infectious individual contributed the disease transmission.

Table 1.1 continued

12	Shi et al., 2018	China	SVEII$_e$QRW • Vaccination had been added into model.	Increasing the rate of virus clearance, vaccinated event and quarantine infectious individuals can effectively control HFMD.
13	Tan & Cao, 2018	China (theoretically study)	SEIVT • Vaccination had been added into model.	Vaccination minimizes the number of infectious cases.

1.6 Effectiveness of control measures

The effectiveness of controlling the spread of HFMD is distancing measures. This is to interrupt the virus transmission from person to person through close contact. Besides, personal hygiene, good sanitation and disinfection of soiled surface with chlorinated disinfectants can lessen the spread of the virus. This is to reduce the risk of virus infection through contact with contaminated surfaces, toys and fomites. Infection control programs such as the closure of child-care centers and public awareness contribute to preventing the rapid spreading of the viruses (Solomon et al., 2010).

1.7 Significant of the study

The study of mathematical modeling provides an insight into the characteristics of the HFMD. The study's goal is aimed to incorporate the behaviors of the HFMD viruses

spreading during the incubation period, infectious period and post-infectious virus shedding period to make a more reliable prediction of the spreading cases. With this, the new formulating simple deterministic SEIPR model is to enhance the predicting of the disease cases based on the behaviors of the HFMD biological factors. SEIPR model shares a comprehensive description of the HFMD transmission dynamics in which, it can help the public heath practitioners to take a more effective control interventions to reduce the effect of the outbreaks.

1.8 Summary

Models incorporated with the epidemiology of the HFMD and assumptions about the disease can help well in interpreting the disease. Next, in Chapter 2, overview of HFMD and methodology are discussed. Whereas, basic SIR model and our new SEIPR model will be analyzed theoretically and numerically in Chapter 3 and in Chapter 4 to comprehend the behaviors of HFMD.

CHAPTER 2

LITERATURE REVIEW

2.1 Introduction

An overall of clinical review will be discussed in this chapter. A more comprehensive study towards the motivation of model formulation and other mathematical models incorporated with the different perspectives to study the behavior of the disease has been done.

2.2 Overview of hand, foot and mouth disease

HFMD is an acute viral illness, mainly affects infants and children under the age of 10, however, older children and adults can also be infected. Viruses is predominantly transmitted via fecal-oral route and mainly caused by coxsackievirus A 16 (CV-A16), human enterovirus (EV-71) or other enteroviruses including coxsackievirus A (CV-A2, CV-A4, CV-A5, CV-A6, CV-A7, CV-A10 and CV-A12) or coxsackievirus B (CV-B1, CV-B2, CV-B3 and CV-B5) (Podin et al., 2006). Viruses can be detected from a patient from nose and throat secretion, blister fluid and stools. Unlike other enteroviruses which usually cause mild HFMD cases, EV-71 is reported to cause neurological and systematic complications (Solomon et al., 2010).

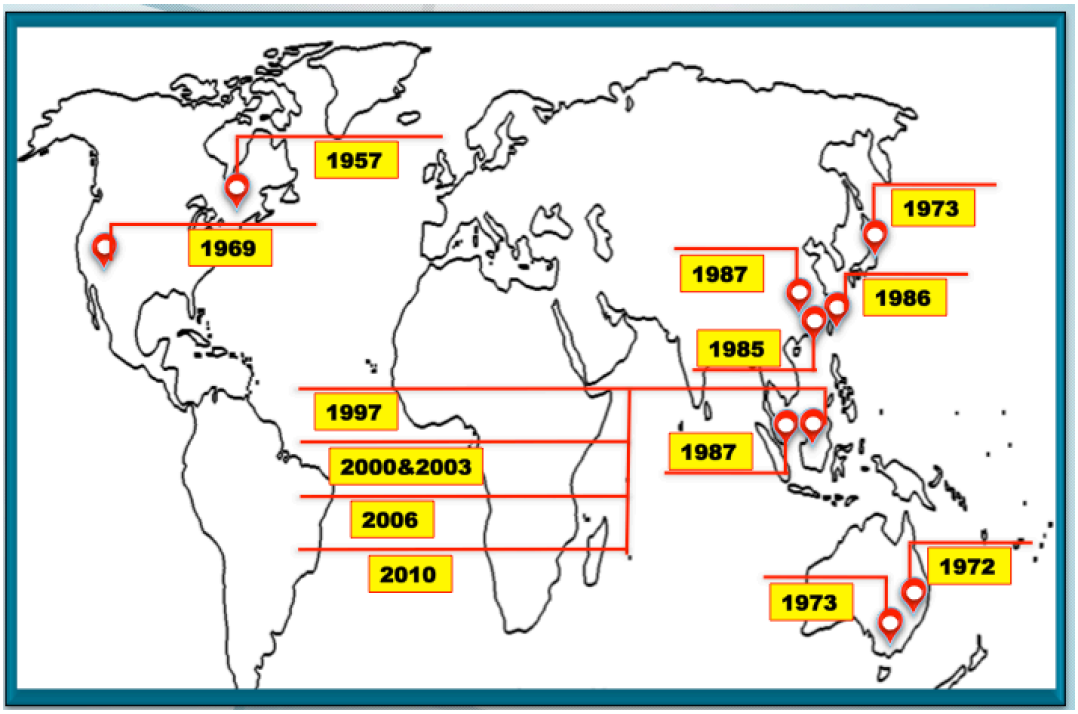

Figure 2.1: World map of HFMD outbreaks throughout the years.

From Figure 2.1, HFMD was first identified in New Zealand in 1957 (Zhu et al., 2014). EV-71 which was firstly isolated in California, USA, 1969, during an outbreak causes neurological disease complication (Han et al., 2010). In Asia-Pacific, early reports of EV-71 associated HFMD outbreaks were reported to be identified in Japan in 1973, Hong Kong, in 1985, Hubei Province, China in 1987, Singapore in 1987, Melbourne, Australia in 1973, eastern Australia in 1972, and Taiwan in 1986 (Huang et al., 2009; McMinn, 2002). In 1997, during an outbreak of HFMD in Sarawak, fatalities in the 29 patients were reported. There were four out of five deceased patients who showed brainstem encephalitis with EV-71 isolated through rectal and throat swabs, serum, pancreatic and lung tissue and spinal cord specimens. In addition to EV-71, other possible factors such as toxins, medicines, environment exposures or other infectious agents have

also been considered in contributing to the fatal outcome of these patients including co-infection of EV-71 and adenovirus (Cardosa et al., 1999; Chan et al., 2000). Meanwhile, (Podin et al., 2006) reported that EV-71 was isolated in Sarawak as the dominant enterovirus serotype during 2000 and 2003 HFMD outbreaks. The HFMD cases began early in the year 2000 and 2003 where the EV-71 cases dropped sharply in June 2000 and April 2003. For the rest of the months until the end of the years (2000 and 2003), the EV-71 cases were replaced by CV-A16 cases. The sentinel surveillance suggested the EV-71 has the ability to spread rapidly within a susceptible community before becoming quiescent during the outbreaks. Whereas, in 2006, another 13 deaths were recorded during HFMD outbreaks (Tiing & Labadin, 2008). It was reported in the study from year 1997 to 2006, major HFMD outbreaks occurred every three years cycle in Sarawak (Podin et al., 2006), and in another other study, Sarawak was reported to have HFMD outbreaks every year (SHD, 2006b, 2015).

From Figure 2.2, when a cohort of children who have not been exposed to the HFMD viruses encounter the viruses, outbreaks will occur (Thomas & Weber, 2001). Once the HFMD virus infects a susceptible individual, after few days of incubation periods (Mandal, 2017; Podin et al., 2006), the patient may start to present symptoms, which start with fever, and sore throat. In a few days, rashes, red spots and blister may develop in the mouth, on the palms, soles of feet, buttocks, knees or other areas and usually accompanied by poor appetite. Anyhow, not all of the infected patients will develop symptoms. Cases may vary between different individuals and different stages of the disease. HFMD is most contagious during the first week of illness. The symptoms of the illness will subside in 7 to 10 days. (CDC, 2015; Mandal, 2017; Ministry of Health, 2014; Podin et al., 2006; Roy & Halder, 2010; SHD, 2018). During the post-infectious periods, the patients can still

transmit the disease even after the symptoms are gone as the persistent viruses can continue to be shed in the throat and stool for up to several weeks (Han et al., 2010; Li et al., 2013; Podin et al., 2006; Teng et al., 2013).

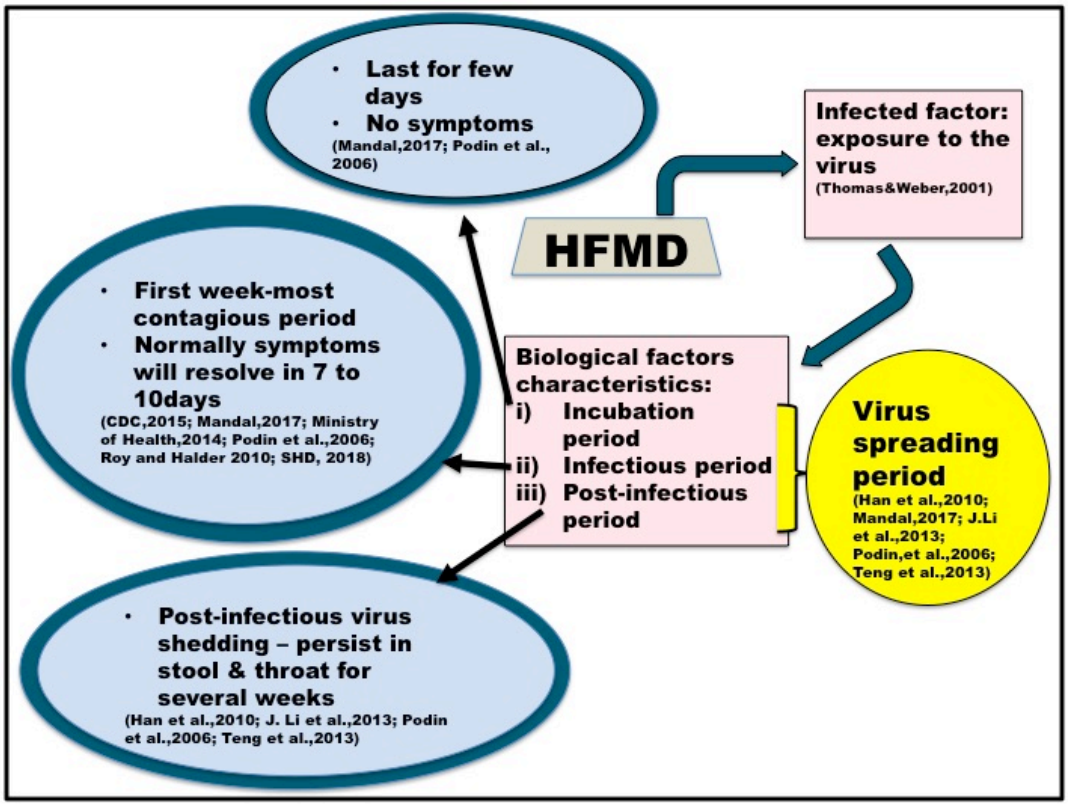

Figure 2.2: Transmission cycle of HFMD.

In a study (Teng et al., 2013), 100% of the patients observed with mild EV-71 cases, severe EV-71 cases and severe CV-A16 cases still had the viruses isolated in the feces after one week of infection. While for mild CV-A16 cases, 94.6% of the patients observed had the virus isolated after one week, followed by the second week, 90.5% of the mild EV-71 cases, 97.1% of the severe EV-71 cases, 87.5% of the mild CV-A16 and 100%

of the severe CV-A16 had the viruses persisted in the stool samples. The maximum duration observed for EV-71 and CV-A16 persisting in stool was 10 weeks and 6 weeks.

Another study showed that 100% of the cases had EV-71 isolated from the patients observed through throat swabs 8 days after case onset. Only half of the patients showed EV-71 negative after two weeks. It is suggested that during the first two weeks of the illness, the patients have high risk to spread the disease. The longest duration for EV-71 persisted in respiratory secretion was 24 days while in stools was 42 days. Although the post-infection virus shedding can still transmit the disease, but it is reported to be less contagious when the illness resolves (Han et al., 2010).

On the other hand, asymptomatic patients contribute as infectious source as well during the incubation period. Incubation period is reported within a range from 1 day to 2 weeks (CDC, 2015; Ministry of Health, 2014). A study done by (Li et al., 2013) showed that the close contact adult group had EV-71 isolated even without showing symptoms and that the virus can persist for one week . Another two close contacts had EV-71 excreted and symptoms were shown only after two days.

There is a short immunity against HFMD but not a permanent immunity after fully recovery. The patients return to being susceptible to HFMD once they lost their immunity. Besides, the patient also can get the disease again from different viruses (CDC, 2015; Chuo, 2008; Mandal, 2017).

As mentioned in Section 1.1, although China has started apply the vaccine EV-71 to against the EV-71 virus, however, the vaccinated individuals do not have life-long immunity and still can be infected by other HFMD viruses besides virus EV71 (Shi et al., 2018; Tan & Cao, 2018). In other countries, there is no vaccine and specific treatment applied to protect against the virus (Ministry of Health, 2014; SHD, 2018).

2.3 Methodology

In order to fulfill the first research objectives, the relevant clinical research done were thoroughly studied. The biological factors of the virus were carefully studied through systematic literature review and oral discussion with domain experts.

Then, the domain problem is characterized whereby the variables that were considered significant were identified and the assumptions made were defined. Hence, the formulation of the model can be done by first abstracting the problem via the drawing of the compartmental diagrams and then the governing equations are constructed. As part of the analysis of this new model, comparison between the basic SIR model with the new model is pertinent in building the first research objective.

Analysis of the new model is done analytically and numerically in fitting the second research objective. Analytical solving method had started with finding equilibrium points, basic reproductive number and threshold value. Analysis of the stability of the equilibrium points used include Jacobian matrix, Routh Hurwitz Criterion and Lyapunov Second Theorem as mentioned in Sections 2.3.1, 2.3.1.1, 2.3.1.2 and 2.3.1.3. Whereas, basic reproductive number and threshold value as mentioned in Sections 2.3.2 and 2.3.3 are used as benchmark in order to analysis the liability of the disease spreading.

Next, numerical solving method allowed us to capture the primary matching results using the visual inspection by comparing the graphs plot between the real and predicted data. Ensuring the well matched between the real and predicted data is then done by model fitting test in Section 2.3.4. The research methodology discussed afore is summarized in the form of a flow chart depicted in Figure 2.3.

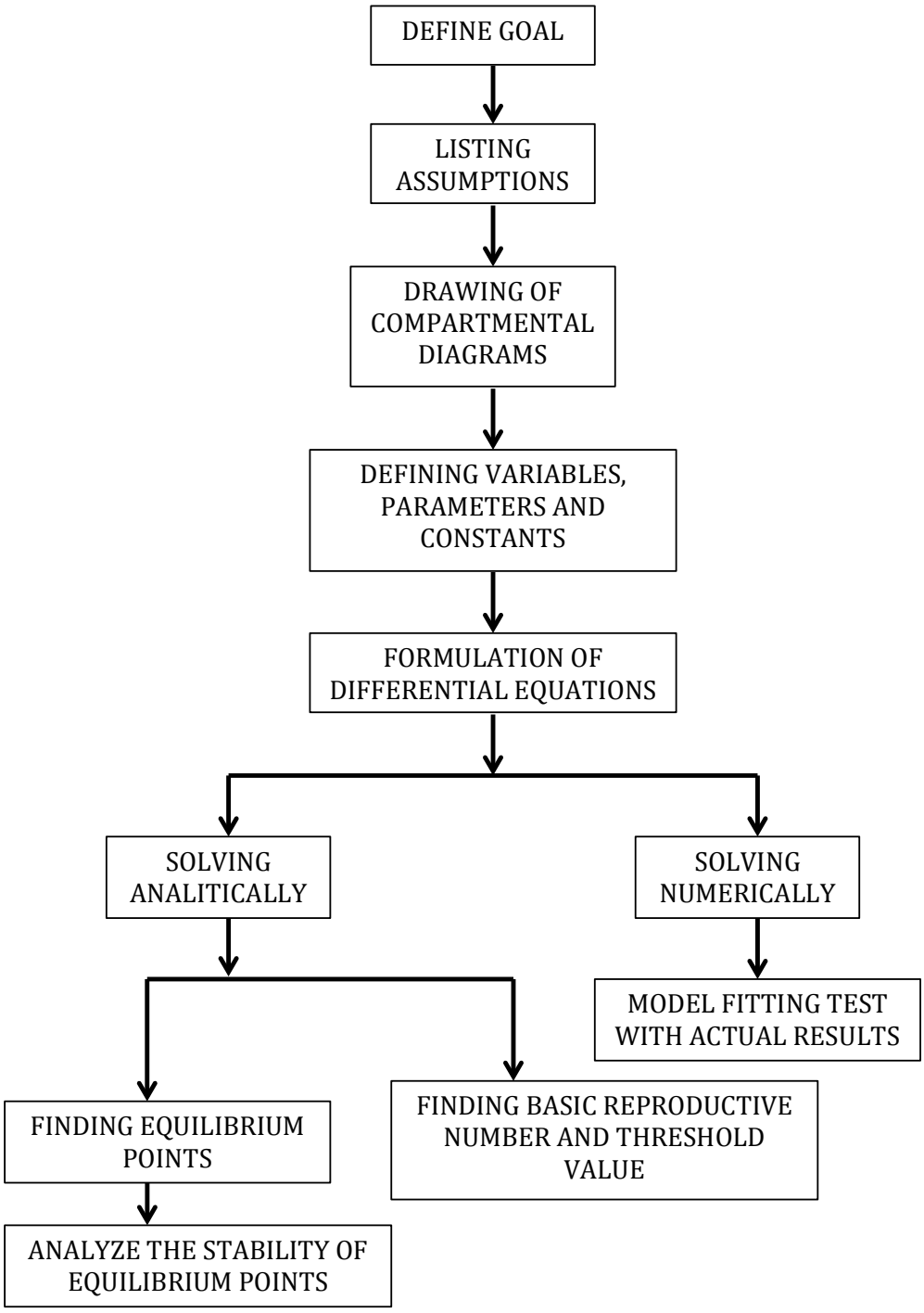

Figure 2.3: Research flow chart.

2.3.1 Equilibrium point

An equilibrium point is a constant solution to a differential equation. It can be referred as a fixed point or a steady state. Given an ordinary differential equation, say, $y' = f(x), x \in R^n$, let $f(x) = 0$ in order to gain the equilibrium point, when $f(x) = 0$ is solved, say, the solution is k, then $f(k) = 0$, where k is known as equilibrium point or equilibrium solution (Hirsch, Smale, & Devaney, 2012).

In this thesis, we analyzed disease-free equilibrium and endemic equilibrium. Disease-free equilibrium points are steady states when the HFMD cannot invade the population. This means all human is in the susceptible state. Whereas endemic equilibrium is a situation when a disease is constantly present in a population. The stability of equilibria study helps us to have better understanding about the disease prevalence. If disease-free equilibrium point is stable, then the outbreak will not occur, and in other words, the endemic state is not globally asymptotically stable. Meanwhile, if disease-free equilibrium point is unstable, the endemic equilibrium exists, which means the endemic steady state is globally asymptotically stable and hence, there is the existence of the disease and cause the outbreak (Heffernan et al., 2005; Ugwa & Agwu, 2013). Thus, it is necessary to study the stability of equilibrium points toward a better understanding when dealing with the disease controlling. Next we will discuss the methods used to study the stability of the disease-free equilibrium in Section 2.3.1.1 and Section 2.3.1.2. In Section 2.3.1.3, we will discuss the method used to study the stability of the endemic equilibrium.

2.3.1.1 Stability of equilibria

Consider a set of equations, $y_i = f_i\left(x_j\right)$, with i =1,2,3, ..., n and j =1, 2, 3, …, n being written as follows:

$$y = \begin{bmatrix} y_1 = f_1\left(x_{1,}x_{2,}\cdots x_n\right) \\ y_2 = f_2\left(x_{1,}x_{2,}\cdots x_n\right) \\ \vdots \\ y_n = f_n\left(x_{1,}x_{2,}\cdots x_n\right) \end{bmatrix} \qquad (2.1)$$

then the Jacobian matrix is defined as

$$J\left(x_{1,}x_{2,}\cdots x_n\right) = \begin{bmatrix} \frac{\partial y_1}{\partial x_1} & \frac{\partial y_1}{\partial x_2} & \cdots & \frac{\partial y_1}{\partial x_n} \\ \frac{\partial y_2}{\partial x_1} & \frac{\partial y_2}{\partial x_2} & \cdots & \frac{\partial y_2}{\partial x_n} \\ \vdots & & & \\ \frac{\partial y_n}{\partial x_1} & \frac{\partial y_n}{\partial x_2} & \cdots & \frac{\partial y_n}{\partial x_n} \end{bmatrix} \qquad (2.2)$$

Hence, the Jacobian's eigenvalues can be determined. The stability of a system of ordinary differential equations is determined by the real parts of the Jacobian's eigenvalues. The equilibria is asymptomatically stable if all the real parts of the Jacobian's eigenvalues are negative values and unstable if there is at least one positive eigenvalue.

2.3.1.2 Routh Hurwitz Criterion

Routh Hurwitz criterion is used to find the number of positive roots and negative roots of a characteristic equation without solving the equation and hence, it can be used to determine the stability of a system. Characteristic equation or polynomial can be written as

$$p(\lambda) = \det(A - \lambda I)$$

$$= \begin{vmatrix} a_{11} - \lambda & a_{12} & \cdots & a_{1n} \\ a_{21} & a_{22-\lambda} & \cdots & a_{2n} \\ \vdots & \vdots & \ddots & \vdots \\ a_{n1} & a_{n2} & \cdots & a_{nn} - \lambda \end{vmatrix}$$

$$= (-1)^n \left[\lambda^n + c_1 \lambda^{n-1} + c_2 \lambda^{n-2} + \ldots + c_{n-1} \lambda + c_n \right], \qquad (2.3)$$

where $A = \left[a_{ij} \right]$ and the coefficients c_i are to be computed by evaluating the determinant (Mondaini, 2002).

In order for a system to be stable, all the roots of the polynomial should have negative real parts and for this to happen, all the coefficients of the polynomial should have positive sign at first. Next, by using Routh Array, the number of the positive real roots is decided for which positive real roots are equivalent to the number of signs changing obtained from Routh Array.

Given a polynomial equation $a_n s^n + a_{n-1} s^{n-1} + \cdots + a_1 s + a_0 = 0$, Routh Array can be filled in as below:

s^n	a_n	a_{n-2}	a_{n-4}	$\cdots$
s^{n-1}	a_{n-1}	a_{n-3}	a_{n-5}	$\cdots$
$\vdots$	$\vdots$	$\vdots$	$\vdots$	$\cdots$
s^0	$\vdots$	$\vdots$	$\vdots$	$\ddots$

Sign changes in $\Delta_0,\ \Delta_1,\ \Delta_2,\ \ldots,\ \Delta_n$ can be determined, where

$$\Delta_0 = a_n,\ \Delta_1 = a_{n-1},\ \Delta_2 = \frac{a_{n-1} \bullet a_{n-2} - a_n \bullet a_{n-3}}{a_{n-1}}, \cdots$$

Thus, if $\Delta_0,\ \Delta_1,\ \Delta_2,\ \ldots,\ \Delta_n$ are all positive, and all the coefficients of the polynomial are positive, then it is said that all the roots of the characteristic equation are all having negative real parts.

2.3.1.3 Lyapunov Second Theorem on stability

Lyapunov function, $V(x)$, can be used to prove the asymptotically stability of the endemic steady state (Abramson, 2001). Let a system $\dot{x} = f(x)$ has a point of equilibrium at $x = 0$ and there exists continuous differentiable function $V(x): \mathbb{R} \to \mathbb{R}$, such that

i) $V(x) = 0 \Leftrightarrow x = 0$

ii) $V(x) > 0 \Leftrightarrow x \neq 0$

iii) There exists continuous function $W(x): \mathbb{R} \to \mathbb{R}$ such that $W(x) \geq 0\ \forall x \in \mathbb{R}$ and $W(x) = 0 \Leftrightarrow x = 0$

iv) $\dot{V}(x) = \sum_j^n \frac{\partial V(x)}{\partial x_j} f_j(x) \leq -cW(x)\ \forall x \in \mathbb{R}$ where $c \geq 0$ is a constant.

Hence, the system is said to be asymptotically stable.

2.3.2 Basic reproductive number

Basic reproductive number, R_0, is the average number of secondary infections produced by an infectious case in a complete susceptible population. R_0 is expressed as the product of the rate of secondary infectious and the duration of the infectious period occur. If $R_0 < 1$, then every wave of the infection in the population has fewer infected individuals being introduced to the susceptible population, and hence, the disease will eventually die out. If $R_0 > 1$, there will be increasing of infected individuals and the disease will spread which the epidemic occur. If $R_0 = 1$, there will approximately be the same number of infected cases all the time, which the endemic occurs (Heffernan et al., 2005).

R_0 is derived by threshold parameter where the average number of new infectious individual is the product of transmission rate and infectious period. This can be done by working the infected compartment in the compartmental model (Keeling & Rohani, 2008). However, when there are more infective compartments involved, we follow the next generation model to obtain the R_0 (Heffernan et al., 2005; van den Driessche, 2017). The next generation model, is a general model derived in such cases where the population is split into discrete and disjoint classes. R_0 is defined as the spectral radius (dominant eigenvalue) of the next generation operator which the formation of the operator will involve two compartments, infected and non-infected, from the model.

Let assume that the model has *n* compartments where $m < n$ compartments contain infected individuals. We define the following (Heffernan et al., 2005; van den Driessche, 2017):

D1) Let $x = x_i$ be the number individuals proportion in the i th compartment where i =1, 2, ..., n.

D2) $F_i(x)$ denotes the rate of new infections cases in the compartment i. $F_i(x)$ is including only the newly arising infection cases but not including the infectious individual who is transferred from one compartment to another.

D3) $V_i(x) = V_i^-(x) - V_i^+(x)$. $V_i(x)$ denotes the rate of other transitions between compartment i and other infected compartments. $V_i^+(x)$ is the individuals transferring rate into compartment i, and $V_i^-(x)$ is the individuals transferring rate out of the compartment i.

D4) The compartment model denotes $\frac{dx_i}{dt} = F_i(x) - V_i(x)$, gives the rate of change of x. Next, we form the next generation matrix (operator) FV^{-1} by using the partial derivatives of F_i and V_i. The entries of matrices F and V are $F = \left[\frac{\partial F_i(x_0)}{\partial x_j}\right]$ and $V = \left[\frac{\partial V_i(x_0)}{\partial x_j}\right]$, where i, j = 1, …, m and x_0 is the disease-free equilibrium. The entries of matrix F is the rate of secondary infections produced in compartment i by an index case in compartment j. The entries of matrix V gives the rate of time an individual spends in a single visit to compartment j. The entries of matrix V^{-1} gives the expected duration of the infectious period. Thus, the FV^{-1} gives the expected number of secondary infections in compartment i produced by an infected

individual introduced in compartment j. R_0 is given by the spectral radius (dominant eigenvalue) of the matrix FV^{-1}.

2.3.3 Threshold value

Threshold value, say S, is used to distinguish the range of the values where the behaviors of the disease discussed may vary in some important way. Given an ordinary differential equation, say, $y_i' = f(x_i)$, where $\in R^n$, $i = 1, 2, \ldots, n$.

Let $f(x_i)>0$, in order to study the minimum proportion of the population in which creates the liability of disease spreading. The threshold is determine by (S-1)>0, where if S >1, thus an outbreak will occur. If S <1, thus the disease will eventually die out (Keeling & Rohani, 2008).

2.3.4 Model fitting test

Goodness of fit is a statistical method used to find out how the observed values are significantly different from the actual values. It is a measurement of how correlated a group of actual observations are to a model's prediction (Trottier & Philippe, 2001). In our study, regression analysis is used to discuss the best fit of the predicted data and actual data. To use regression analysis, we need to get simple linear regression, linear regression

equation, correlation coefficient and residuals plot, which are discussed in Sections 2.3.4.1 until 2.3.4.4. Besides, root square mean error (RMSE) for sensitivity analysis is discussed in Section 2.3.5.

2.3.4.1 Simple linear regression

A simple linear regression is the best fitting straight line through a set of points. Firstly, a scatterplot is chosen by plotting the predicted values on the x-axis and observed values on the y-axis. Scatterplot is used to determine the strength of the goodness of fit of the model (predicted values) to the observed data. Next, we will find linear regression equation for the best fitting straight line to provide a solution to the problem.

2.3.4.2 Linear regression equation

Linear regression equation is line of best fit, which is formed by using the linear least squares fitting. Vertical least squares fitting proceeds by finding the sum of the squares of the vertical deviations R^2 of a set of n data points (Keeping, 1962).

$$R^2 = \sum \left[y_i - f\left(x_i, a_1, a_2, \cdots, a_n\right) \right]^2 \qquad (2.4)$$

R^2 minimum when,

$$\frac{\partial\left(R^2\right)}{\partial a_i} = 0, \; i = 1,\ldots,n$$

For a linear fit,

$$f(a,b)=a+bx\,, \tag{2.5}$$

so,

$$R^2(a,b)=\sum_{i=1}^{n}\left[y_i-\left(a+bx_i\right)\right]^2 \tag{2.6}$$

$$\frac{\partial\left(R^2\right)}{\partial a}=-2\sum_{i=1}^{n}\left[y_i-\left(a+bx_i\right)\right]=0$$
$$\frac{\partial\left(R^2\right)}{\partial b}=-2\sum_{i=1}^{n}\left[y_i-\left(a+bx_i\right)x_i\right]=0$$

These give the following:

$$na+b\sum_{i=1}^{n}x_i=\sum_{i=1}^{n}y_i \tag{2.7}$$

$$a\sum_{i=1}^{n}x_i+b\sum_{i=1}^{n}x^2{}_i=\sum_{i=1}^{n}x_iy_i \tag{2.8}$$

We put them in matrix form,

$$\begin{bmatrix} n & \sum_{i=1}^{n}x_i \\ \sum_{i=1}^{n}x_i & \sum_{i=1}^{n}x_i{}^2 \end{bmatrix}\begin{bmatrix} a \\ b \end{bmatrix}=\begin{bmatrix} \sum_{i=1}^{n}y_i \\ \sum_{i=1}^{n}x_iy_i \end{bmatrix},$$

so, we get ,

$$\begin{bmatrix} a \\ b \end{bmatrix}=\begin{bmatrix} n & \sum_{i=1}^{n}x_i \\ \sum_{i=1}^{n}x_i & \sum_{i=1}^{n}x_i{}^2 \end{bmatrix}^{-1}\begin{bmatrix} \sum_{i=1}^{n}y_i \\ \sum_{i=1}^{n}x_iy_i \end{bmatrix}$$

$$\begin{bmatrix} a \\ b \end{bmatrix}=\frac{1}{n\sum_{i=1}^{n}x_i{}^2-\left(\sum_{i=1}^{n}x_i\right)^2}\begin{bmatrix} \sum_{i=1}^{n}y_i\sum_{i=1}^{n}x_i{}^2-\sum_{i=1}^{n}x_i\sum_{i=1}^{n}x_iy_i \\ n\sum_{i=1}^{n}x_iy_i-\sum_{i=1}^{n}x_i\sum_{i=1}^{n}y_i \end{bmatrix}. \tag{2.9}$$

Thus, we get,

$$a = \frac{\sum_{i=1}^{n} y_i \sum_{i=1}^{n} x_i^2 - \sum_{i=1}^{n} x_i \sum_{i=1}^{n} x_i y_i}{n\sum_{i=1}^{n} x_i^2 - \left(n\sum_{i=1}^{n} x_i \right)^2} \quad (2.10)$$

$$b = \frac{\sum_{i=1}^{n} x_i y_i - \sum_{i=1}^{n} x_i \sum_{i=1}^{n} y_i}{n\sum_{i=1}^{n} x_i^2 - \left(n\sum_{i=1}^{n} x_i \right)^2} \quad (2.11)$$

Hence, the linear regression equation, $y = a + bx$ is formed. This linear regression equation can help to get the new predicted value in Section 2.3.4.4. Next, we will get the correlation coefficient, r^2, which can be used to measure the overall quality of the goodness of fit.

2.3.4.3 Correlation coefficient

R-square, r^2, is the correlation coefficient that can take on any value between 0 and 1, with a larger number indicating a better fit and 1 is perfect fit between the predicted data and observed data. R-square, r^2 is used to read the respond of the variability between the actual data and the predicted data around its mean. The higher the value of the r^2 means that the variability of the actual and predicted data had higher respond around its mean and indicating a better fit (Benesty et al., 2009; Keeping, 1962) .

The correlation coefficient, $r^2 = \frac{ss_{xy}^2}{ss_{xx} ss_{yy}}$.

$$ss_{xx} = \sum_{i=1}^{n} \left(x_i - \bar{x} \right)^2 \quad (2.12)$$

where ss_{xx} is sum of variance of data x, $\bar{x}$ is mean of data x and $\sum_{i=1}^{n}$ is sum of n data.

$$ss_{yy} = \sum_{i=1}^{n}\left(y_i - \bar{y}\right)^2 \qquad (2.13)$$

where ss_{yy} is sum of variance of data y, $\bar{y}$ is mean of data y and $\sum_{i=1}^{n}$ is sum of n data.

$$ss_{xy} = \sum_{i=1}^{n}\left(x_i - \bar{x}\right)\left(y_i - \bar{y}\right) \qquad (2.14)$$

where ss_{xy} is sum of cross-correlation between data x and data y, $\sum_{i=1}^{n}$ is sum of n data.

After obtain the r^2, we then validate again the model by using residuals plot.

2.3.4.4 Residuals plot

First, we need to get the residual, the formula is as following:

$$e = y - \hat{y} \qquad (2.15)$$

where e is residual, y is scatterplot obtain from the Section 2.3.4.1 and $\hat{y}$ is predicted value obtain from the linear regression equation discussed in the Section 2.3.4.2.

Next, we will plot the residuals plot by using scatterplot. It is a graph that all the residuals are plotted on the *y*-axis and predicted values obtained from numerical result are plotted on the *x*-axis. If the points in a residual plot are dispersed randomly around the observed data (horizontal line), thus the linear regression model is appropriate for the data. Hence, the validation of the mathematical model is convincing (Weisstein, 2002).

2.3.5 Root square mean error (RMSE)

RMSE is the prediction error, obtains by calculating the standard deviation of the residuals, e (Section 2.3.4.4). With RMSE, we measure how far the residuals are from the linear regression equation (Section 2.3.4.2) data points. The smaller the RMSE, the better the prediction, which means, the residuals are not spread out far from the line of best fit and in other words, it tells us the data is concentrated around the line of best fit (Zhao et al., 2018). The formula of RMSE is as following:

$$RMSE = \sqrt{\frac{\sum_{i=1}^{n}(e)^2}{n}} \qquad (2.16)$$

where e is the residuals calculated in Section 2.3.4.4, n is total number of data and $\sum_{i=1}^{n}$ is sum of n data.

2.4 Thesis outline

The following is the arrangement of the thesis. Formulation, theoretical analysis, numerical results, verifying technique for predicting cases and summarizes of the results for the basic SIR model will be described in Chapter 3. In Chapter 4, formulation, addition, changes made and modification on the basic model to create a new SEIPR model are described. Theoretical analysis, numerical results, summarizes of the results for the modified model and verifying technique for predicting cases are shown. Chapter 5 concluded the contribution of the models, the limitation of the models and further future work on HFMD.

CHAPTER 3

FORMULATION AND ANALYSIS OF THE BASIC SIR MODEL

3.1 Introduction

In Chapter 2, a lot of researches have been done to study the epidemiology of hand, foot and mouth disease (HFMD). Some of the mathematical models from other researchers have been published to highlight the HFMD spreading causes. SIR model was then the first mathematical model being used to discuss the behavior of HFMD in Sarawak. Here, we reproduced the SIR model to be read as benchmark for our improvement SEIPR model. In Chapter 3, compartmental diagrams for basic model are drawn in order to describe the behaviors of the HFMD comprehensively. A system of nonlinear differential equations is formulated. The basic SIR model is being analyzed theoretically. Equilibrium points, basic reproductive number and threshold value are discussed. Later, numerical result is obtained and lastly, analysis for verifying the cases is done. Discussion and summary are made from the results obtained.

3.2 Basic SIR model formulation

First of all, a simple basic SIR model which consists of three differential equations have been studied to describe the epidemiology of the HFMD disease (Keeling & Rohani,

2008). Hence, we will study the basic SIR model developed by (Tiing & Labadin, 2008) to describe the HFMD. To study the behaviors of the infectious HFMD based on mathematically modeling, the following assumptions are made (Giesecke, 2017; Tiing & Labadin, 2008):

i) All newborns are not infected at birth.

ii) The susceptible group is made up of children under age of nine.

iii) The disease is transmitted through the infectious patient.

iv) Individuals are mixed randomly within the population.

v) The infectious occur randomly based on the contact and transmission rate between the susceptible and the infected individuals.

vi) All the parameters values and initial values are constants.

vii) There is no intervention to curb the spreading disease.

viii) Patients who have recovered have a temporary immunity before they return to the susceptible.

ix) The transmission only occurs when susceptible meets with the infectious.

Now, we will look at the basic SIR model (Keeling & Rohani, 2008). This model consists of three compartments that are susceptible (*S*), infectious (*I*) and fully recovered (*R*). In this simple scenario, we have the transitions $S \to I \to R$. The movement from *S* to *I* is the disease transmission progression. Whereas, the movement from *I* to *R* shows that the infected patients has fought off the infection and moving from infectious compartment to the fully recovered compartment. The duration progress from being infected until recovered is taken into account.

The scenario above has been used to study the behaviors of the HFMD (Tiing & Labadin, 2008), basic SIR model used is shown in Figure 3.1, the population is split into three compartments namely susceptible (*S*), infectious (*I*) and fully recovered (*R*).

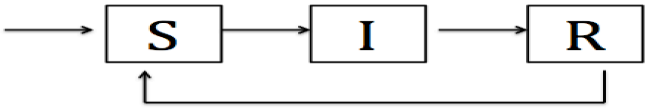

Figure 3.1: A compartmental diagram of SIR basic model (Susceptible-Infectious-Fully recovered). (Tiing & Labadin, 2008)

From Figure 3.2, the susceptible compartment is increased through the nature birth rate, k_1, that is dependent on total susceptible population, *N*. Also, the fully recovered individuals who have lost their immunity return to the susceptible group at the rate of α_2. Besides, the susceptible compartment is decreased through natural death at the rate of k_2. When susceptible meets with the infectious individuals, transmission occurs with the rate of α_1 and the infected individual will move to infectious compartment.

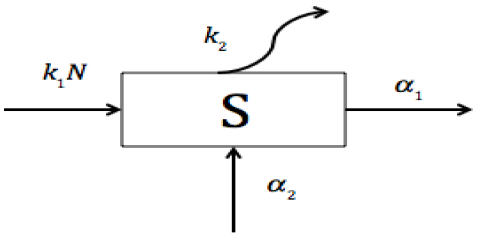

Figure 3.2: Susceptible compartmental diagram, *S*.

As shown in Figure 3.3, once the infectious individual departs from susceptible compartment, the patient will enter the infectious compartment. After a period of time, the infectious individual will depart from the infectious compartment due to death which are

caused by the disease with the rate of k_3, natural death with rate of k_2 or fully recovered from the disease after time D, thus the fully recovery rate is $\alpha_3 = \frac{1}{D}$.

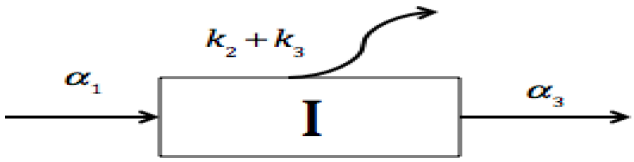

Figure 3.3: Infectious compartmental diagram, *I*.

After time *D*, the fully recovered individuals from the infectious compartment will enter the fully recovered compartment as shown in Figure 3.4. An individual will attain a short immunity after fully recovered from the disease. Once the immunity is lost after time G, the individual will return to the susceptible compartment and capable to being infected again. The rate at which the individual loses its immunity is $\alpha_2 = \frac{1}{G}$. At the meantime, the fully recovered compartment has the population decreased due to the death which is caused by the natural death, with the rate of k_2.

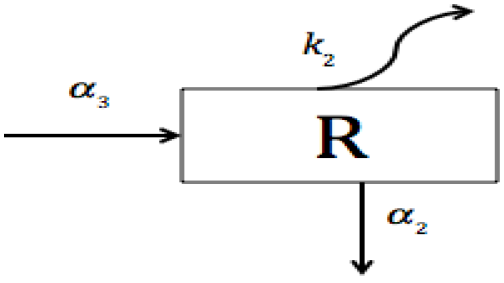

Figure 3.4: Fully recovered compartmental diagram, R.

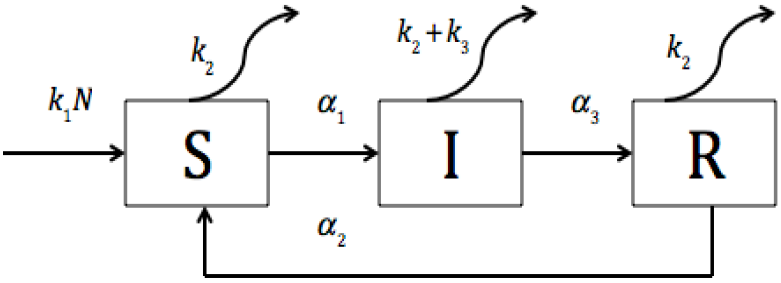

Figure 3.5: The combined compartmental diagram of SIR basic model.

The overview of the complete SIR model compartmental diagram can be seen at Figure 3.5. The susceptible compartment is increased through the nature birth rate, k_1 multiply with total susceptible population, *N*. The transition $S \rightarrow I$ is the disease transmission progression. Let β_ω is the $\Lambda \times \kappa$, where Λ is the average number of contacts any person in the population and κ is the transmission probability. When we multiply β_ω with $\frac{I}{N}$, where $\frac{I}{N}$ are the contacts with infected individuals, force of infection is defined as per capita rate at which susceptible individuals contact the infection. Finally, to obtain the actual number of infectious individual, we will have $\alpha_1 \times I \times S, \alpha_1 = \frac{\beta_w}{N}$. The infectious individual will then depart from susceptible compartment and move to infectious compartment.

Next, the transition $I \rightarrow R$ is the movement where an infectious individual has fully recovered and moves to fully recovered compartment with the rate α_3. Whereas $R \rightarrow S$ is the immunity lost individual enters the susceptible compartment again with the

rate α_2. Besides, the compartments *S*, *I* and *R* have the population decreased with natural death at the rate of k_2 and at the same time, compartment *I* has population decreased through death which is caused by the disease with the rate of k_3. The system of differential equations for SIR model is formed and discussed next.

The differential equations are made as follows:

$$\frac{dS}{dt} = k_1 N - \alpha_1 SI - k_2 S + \alpha_2 R \qquad (3.1)$$

$$\frac{dI}{dt} = \alpha_1 SI - \alpha_3 I - \left(k_2 + k_3\right) I \qquad (3.2)$$

$$\frac{dR}{dt} = \alpha_3 I - \alpha_2 R - k_2 R \qquad (3.3)$$

The total population is $N = S + I + R$ so that,

$$\frac{dN}{dt} = \frac{dS}{dt} + \frac{dI}{dt} + \frac{dR}{dt} \qquad (3.4)$$

hence, we obtain,

$$\frac{dN}{dt} = k_1 N - k_2 S - k_2 I - k_3 I - k_2 R$$

$$\frac{dN}{dt} = k_1 N - k_3 I - k_2 \left(S + I + R\right)$$

$$\frac{dN}{dt} = k_1 N - k_3 I - k_2 N^*, \ (N^* = S + I + R) \qquad (3.5)$$

N^* represents the changing of total population over time, whereas, *N* is the total population at initial time.

3.3 Theoretical analysis of the basic SIR model

Theoretical analysis of SIR model is made based on the differential equations (3.1 – 3.3). The SIR model that describes the population should be positive all the time. From the equations (3.2) and (3.3), the domain of the solution is as follow:

$$\Omega = \left\{ \left(I,R \right) \in R_{+}^{2} \middle| I + R \le N, N > 0 \right\} \quad (3.6)$$

The system of differential equations for the model above has a unique solution with the initial condition lies in Ω, for all $t \ge 0$. The number of population does not change with time, with this we can find the steady state equilibrium point. We set the equations (3.2), (3.3) and (3.5) to zero (Hethcote, 2000).

$$\frac{dI}{dt} + \frac{dR}{dt} + \frac{dN}{dt} = 0 \quad (3.7)$$

To solve (3.7), we denote the equilibrium points as following

$$E_e = \left(I^*, R^*, N^* \right) \quad (3.8)$$

where corresponding equilibrium points I^*, R^* and $N*$ are as follows:

$$I^* = \frac{k_2\left(\alpha_3 + k_2 + k_3\right)}{\alpha_3} - \alpha_2 R^* - k_1 N^*$$

$$R^* = \frac{\alpha_3 I^*}{\alpha_2 + k_1}$$

$$N^* = \frac{k_1 N - k_3 I^*}{k_2} \quad (3.9)$$

From equations (3.7 – 3.9), we obtain the steady state equations. When we set $I^* = 0$, we can get disease-free equilibrium point, $E_e = \left(I^*, R^*, N^*\right)$, which by solving the equations (3.7 – 3.9), we obtain the following:

$$R^* = 0 \text{ and } N^* = \frac{k_1 N}{k_2} \qquad (3.10)$$

Hence,

$$E_0 = \left(0, 0, \frac{k_1 N}{k_2}\right) \qquad (3.11)$$

3.3.1 Disease-free equilibrium point

The disease-free equilibrium point, E_0, is a steady state where the infectious compartment is zero. This means there is no existent of HFMD in the population and the number of the population remains same.

Proof

From the equation (3.3), when $\frac{dR}{dt} = 0$,

$$\alpha_3 I = R\left(\alpha_2 + k_2\right)$$

$$\therefore I = 0 \Leftrightarrow R = 0$$

Thus, from the disease-free equilibrium point, we can see that the infectious compartment will determine the existence of the HFMD. To eradicate the disease, the patients have to be treated early. Next, we will discuss the basic reproductive number that helps to indicate the prevalence of the disease.

3.3.2 Basic reproductive number for basic SIR model

As mentioned in Section 2.3.2, basic reproductive number, $R_\circ$, is the average number of the secondary infectious which is infected by a single infected individual during his or her entire infectious period. It can be expressed as the product of the expected duration of the infectious period and the rate of secondary infectious occurs (Heffernan et al., 2005; Keeling & Rohani, 2008; van den Driessche & Watmough, 2008). Here, the basic reproductive number described by (Keeling & Rohani, 2008) is used.

From equation (3.2),

$$\frac{dI}{dt} = \alpha_1 SI - \alpha_3 I - \left(k_2 + k_3\right) I$$

$$= I\left(\alpha_1 S - \alpha_3 - \left(k_2 + k_3\right)\right)$$

$$\frac{dI}{dt} = I\left(\alpha_1 S - \left(\alpha_3 + k_2 + k_3\right)\right)$$

$$= I\left(\alpha_3 + k_2 + k_3\right)\left(\frac{\alpha_1 S}{\alpha_3 + k_2 + k_3} - 1\right) \qquad (3.12)$$

At the outset of an epidemic, disease-free equilibrium, I=0, thus $S = N = S_0$

$$\therefore R_0 = \frac{\alpha_1 S}{\alpha_3 + k_2 + k_3} = \frac{\alpha_1 S_0}{\alpha_3 + k_2 + k_3} \qquad (3.13)$$

In the next section, we will look at the threshold value analysis.

3.3.3 Threshold value analysis of the basic SIR model

As mentioned in section 2.3.3, if $\frac{dI}{dt} < 0$, then the infectious will die out. From equation (3.12),

$$\frac{dI}{dt} = I\left(\alpha_3 + k_2 + k_3\right)\left(\frac{\alpha_1 S}{\alpha_3 + k_2 + k_3} - 1\right)$$

If $\frac{dI}{dt} < 0$, then $\frac{\alpha_1 S}{\alpha_3 + k_2 + k_3} - 1 < 0$, since $I > 0$ and $\alpha_3 + k_2 + k_3 > 0$. Hence,

$$\frac{\alpha_1 S}{\alpha_3 + k_2 + k_3} - 1 < 0$$

$$\frac{\alpha_1 S}{\alpha_3 + k_2 + k_3} < 1$$

$$S < \frac{\alpha_3 + k_2 + k_3}{\alpha_1} \qquad (3.14)$$

We note that if $S < \frac{\left(\alpha_3 + k_2 + k_3\right)}{\alpha_1}$, then $\frac{dI}{dt} < 0$. Thus, $\frac{\alpha_3 + k_2 + k_3}{\alpha_1}$ is referred as threshold phenomenon where the proportion of susceptible must exceed this critical threshold for an infection to invade. Also, from equation (3.13), we notice that $\frac{\alpha_3 + k_2 + k_3}{\alpha_1} = \frac{S_0}{R_0}$ (Keeling

& Rohani, 2008). Next sections, we are going to prove that if R_0<1, then disease-free equilibrium is stable and the disease will eventually die out. If R_0>1, the disease-free equilibrium is not stable and the disease will prevail.

3.3.4 Stability of disease-free equilibrium point of basic SIR model

Theorem 3.3.4 The disease-free equilibrium is stable if R_0<1 and is not stable if R_0>1 (Keeling & Rohani, 2008)

Proof

The stability of the equilibrium can be determined by using Jacobian matrix. The disease-free equilibrium is stable when all the eigenvalues are negative. At disease-free equilibrium point, $I = R = 0$. Next, we will show the Jacobian matrix from equations (3.2 – 3.3).

$$J_{(I,R)} = \begin{pmatrix} \frac{\partial}{\partial I}\left(\frac{dI}{dt}\right) & \frac{\partial}{\partial R}\left(\frac{dI}{dt}\right) \\ \frac{\partial}{\partial I}\left(\frac{dR}{dt}\right) & \frac{\partial}{\partial R}\left(\frac{dR}{dt}\right) \end{pmatrix} \qquad (3.15)$$

$$J_{(I,R)} = \begin{pmatrix} E_{11} & E_{12} \\ E_{21} & E_{22} \end{pmatrix} \qquad (3.16)$$

where

$$E_{11} = \alpha_1 S - \left(\alpha_3 + k_2 + k_3\right)$$

$$E_{21} = \alpha_3$$

$$E_{22} = -\left(\alpha_2 + k_2\right)$$

$$\det\left(E - \lambda I\right) = 0$$

$$\begin{vmatrix} E_{11} - \lambda & 0 \\ E_{21} & E_{22} - \lambda \end{vmatrix} = 0$$

$$\left(E_{11} - \lambda\right)\left(E_{22} - \lambda\right) = 0$$

We have two solutions:

$$\lambda = E_{11} = \alpha_1 S - \left(\alpha_3 + k_2 + k_3\right) \text{ and } \lambda = E_{22} = -\left(\alpha_2 + k_2\right)$$

For the disease-free equilibrium to be stable, we need to ensure that all eigenvalues have to be negative. Hence, the stability criterion has to be $\alpha_1 S < \left(\alpha_3 + k_2 + k_3\right)$, which means $R_0 < 1$. However, when $\alpha_1 S > \left(\alpha_3 + k_2 + k_3\right)$, we have a positive eigenvalue and the disease-free equilibrium is not stable meaning there is the existence of the disease.

3.3.5 Endemic equilibrium points for basic SIR model

Theorem 3.3.5 When $R_0 > 1$, the disease-free equilibrium is unstable, and the endemic equilibrium exists.

Proof

We will analyze the model from equations (3.1 – 3.3)

$$\frac{dS}{dt} = k_1 N - \alpha_1 SI - k_2 S + \alpha_2 R$$

$$\frac{dI}{dt} = \alpha_1 SI - \alpha_3 I - \left(k_2 + k_3\right) I$$

$$\frac{dR}{dt} = \alpha_3 I - \alpha_2 R - k_2 R$$

To find the equilibrium point, we set the right hand side of the system above to zero. When $\frac{dI}{dt} = 0$, we obtain $S^* = \frac{\alpha_3 + k_2 + k_3}{\alpha_1} = \frac{S_0}{R_0}$

When $\frac{dR}{dt} = 0$,

$$\alpha_3 I - \alpha_2 R - k_2 R = 0$$

$$\left(\alpha_2 + k_2\right)\left(N - S - I\right) = \alpha_3 I$$

$$\left(\alpha_2 + k_2\right) N - \left(\alpha_2 + k_2\right) S - \left(\alpha_2 + k_2\right) I = \alpha_3 I$$

$$\left(\alpha_2 + k_2\right) N - \left(\alpha_2 + k_2\right)\left(\frac{\alpha_3 + k_2 + k_3}{\alpha_1}\right) = \left(\alpha_3 + \alpha_2 + k_2\right) I$$

$$I = \frac{\alpha_1\left(\alpha_2 + k_2\right) N - \left(\alpha_2 + k_2\right)\left(\alpha_3 + k_2 + k_3\right)}{\alpha_1\left(\alpha_3 + \alpha_2 + k_2\right)}$$

$$= \frac{\left(\alpha_2 + k_2\right)\left(\alpha_1 N - \left(\alpha_3 + k_2 + k_3\right)\right)}{\alpha_1\left(\alpha_3 + \alpha_2 + k_2\right)}$$

$$= \frac{\left(\alpha_2 + k_2\right)}{\alpha_1\left(\alpha_3 + \alpha_2 + k_2\right)}\left(\alpha_1 N - \left(\alpha_3 + k_2 + k_3\right)\right)$$

$$= \frac{\left(\alpha_2 + k_2\right)}{\alpha_1\left(\alpha_3 + \alpha_2 + k_2\right)}\left(\alpha_3 + k_2 + k_3\right)\left(\frac{\alpha_1 N}{\alpha_3 + k_2 + k_3} - 1\right)$$

$$= \frac{\left(\alpha_2 + k_2\right)}{\alpha_1\left(\alpha_3 + \alpha_2 + k_2\right)}\left(\alpha_3 + k_2 + k_3\right)\left(\frac{\alpha_1 S_0}{\alpha_3 + k_2 + k_3} - 1\right)$$

$$= \frac{\left(\alpha_2 + k_2\right)}{\alpha_1\left(\alpha_3 + \alpha_2 + k_2\right)}\left(\alpha_3 + k_2 + k_3\right)\left(R_0 - 1\right)$$

$$\therefore I^* = \frac{\left(\alpha_3 + k_2\right)}{\alpha_1\left(\alpha_3 + \alpha_2 + k_2\right)}\left(\alpha_3 + k_2 + k_3\right)\left(R_0 - 1\right)$$

Hence, the endemic equilibrium point, $E_e = \left(S^*, I^*, R^*\right)$, is as follow:

$$E_e = \left(\frac{S_0}{R_0}, \frac{\left(\alpha_3 + k_2\right)}{\alpha_1\left(\alpha_3 + \alpha_2 + k_2\right)}\left(\alpha_3 + k_2 + k_3\right)\left(R_0 - 1\right), S_0 - \frac{S_0}{R_0} - \frac{\left(\alpha_3 + k_2\right)}{\alpha_1\left(\alpha_3 + \alpha_2 + k_2\right)}\left(\alpha_3 + k_2 + k_3\right)\left(R_0 - 1\right)\right) \quad (3.17)$$

The disease is to prevail in the population when $I^* > 0$. Thus, when $R_0 > 1$, the endemic equilibrium point exist meaning that the disease remains in the population and an outbreak occurs. When $R_0 = 1$, it is given us the disease-free equilibrium point. Also, if $R_0 = 1$, it also means that there will approximately the same number of infected cases all the time (Heffernan et al., 2005).

Lemma 3.3.5 The endemic steady state is globally asymptotically stable (Keeling & Rohani, 2008).

Proof

As mentioned in Section 2.3.1.3, Lyapunov function, $V\left(x\right)$, can be used to prove the asymptotically stability of the endemic steady state (Abramson, 2001).

$$V(S,I) = S - S^* \ln S + I - I^* \ln I$$

$$\frac{dV}{dt} = \frac{\partial V}{\partial S}\left(\frac{\partial S}{\partial t}\right) + \frac{\partial V}{\partial I}\left(\frac{\partial I}{\partial t}\right)$$

$$= \left(1 - \frac{S^*}{S}\right)\left(k_1 N - \alpha_1 SI - k_1 S + \alpha_2 R\right) + \left(1 - \frac{I^*}{I}\right)\left(\alpha_1 SI - \alpha_3 I + \left(k_2 + k_3\right)I\right)$$

$$= \left(S - S^*\right)\left(\frac{k_1 N}{S} - \alpha_1 I - k_2 + \frac{\alpha_2 R}{S}\right) + \left(I - I^*\right)\left(\alpha_1 S - \alpha_3 + \left(k_2 + k_3\right)\right)$$

$$= \left(S - S^*\right)\left(\frac{k_1 N}{S} - \alpha_1 I - k_2 + \left(\frac{k_2 S^* + \alpha_1 S^* I^* - k_1 N}{S}\right)\right)$$

For $\frac{k_2 S^* + \alpha_1 S^* I^* - k_1 N}{S}$, let $S^* = S$, $I^* = I$

Thus, $\frac{k_2 S^* + \alpha_1 S^* I^* - k_1 N}{S^*} = k_2 + \alpha_1 I - \frac{k_1 N}{S^*}$

Hence,

$$\frac{dV}{dt} = \left(S - S^*\right)\left(\frac{k_1 N}{S} - \alpha_1 I - k_2 + \left(k_2 + \alpha_1 I - \frac{k_1 N}{S^*}\right)\right)$$

$$= \left(S - S^*\right)\left(\frac{k_1 N}{S} - \frac{k_1 N}{S^*}\right)$$

$$= -\frac{k_1 N}{SS^*}\left(S - S^*\right)^2 \qquad (3.18)$$

With this, the system is said to be asymptotically stable in the sense of Lyapunov.

3.4 Numerical results for basic SIR model

The governing equations are nonlinear and cannot be solved analytically. The system is to be solved numerically. The method used is based on fourth-order Runge Kutta method in MatLab program. The ordinary differential equations in (3.1 – 3.3) are in the form of

$$\begin{aligned}
\frac{dy_1}{dt} &= f\left(y_1, y_2, \ldots, y_n, t\right), \\
\frac{dy_2}{dt} &= f\left(y_1, y_2, \ldots, y_n, t\right), \\
&\vdots \\
\frac{dy_n}{dt} &= f\left(y_1, y_2, \ldots, y_n, t\right).
\end{aligned}$$

Here, $y_1 = S, y_2 = I$ and $y_3 = R$. A column vector y with t is a scalar is applied and to be solved from $\frac{dy(t)}{dt} = y' = f\left(y(t), t\right)$, with initial condition $y(t_0) = y_0$, at initial time, t_0. The governing equations (3.1 – 3.3) are written into a column vector system, after running the program, the system will return us a column vector $f\left(y(t), t\right)$. The time span for simulation is needed so that the interval of the integration can allow the problem to be solved by running the program. The time span used for our simulation is $t_0 = 0$ (initial value) to $t = 50$ (terminal value). The basic SIR model provides a basic framework will be used as benchmark for the investigation of the HFMD spread (Bhattacharya et al., 2015). Parameter and initial values are taken from (Tiing & Labadin, 2008) as benchmark to simulate the model as their study area is same with us. The model is used to compare the HFMD clinical data, year 2006.

Initial conditions are $S = 10000$, $I = 4$ and $R = 0$ where S is susceptible, I is infected individuals and R is fully recovered individual. Parameter values are

$k_1 = 0.0002923,\ \ k_2 = 0.0001077,\ \ k_3 = 0.00001731,\ \ \alpha_1 = 0.00015,\ \ \ \alpha_2 = 0.07$ and $\alpha_3 = 0.8325$ where the unit of time is per week. k_1 is the natural birth rate, k_2 is the natural death rate, k_3 is the death rate caused by the disease, α_1 is the transmission coefficient, α_2 is the rate of losing immunity and α_3 is the fully recovery rate.

The initial condition for susceptible, *S*, was taken based on estimation, α_2, the period of losing immunity predicted is 100 days and α_3, the prediction for the infected individual to reach recovered stage was 8.5 days. α_2 and α_3 are taken from the best simulation results after so many times of the simulation conducted. Whereas, *I*, the initial condition for infectious individual was taken based on the clinical data from Sarawak Health Department. On the other hand, k_1, k_2 and k_3 were calculated based on the crude birth rate, crude death rate and fatality rate taken from Department of Statistic Malaysia. The SIR model simulation result is shown below in the Figure 3.6.

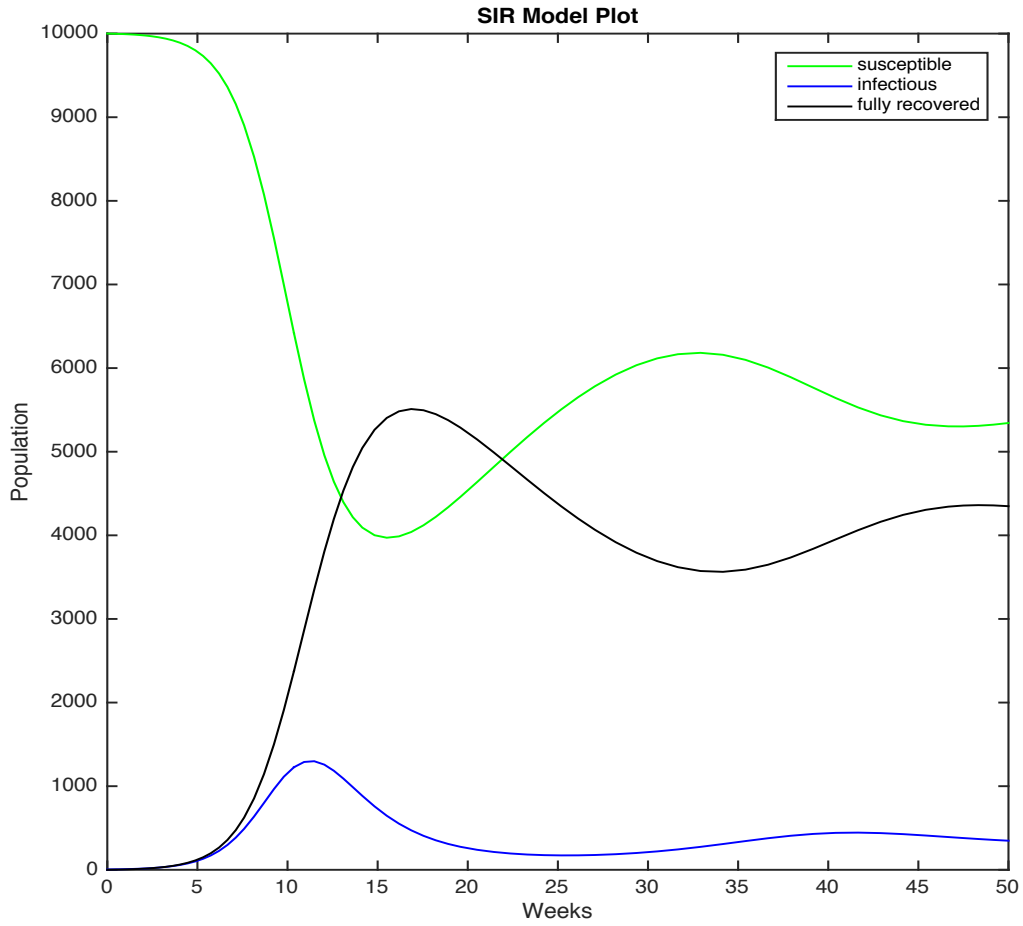

Figure 3.6: The predicted cases of the basic SIR model for susceptible, infectious and fully recovered over the time.

From Figure 3.6, the graphs are governed by the graphs of susceptible, predicted infectious cases and fully recovered individual. As we can see when the infectious cases increasing rapidly, the number of susceptible drops sharply. And, when the infectious cases start to drop, the recovered individuals increase a lot and the number of susceptible is started to rebound.

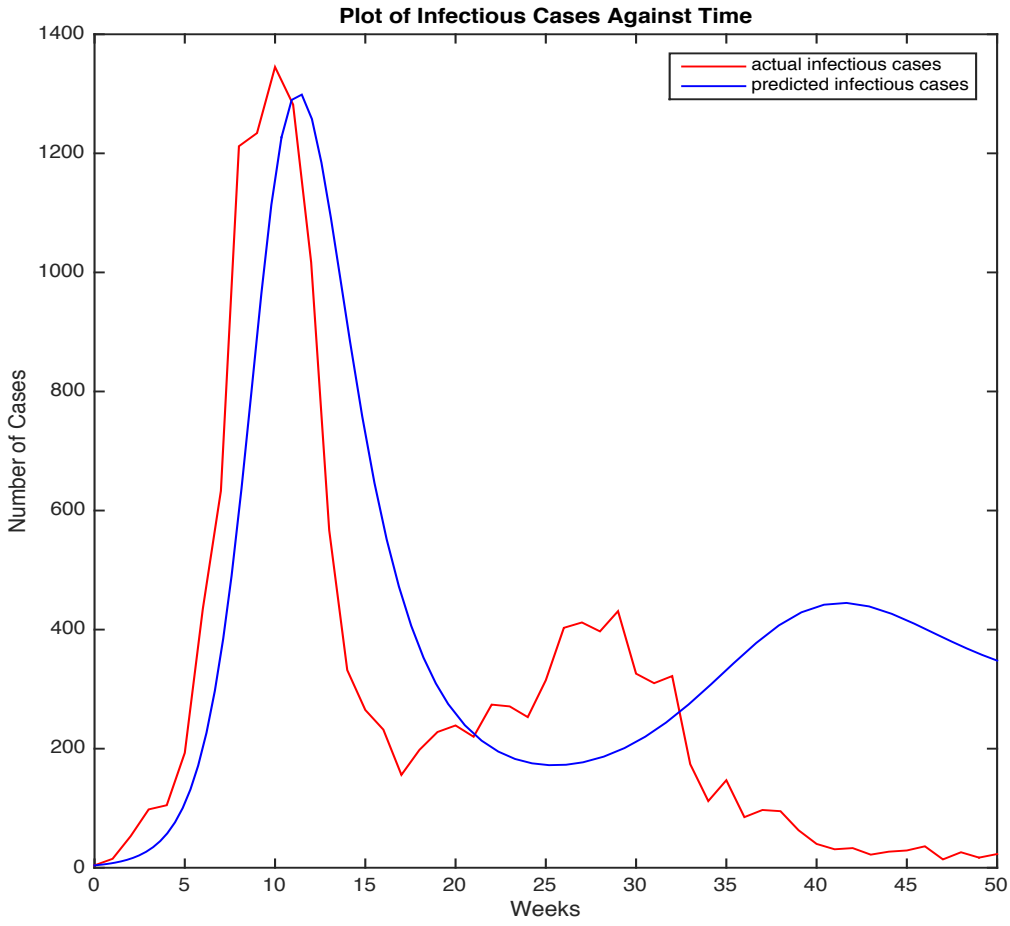

Figure 3.7: Comparison of the actual infectious cases and predicted infectious cases.

Figure 3.7 is the plot of comparison between the predicted infectious cases and actual infectious cases. By using visual inspection, the fitting between predicted infectious cases and actual infectious cases is not well matched. The predicted curve shifts slower and reach the peak later compare to actual data shows slower spreading. We then try to change the parameters to do other sensitivity tests.

Table 3.1: Parameters values of SIR model for sensitivity analysis.

Parame-ters Values	**Trial tests for sensitivity analysis**		
	First trial	**Second trial**	**Third trial**
k_1	2.923×10^{-4}	2.923×10^{-4}	2.923×10^{-4}
k_2	1.077×10^{-4}	1.077×10^{-4}	1.077×10^{-4}
k_3	1.731×10^{-5}	1.731×10^{-5}	1.731×10^{-5}
α_1	1.5×10^{-4}	1.771×10^{-4}	1.18×10^{-4}
α_2	0.07	0.07	0.07
α_3	0.8325	0.8325	0.8325
I	4	4	4
N	10,000	9,000	12,000
R	0	0	0
S	10,000	9,000	12,000

Table 3.1 above shows the parameter values of SIR model for the other two sensitivity tests, which are second trial and third trial besides the first trial. The sensitivity analysis results are used to compare with actual HFMD cases in year 2006. The following are the numerical results for the sensitivity analysis.

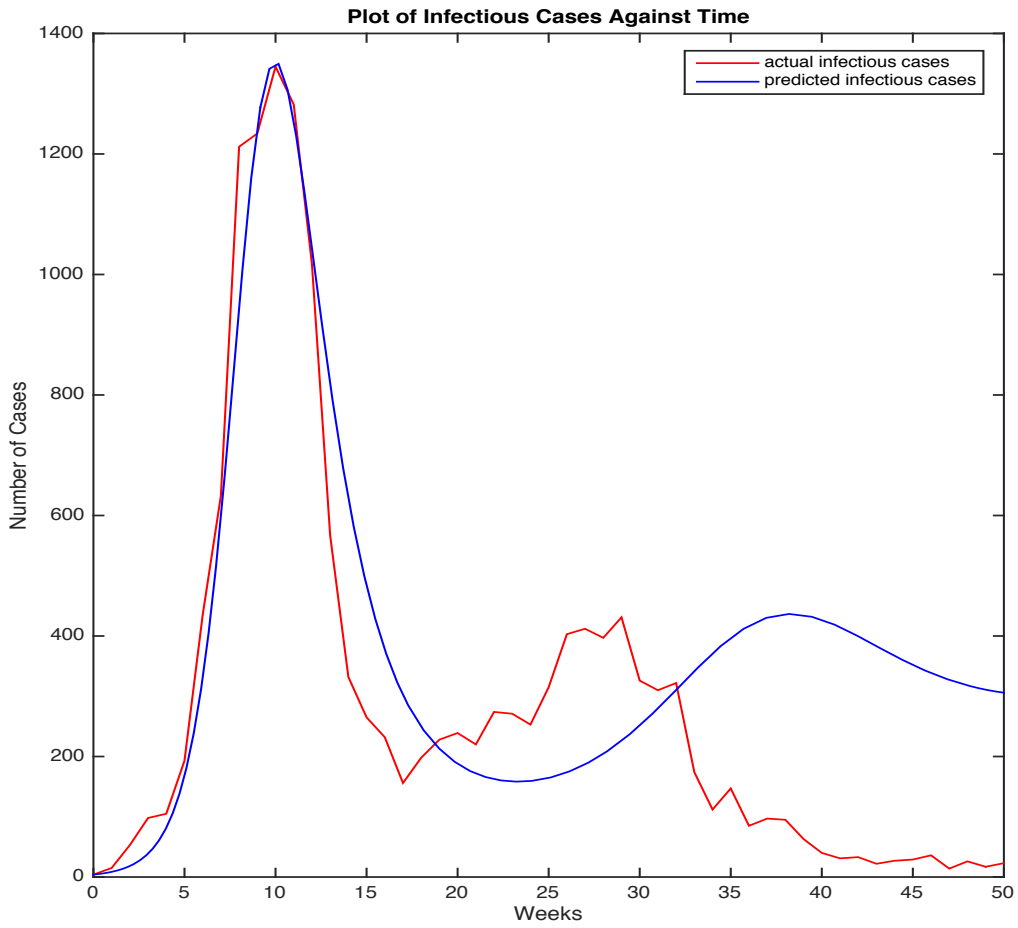

Figure 3.8: Comparison of the actual infectious cases and predicted infectious cases, second trial.

Figure 3.8 shows the comparison between the actual infectious cases and predicted infectious cases. Notice that, the graphs show a better match by visual inspection compare to Figure 3.7 during the first wave when *S* is changed to 9000. The predicted infectious can reach the peak almost same as the actual data. Next, we will change the parameters again for another sensitivity analysis. Figure 3.9 below shows the numerical results for third trial test.

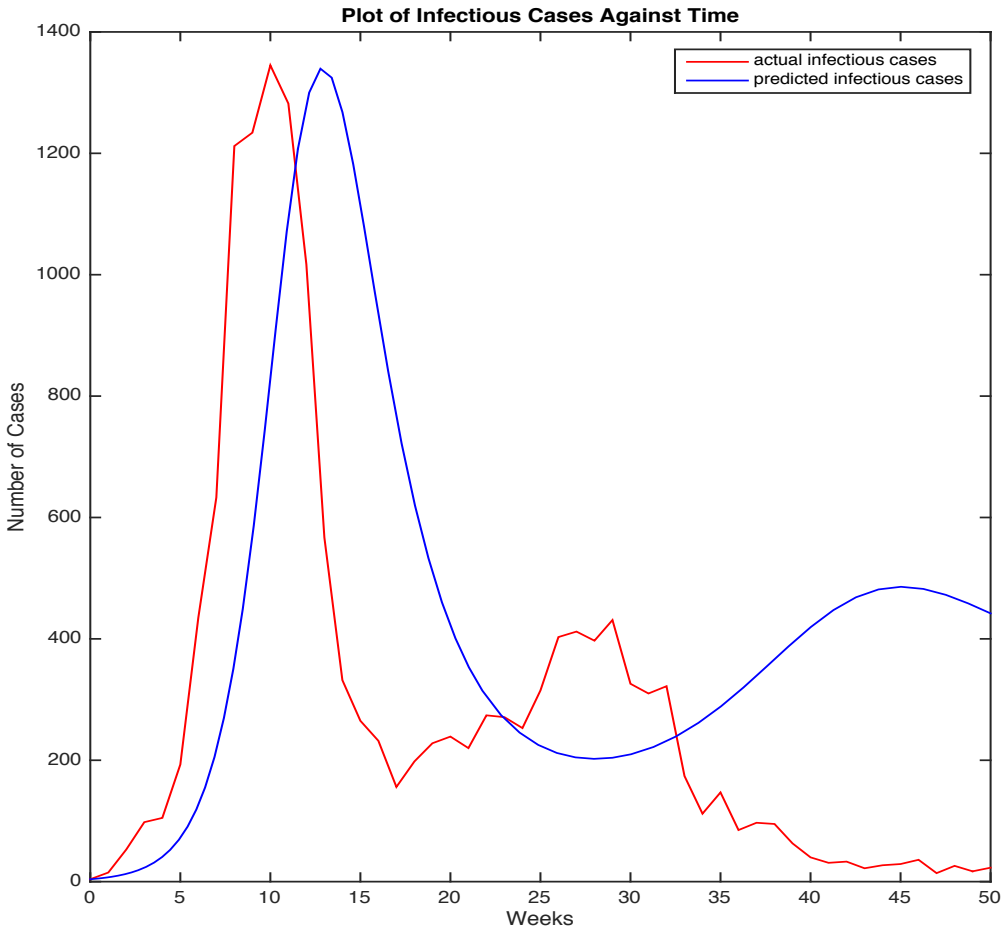

Figure 3.9: Comparison of the actual infectious cases and predicted infectious cases, third trial.

From Figure 3.9, the predicted infectious cases dispersed more when *S* is put as 12000. The predicted infectious cases show a slower spreading and reach the peak a bit later than the actual cases. Next, we will use RMSE in MatLab program to calculate the prediction error by comparing the actual infectious cases and the predicted infectious cases of sensitivity analysis. As mentioned in Section 2.3.5, the smaller the RMSE, the better the prediction, which means, the predicted results are closer to the actual results and parameters used are more suitable for the prediction. By visual inspection, Figure 3.8

shows a better fit during the first wave, by estimation, we then choose the first thirteen weeks of the results to have the prediction error test for all the trial tests. The results data is shown in Table 3.2.

Table 3.2: Results of the actual infectious cases in 2006, predicted infectious cases of sensitivity analysis and RMSE values by using SIR model for first until third trial.

Weeks	**Actual infectious cases**	**Predicted infectious cases of sensitivity analysis**		
		First trial	**Second trial**	**Third trial**
0	4	4	4	4
1	15	11	14	10
2	53	21	28	15
3	98	45	61	24
4	105	58	1065	52
5	193	132	180	91
6	435	227	404	155
7	633	490	667	270
8	1212	800	1160	449
9	1234	1114	1277	586
10	1345	1290	1350	911
11	1282	1299	1230	1208
12	1017	1258	1027	1300
13	567	988	679	1325
RMSE values		194.4	44.65	371.1

Table 3.2 shows the actual data for HFMD cases in 2006, predicted data and RMSE values for sensitivity analysis of SIR model from first trial until third trial. From table 3.2, the lowest prediction error happens at the second trial sensitivity analysis test shows that the parameters values from second trial are suitable to use for further analytical analysis. After this, we will further analyze the result by using threshold value and basic reproductive number, R_0 based on the data that produces the least RMSE from which the data is second trial of the sensitivity analysis.

Threshold value is the maximum or minimum number of susceptible predicted which serves as a benchmark to have a complete review of the proportion of the population that creates the liability of disease spreading. As mentioned in Section 3.3.3, threshold value is $\frac{\alpha_3 + k_2 + k_3}{\alpha_1}$. Hence, by calculating, we get threshold value estimation as 4701. By graph, Figure 3.10 below shows the threshold value when S = 9000, the outbreak occurs when the threshold value is 4701. When the number of susceptible is above the minimum proportion of 4701, outbreak occurs, otherwise, no outbreak.

Whereas, R_0, is showing the average number of infectious cases infected by an infectious case during his or her entire infectious period. By using equation (3.19), R_0 is approximately 1.91.

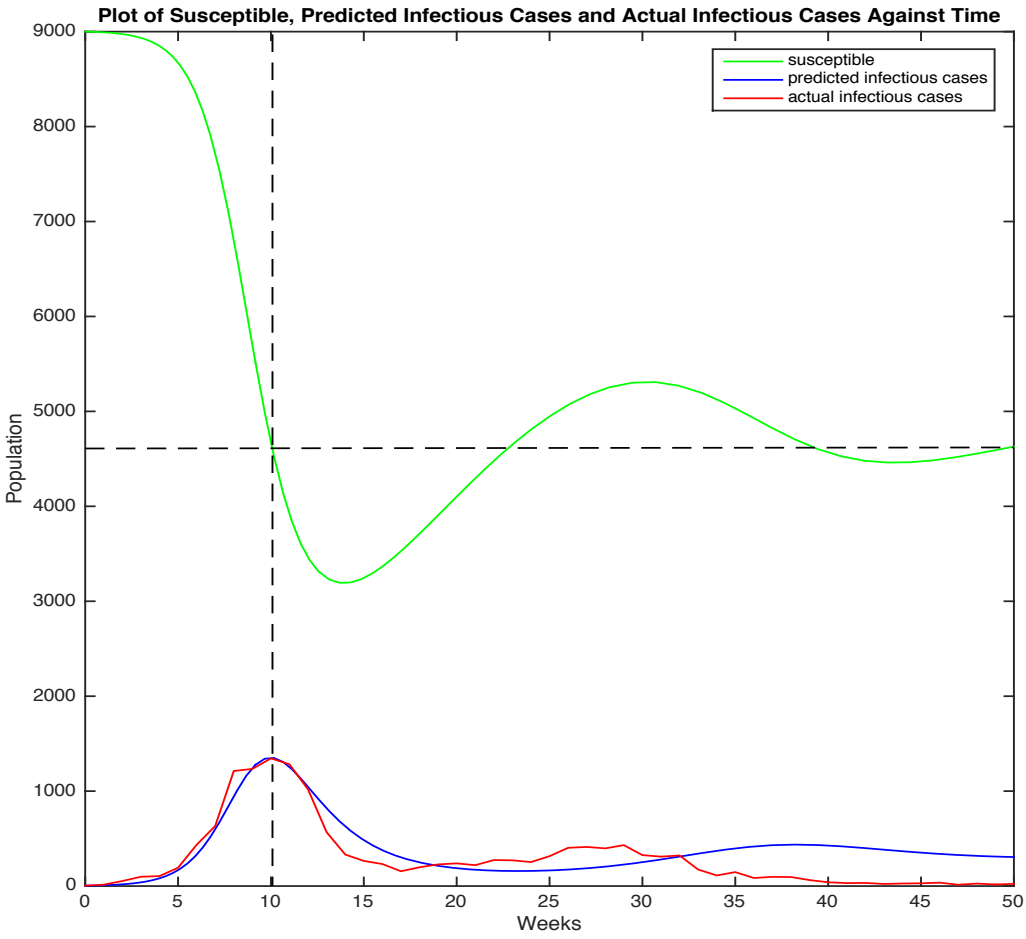

Figure 3.10: Susceptible, predicted infectious cases and actual infectious cases of second trial sensitivity analysis. Dashed line indicated threshold value.

3.5 Summary

From the basic SIR model, we can calculate the threshold value by using the parameter values. It shows that the predicted threshold value is 4701, which means when there is the cohort of the susceptible exceeds this value, then the outbreak will occur. This can be seen at the Figure 3.10. On the other hand, R_0 is calculated. The R_0 is 1.91, indicating that the

disease invades the susceptible and outbreak occurs. An R_0 = 1.91, means that every infectious child would infect almost two children during the outbreak.

However, since the basic SIR model provides only a basic framework for the HFMD spreading investigation (Bhattacharya et al., 2015), and after so many study done on the biological factors as mentioned in Section 2.2, we decide to extend the basic SIR to SEIPR model.

The biological factors contribute to HFMD spreading are incubation period, infectious period and post-infectious virus shedding period (Han et al., 2010; Li et al., 2013; Mandal, 2017; Podin et al., 2006; Teng et al., 2013). Throughout the years, a lot of studies have mentioned incubation period and post-infectious virus shedding period together with the infectious period contribute to the disease transmission (Chadsuthi & Wichapeng, 2018; Phutthichayanon & Naowarat, 2015; Podin et al., 2006; Shi et al., 2018; Teng et al., 2013).

Thus, we cannot ignore some of the known biological factors while discussing the HFMD behaviors. With this, SEIPR model adds in the compartments of incubation period and post-infectious virus shedding period together with the infectious period compartment as infected compartments in order to provide complete biological factors to discuss the characteristic of HFMD. In next chapter, we will further discuss our new SEIPR model.

CHAPTER 4

FORMULATION AND ANALYSIS OF THE SEIPR MODEL

4.1 Introduction

As mentioned in Chapter 2, the concern towards the contact pattern in the population is highlighted, hence contributed to the formulation of a refined model, SEIPR model. In this chapter, schematics diagrams for SEIPR model are drawn to describe the characteristic of the HFMD. A system of nonlinear differential equations is formulated and SEIPR model is analyzed theoretically. Also, the equilibrium points, basic reproductive number and threshold value are discussed. Sensitivity analysis is done. Numerical results are obtained and lastly, the goodness of fit test is used to verify the results. Discussion and summary are made from the results obtained.

4.2 SEIPR model formulation

The behaviors of the infectious HFMD based on SEIPR mathematical model is studied, the following assumptions are made:

i) All newborns are not infected at birth.

ii) The susceptible group is made up of children under age of nine.

iii) The disease is transmitted through the infected patient.

iv) Individuals are mixed randomly within the population.

v) The infectious occur randomly based on the contact and transmission rate between the susceptible and the infected individuals (incubation period).

vi) The infectious occur randomly based on the contact and transmission rate between the susceptible and the infected individuals (infectious period).

vii) The infectious occur randomly based on the contact and transmission rate between the susceptible and the infected individuals (post-infectious period).

viii) All the parameters values and initial values are constants.

ix) There is no intervention to curb the spreading disease.

x) Patients who have recovered have a temporary immunity before they return to the susceptible.

xi) The transmission only occurs when susceptible meets with the infected patients.

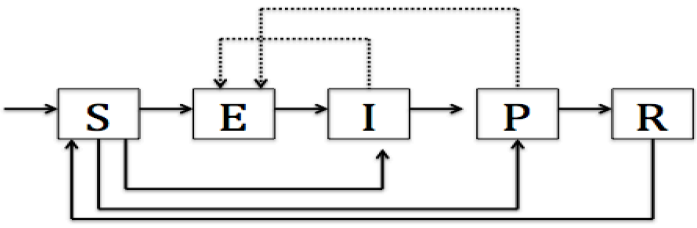

Figure 4.1: A schematic diagram of SEIPR basic model (Susceptible-Incubation period-Infectious-Post infectious virus shedding-Fully recovered).

The compartmental SEIPR model is shown in Figure 4.1. The model consists of five compartments that are susceptible (S), incubation period (E), infectious period (I), post-infectious virus shedding period (P) and fully recovered (R). The transitions are $S \to I$, $S \to P$, $I \dashrightarrow E$, $P \dashrightarrow E$ and $S \to E \to I \to P \to R$. The movement from S to E, S to I, and S to P are the disease transmission progression. The infection that is transmitted from

the incubation period patients resulted the movement from *S* to *E*. The movement from *S* to *E* together with the movements from *I* to E and P to E both shown as dotted arrow lines in Figure 4.1 are the infected patients having the incubation period and at the asymptomatic stage. These infected patients are the susceptible (*S*) that are initially gained the infection from incubation (*E*), infectious (*I*) and post-infectious virus shedding or is known as clinically recovered (*P*) patients. Once infected, these infected asymptomatic patients will move to the incubation compartment. The movement from E to I shows that the patients have shown the HFMD symptoms. And, from I to P, the patients have the symptoms subsided and carrying the post-infectious virus shedding. Lastly, the patients has fought off the infection and moving from post-infectious compartment to the fully recovered compartment. The duration progress from being infected until fully recovered is taken into account. The scenario mentioned above has been used to study the biological behaviors of the HFMD comprehensively. Next, we will discuss Figure 4.2, the susceptible compartment.

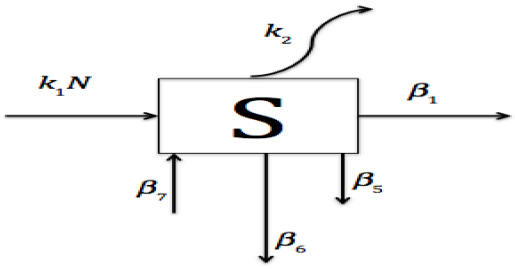

Figure 4.2: Susceptible compartmental diagram, *S*.

In Figure 4.2, susceptible compartment is increased through the nature birth rate, k_1, that dependents on total susceptible population, *N* and decreased through natural death at the rate of k_2. Meanwhile, the recovered individuals who have lost their immunity

return to the susceptible group at the rate of β_7. When susceptible meets with the infected individual during incubation period, infected individual during infectious period and infected individual during post-infectious period (clinically recovered individual), transmission can occur and newly infected individual has produced and this leads to these newly infected individuals depart from susceptible compartment with the transmission coefficient of β_1, β_5 and β_6. Once an infected individual departs from susceptible compartment, the patient will enter the incubation period compartment where the individual is at asymptomatic stage which is shown in Figure 4.3.

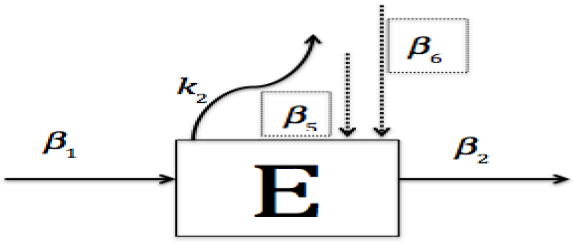

Figure 4.3: Incubation period compartmental diagram, E.

As shown in Figure 4.3, the increasing population is gained from the transmission rates of β_1, β_5 and β_6. β_1 is the transmission coefficient obtained from the exposed individual to susceptible, it is directly move from susceptible to incubation period group. β_5 is the transmission coefficient obtained from the infectious individual to susceptible. It is at first caused by the contact between the susceptible and the infectious individual, when the susceptible being infected and soon the infected individual will move to the incubation period group where the individual is at asymptomatic stage and capable to transmit the

disease to other susceptible when there is close contact. Meanwhile, β_6 is the transmission coefficient obtained from the close contact between clinically recovered individual and susceptible. Once being infected, the infected individual soon will move to incubation period compartment as symptoms have not yet developed but the infected individual as well can transmit the disease to other susceptible. At the same time, the decreasing population at this compartment can occur due to the natural death with rate of k_2. After a period of time, these infected individuals will depart from the incubation period compartment after time W, thus, the rate at which an asymptomatic patient develops the symptoms is $\beta_2 = \frac{1}{W}$ and depart to infectious compartment shown in Figure 4.4.

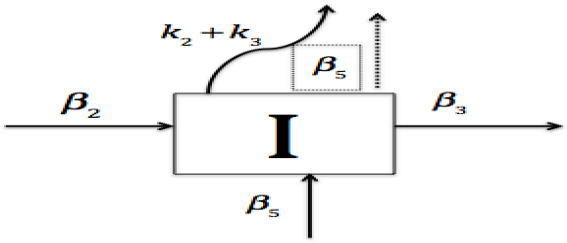

Figure 4.4: Infectious compartmental diagram, I.

Figure 4.4 shows the infectious individuals have shown the disease symptoms. At this stage, it is a highly contagious period and the infectious individual is easily to transmit the disease to the susceptible when there is close contact. Once the susceptible being infected, the infected individual will soon move out from the infectious compartment and enter the incubation period group. This can be seen from Figure 4.4, the move in rate of β_5

shown with solid arrow line and also the move out rate of β_5 shown with dotted arrow line. At the meantime, the infectious compartment has the population decreased due to natural death, with the rate of k_2 and death which is caused by the disease, with the rate of k_3. On the other hand, for the infectious symptomatic individuals who stay in this compartment, after time Q, when the symptoms subside, they will move out and enter the clinically recovered compartment or we called it post-infectious virus shedding compartment shown in Figure 4.5. Hence, the rate at which an infectious individual reach the clinically recovered stage is $\beta_3 = \frac{1}{Q}$.

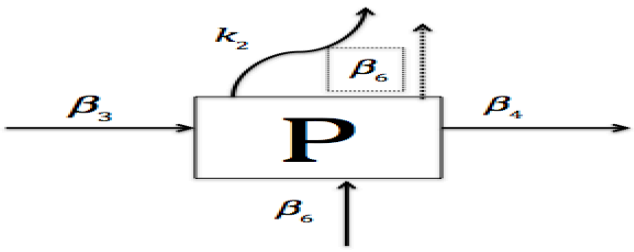

Figure 4.5: Clinically recovered compartmental diagram, P.

From Figure 4.5, after time Q, the infectious asymptomatic individuals from the infectious compartment will enter the clinically recovered compartment. Here, the infectious individuals have the disease symptoms subsided. However, the clinically recovered individuals still carry the post-infectious virus shedding and able to transmit the disease when there is close contact with the susceptible. Once being infected, soon, the newly infected individuals will move out and enter the incubation compartment. This is shown by solid arrow line, moving in with rate of β_6 and dotted arrow line, moving out

with the rate β_6. After time Z when the clinically recovered individual has fully recovered, they will depart from this compartment with the rate of $\beta_4 = \frac{1}{Z}$ and enter fully recovered compartment, shown in Figure 4.6. Also, the clinically recovered compartment has the population decreased due to natural death, with the rate of k_2.

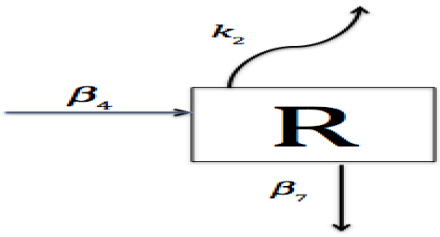

Figure 4.6: Fully recovered compartmental diagram, R.

Clinically recovered individuals will reach fully recovered stage when they are not capable to transmit the disease. In Figure 4.6, after time Z, the infected patients are not carrying the post-infectious virus shedding anymore and they will enter to the fully recovered compartment. An individual will attain a short immunity after fully recover from the disease. Once the immunity is lost after time G, the individual will return to the susceptible compartment and capable to being infected again. The rate at which the individual loses its immunity is $\beta_7 = \frac{1}{G}$. At the meantime, the fully recovered compartment has the population decreased due to natural death, with the rate of k_2.

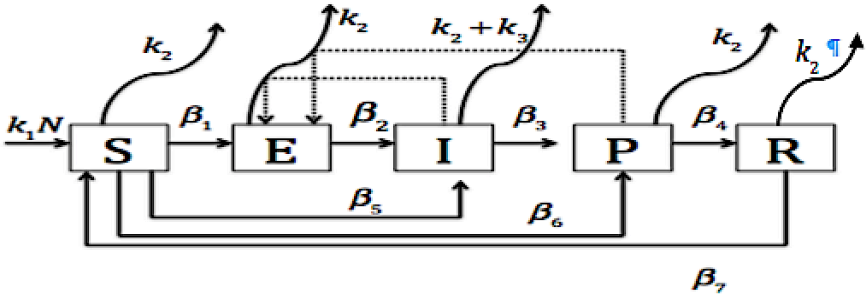

Figure 4.7: The combined compartmental diagram of SEIPR model.

Figure 4.7 shows an overview of the compartmental diagram of SEIPR model. The susceptible compartment is increased through the nature birth rate, k_1 multiply with total susceptible population, N. The transitions $S \to E$, $S \to I$ and $S \to P$ are disease transmissions progression. The transition $S \to E$ is the transmission where susceptible get infected when meets with the asymptomatic infected patient (E). Let β_ς is $b \times c$, where b is the average number of contacts any person in the population and c is the transmission probability. The multiplication of β_ς and $\frac{E}{N}$, where $\frac{E}{N}$ are the infected asymptomatic individuals, force of infection is occurred as per capita rate at which susceptible individual contact with the infected individual. To obtain the actual number of infected individual, we have $\beta_1 \times E \times S$, $\beta_1 = \frac{\beta_\varsigma}{N}$.

For next case, we will look at the transition $S \to I$. Let β_ω is the $\Lambda \times \kappa$, where Λ is the average number of contacts any person in the population and κ is the transmission probability. When we multiply β_ω with $\frac{I}{N}$, where $\frac{I}{N}$ are the infectious individuals, force of infection is defined as per capita rate at which susceptible individual contacts the

infectious individual. Finally, to obtain the actual number of infected individual causes from infectious compartment, we will have $\beta_5 \times I \times S$, $\beta_5 = \frac{\beta_\omega}{N}$.

At another scenario where susceptible meets with the post-infectious individual (*P*) or clinically recovered individual, the transition $S \to P$ occurs. The disease transmission happens as well when there is close contact via droplets or fomites that are carrying the infectious virus. Post-infectious individual has the symptoms subsided, but the virus may continue to shed for several weeks after the symptoms gone. Hence, the scenario leads to another force of infection. Let β_ε is $m \times n$, m is the average number of contacts any person in the population and n is the transmission probability. We multiply the β_ε and $\frac{P}{N}$, where $\frac{P}{N}$ are the post-infectious individual who is still carrying the post-infectious virus shedding, force of infection happens as per capita rate at which susceptible individual contacts with the post-infectious virus shedding carrier. To get the actual infected individual, we have $\beta_6 \times P \times S$, $\beta_6 = \frac{\beta_\varepsilon}{N}$.

After time *Z* as mentioned above, the clinically recovered individual will move to fully recovered compartment, $P \to R$, with rate of β_4. And after time G, the fully recovered individual lost the immunity and move to susceptible compartment again with rate of β_7. Besides, the compartments *S*, *E*, *I*, *P* and *R* have the population decreased with natural death at the rate of k_2 and at the same time, compartment *I* has population decreased through death which is caused by the disease with the rate of k_3. The system of differential equations for SEIPR model is formed and discussed next.

The differential equations are made as follow:

$$\frac{dS}{dt} = k_1 N + \beta_7 R - \beta_1 SE - \beta_5 SI - \beta_6 SP - k_2 S \quad (4.1)$$

$$\frac{dE}{dt} = \beta_1 SE + \beta_5 SI + \beta_6 SP - \beta_2 E - k_2 E \quad (4.2)$$

$$\frac{dI}{dt} = \beta_2 E - \beta_3 I - \left(k_2 + k_3\right) I \quad (4.3)$$

$$\frac{dP}{dt} = \beta_3 I - \beta_4 P - k_2 P \quad (4.4)$$

$$\frac{dR}{dt} = \beta_4 P - k_2 R - \beta_7 R \quad (4.5)$$

The total population is $N = S + E + I + P + R$, so that,

$$\frac{dN}{dt} = \frac{dS}{dt} + \frac{dE}{dt} + \frac{dI}{dt} + \frac{dP}{dt} + \frac{dR}{dt} \quad (4.6)$$

hence, we obtain,

$$\frac{dN}{dt} = k_1 N - k_2 S - k_2 E - k_2 I - k_3 I - k_2 P - k_2 R$$

$$\frac{dN}{dt} = k_1 N - k_3 I - k_2 \left(S + E + I + P + R\right)$$

$$\frac{dN}{dt} = k_1 N - k_3 I - k_2 N^*, \ (N^* = S + E + I + P + R) \quad (4.7)$$

N^* represents the changing of total population over time, whereas, N is the total population at initial time.

4.3 Theoretical analysis of the SEIPR model

Theoretical analysis of SEIPR model is made based on the differential equations (4.2 – 4.5). The SEIPR model which describes the population should be positive all the time. From equations (4.2 – 4.5), the domain of the solution is as follow:

$$\Omega = \left\{ \left(E, I, P, R \right) \in R_{+}^{4} \middle| E + I + P + R \le N, N > 0 \right\} \quad (4.8)$$

Hence, the steady state equilibrium point can be found. We set the equations (4.2 – 4.5 and 4.7) to zero (Hethcote, 2000).

$$\frac{dE}{dt} + \frac{dI}{dt} + \frac{dP}{dt} + \frac{dR}{dt} + \frac{dN}{dt} = 0 \quad (4.9)$$

To solve equation (4.9), we denote the equilibrium point as following

$$E_e = \left(E^*, I^*, P^*, R^*, N^* \right) \quad (4.10)$$

where

$$E^* = \frac{\left(\beta_5 I^* + \beta_6 P^* \right) S^*}{\beta_2 + k_2 - \beta_1 S^*}$$

$$I^* = \frac{\beta_2 E^*}{\beta_3 + k_2 + k_3}$$

$$P^* = \frac{\beta_3 I^*}{\beta_4 + k_2}$$

$$R^* = \frac{\beta_4 P^*}{k_2 + \beta_7}$$

$$N^* = \frac{k_1 N - k_3 I^*}{k_2} \quad (4.11)$$

When we set $E^*, I^*, P^* = 0$ we can get disease-free equilibrium point, $E_0 = \left(E^*, I^*, P^*, R^*, N^*\right)$ by solving the equations (4.9 – 4.11), we obtain the following:

$$E^* = 0,\ I^* = 0,\ P^* = 0,\ R^* = 0 \text{ and } N^* = \frac{k_1 N}{k_2} \qquad (4.12)$$

Hence,

$$E_0 = \left(0,0,0,0,\frac{k_1 N}{k_2}\right) \qquad (4.13)$$

4.3.1 Disease-free equilibrium point

As mentioned in Section 3.3.1, the disease-free equilibrium point, E_0, is a steady state where the infectious compartment is zero. This means there is no existent of HFMD in the population and the number of the population remains same.

Proof

From the equation (4.2), when $\frac{dI}{dt} = 0$,

$$\beta_2 E = \left(\beta_5 + k_2 + k_3\right) I$$

$$I = 0 \Leftrightarrow E = 0$$

From the equation (4.3), when $\frac{dP}{dt}=0$,

$$\left(\beta_4+k_2\right)P=\beta_3 I$$

$$I=0\Leftrightarrow P=0$$

From the equation (4.4), when $\frac{dR}{dt}=0$,

$$\left(k_2+\beta_7\right)R=\beta_4 P$$

$$P=0\Leftrightarrow R=0$$

Here, we can see that the infectious compartment will determine the existence of the HFMD. Next, we will discuss the basic reproductive number, R_0, that helps to indicate the prevalence of the disease.

4.3.2 Basic reproductive number for SEIPR model

As mentioned in Section 2.3.2, we follow the next generation model to obtain the R_0 (Heffernan et al., 2005).

Let function F_i represents new infections and cannot be negative. From equations (4.1–4.5), we obtain

$$F_i=\begin{pmatrix}\beta_1 SE+\beta_5 SI+\beta_6 SP\\0\\0\end{pmatrix} \qquad (4.14)$$

Let V_i^- is the rate of transfer of individuals out of the i^{th} compartment.

$$V_i^- = \begin{pmatrix} k_2 E + \beta_2 E \\ \beta_3 I + \left(k_2 + k_3\right) I \\ \beta_4 P + k_2 P \end{pmatrix} \tag{4.15}$$

Let V_i^+ is the rate of transfer of individuals into the i^{th} compartment.

$$V_i^+ = \begin{pmatrix} 0 \\ \beta_2 E \\ \beta_3 I \end{pmatrix} \tag{4.16}$$

$$V_i = V_i^- - V_i^+$$

$$V_i = \begin{pmatrix} k_2 E + \beta_2 E \\ \beta_3 I + \left(k_2 + k_3\right) I - \beta_2 E \\ \beta_4 P + k_2 P - \beta_3 I \end{pmatrix} \tag{4.17}$$

$$F = \begin{pmatrix} \frac{\partial F_1}{\partial E_1} & \frac{\partial F_1}{\partial I_1} & \frac{\partial F_1}{\partial P_1} \\ \frac{\partial F_2}{\partial E_2} & \frac{\partial F_2}{\partial I_2} & \frac{\partial F_2}{\partial P_2} \\ \frac{\partial F_3}{\partial E_3} & \frac{\partial F_3}{\partial I_3} & \frac{\partial F_3}{\partial P_3} \end{pmatrix} = \begin{pmatrix} \beta_1 S & \beta_5 S & \beta_6 S \\ 0 & 0 & 0 \\ 0 & 0 & 0 \end{pmatrix} \tag{4.18}$$

$$V = \begin{pmatrix} \frac{\partial V_1}{\partial E_1} & \frac{\partial V_1}{\partial I_1} & \frac{\partial V_1}{\partial P_1} \\ \frac{\partial V_2}{\partial E_2} & \frac{\partial V_2}{\partial I_2} & \frac{\partial V_2}{\partial P_2} \\ \frac{\partial V_3}{\partial E_3} & \frac{\partial V_3}{\partial I_3} & \frac{\partial V_3}{\partial P_3} \end{pmatrix} = \begin{pmatrix} k_2 + \beta_2 & 0 & 0 \\ -\beta_2 & \beta_3 + k_2 + k_3 & 0 \\ 0 & -\beta_3 & k_2 + \beta_4 \end{pmatrix} \tag{4.19}$$

With this, we obtain R_0 by using the spectral radius of the matrix FV^{-1}. The operation gives the rate at which an infected individual produces new infections times the length of time an individual spends in single visit to the infectious compartments. Hence, to get R_0, first we need to get V^{-1}. We use inverse matrix formula to obtain V^{-1}.

$$V^{-1} = \frac{1}{|V|} adjoint\ V$$

Let

$$V = \begin{pmatrix} k_2+\beta_2 & 0 & 0 \\ -\beta_2 & \beta_3+k_2+k_3 & 0 \\ 0 & -\beta_3 & k_2+\beta_4 \end{pmatrix} = \begin{pmatrix} a & 0 & 0 \\ b & c & 0 \\ 0 & d & e \end{pmatrix} \qquad (4.20)$$

Where

$$a = k_2+\beta_2,$$
$$b = -\beta_2,$$
$$c = \beta_3+k_2+k_3,$$
$$d = -\beta_3,$$
$$e = k_2+\beta_4$$

$$|V| = ace$$

$$\text{cofactor of } V = \begin{pmatrix} ce & -be & bd \\ 0 & ae & -ad \\ 0 & 0 & ac \end{pmatrix} \qquad (4.21)$$

$$\text{adjoint of } V = \begin{pmatrix} ce & 0 & 0 \\ -be & ae & 0 \\ bd & -ad & ac \end{pmatrix} \qquad (4.22)$$

$$V^{-1}=\frac{1}{ace}\begin{pmatrix} ce & 0 & 0 \\ -be & ae & 0 \\ bd & -ad & ac \end{pmatrix}$$

$$=\begin{pmatrix} \frac{1}{a} & 0 & 0 \\ \frac{-b}{ac} & \frac{1}{c} & 0 \\ \frac{bd}{ace} & \frac{-d}{ce} & \frac{1}{e} \end{pmatrix} \qquad (4.23)$$

$$FV^{-1}=\begin{pmatrix} \beta_1 S & \beta_5 S & \beta_6 S \\ 0 & 0 & 0 \\ 0 & 0 & 0 \end{pmatrix}\begin{pmatrix} \frac{1}{a} & 0 & 0 \\ \frac{-b}{ac} & \frac{1}{c} & 0 \\ \frac{bd}{ace} & \frac{-d}{ce} & \frac{1}{e} \end{pmatrix}$$

$$=\begin{pmatrix} \frac{\beta_1 S}{a}+\frac{\beta_5 S(-b)}{ac}+\frac{\beta_6 S(bd)}{ace} & \frac{\beta_5 S}{c}+\frac{\beta_6 S(-d)}{ce} & \frac{\beta_6 S}{e} \\ 0 & 0 & 0 \\ 0 & 0 & 0 \end{pmatrix} \qquad (4.24)$$

Thus,

$$R_0=\frac{\beta_1 S}{a}+\frac{\beta_5 S(-b)}{ac}+\frac{\beta_6 S(bd)}{ace}$$

$$=\frac{\beta_1 S}{k_2+\beta_2}+\frac{\beta_5\beta_2 S}{(k_2+\beta_2)(\beta_3+k_2+k_3)}+\frac{\beta_6\beta_2\beta_3 S}{(k_2+\beta_2)(\beta_3+k_2+k_3)(k_2+\beta_4)} \qquad (4.25)$$

Disease-free equilibrium, I=0, thus $S=N=S_0$, thus

$$R_0=R_1+R_2+R_3$$

$$R_0 = \frac{\beta_1 S_0}{k_2 + \beta_2} + \frac{\beta_5 \beta_2 S_0}{\left(k_2 + \beta_2\right)\left(\beta_3 + k_2 + k_3\right)} + \frac{\beta_6 \beta_2 \beta_3 S_0}{\left(k_2 + \beta_2\right)\left(\beta_3 + k_2 + k_3\right)\left(k_2 + \beta_4\right)} \qquad (4.26)$$

Hence, we have obtained R_0 from our new SEIPR model. The R_0 consists of three terms. The first term, R_1, is representing the number of secondary infectious during the asymptomatic stage. The denominator of the first term is the inverse of the natural death rate plus the transition rate from asymptomatic to symptomatic cases, $k_2 + \beta_2$. The second term, R_2, gives contributions from the infectious compartments. The denominator of the second term is the multiplication of $k_2 + \beta_2$ with the inverse of the natural death rate plus death rate which is caused by disease plus the transition rate from symptomatic to clinically recovered cases, $\beta_3 + k_2 + k_3$. Lastly, the third term, R_3, is the number of secondary infectious during the clinically recovered stage. The denominator of the third term is the multiplication of $\left(k_2 + \beta_2\right)\left(\beta_3 + k_2 + k_3\right)$ with the inverse of the death rate plus the transition rate from the clinically recovered to the fully recovered cases, $k_2 + \beta_4$ (van den Driessche, 2017). In the next section, we will discuss the threshold value analysis.

4.3.3 Threshold value analysis of the SEIPR model

As mentioned in Section 2.3.3, if $\frac{dI}{dt} < 0$, then the infectious will die out. From equations (4.2 – 4.4),

We let $\frac{dE}{dt}=\frac{dI}{dt}=\frac{dP}{dt}=0$, and, we obtain the following:

$$\beta_1 SE+\beta_5 SI+\beta_6 SP-k_2 E-\beta_2 E=0$$

$$E^*=\frac{-\beta_5 S^* I^*-\beta_6 S^* P^*}{\beta_1 S^*-k_2-\beta_2} \quad (4.27)$$

$$\beta_3 I-\beta_4 P-k_2 P=0$$

$$P^*=\frac{\beta_3 I^*}{\beta_4+k_2} \quad (4.28)$$

$$\beta_2 E-\beta_3 I-\left(k_2+k_3\right)I=0 \quad (4.29)$$

Substitute equation (4.27) and equation (4.28) into equation (4.29),

$$\beta_2\left(\frac{-\beta_5 S^* I^*-\beta_6 S^* P^*}{\beta_1 S^*-k_2-\beta_2}\right)-\beta_3 I-\left(k_2+k_3\right)I=0$$

$$\beta_2\left(\frac{-\beta_5 S^* I^*-\beta_6 S^*\left(\frac{\beta_3 I^*}{\beta_4+k_2}\right)}{\beta_1 S^*-k_2-\beta_2}\right)-\beta_3 I-\left(k_2+k_3\right)I=0$$

$$\beta_2\left(\frac{-\beta_5 S^*-\beta_6 S^*\left(\frac{\beta_3}{\beta_4+k_2}\right)}{\beta_1 S^*-k_2-\beta_2}\right)=\beta_3+k_2+k_3$$

$$\beta_2 S^*\left(-\beta_5-\beta_6\left(\frac{\beta_3}{\beta_4+k_2}\right)\right)=\left(\beta_3+k_2+k_3\right)\left(\beta_1 S^*-k_2-\beta_2\right)$$

$$\beta_2 S^*\left(-\beta_5-\beta_6\left(\frac{\beta_3}{\beta_4+k_2}\right)\right)=\beta_3\beta_1 S^*-\beta_3 k_2-\beta_3\beta_2+k_2\beta_1 S^*-k_2^{\,2}-k_2\beta_2+k_3\beta_1 S^*-k_2 k_3-\beta_2 k_3$$

$$S^*\left(\beta_2\left(-\beta_5-\beta_6\left(\frac{\beta_3}{\beta_4+k_2}\right)\right)-\left(\beta_3\beta_1+k_2\beta_1+k_3\beta_1\right)\right)=-\beta_3k_2-\beta_3\beta_2-k_2^{\,2}-k_2\beta_2-k_2k_3-\beta_2k_3$$

$$S^*=\frac{-\beta_3k_2-\beta_3\beta_2-k_2^{\,2}-k_2\beta_2-k_2k_3-\beta_2k_3}{\beta_2\left(-\beta_5-\beta_6\left(\frac{\beta_3}{\beta_4+k_2}\right)\right)-\left(\beta_3\beta_1+k_2\beta_1+k_3\beta_1\right)}$$

$$S^*=\frac{-\beta_3k_2-\beta_3\beta_2-k_2^{\,2}-k_2\beta_2-k_2k_3-\beta_2k_3}{\beta_2\left(\frac{-\beta_5\left(\beta_4+k_2\right)-\beta_6\beta_3}{\beta_4+k_2}\right)-\left(\beta_3\beta_1+k_2\beta_1+k_3\beta_1\right)}$$

$$S^*=\frac{\left(-\beta_3k_2-\beta_3\beta_2-k_2^{\,2}-k_2\beta_2-k_2k_3-\beta_2k_3\right)\left(\beta_4+k_2\right)}{\beta_2\left(-\beta_5\left(\beta_4+k_2\right)-\beta_6\beta_3\right)-\left(\beta_3\beta_1+k_2\beta_1+k_3\beta_1\right)\left(\beta_4+k_2\right)} \qquad (4.30)$$

With this, we have found the threshold value, S^*.

If $S^*>\frac{\left(-\beta_3k_2-\beta_3\beta_2-k_2^{\,2}-k_2\beta_2-k_2k_3-\beta_2k_3\right)\left(\beta_4+k_2\right)}{\beta_2\left(-\beta_5\left(\beta_4+k_2\right)-\beta_6\beta_3\right)-\left(\beta_3\beta_1+k_2\beta_1+k_3\beta_1\right)\left(\beta_4+k_2\right)}$, then $\frac{dI}{dt}>0$, there must be an epidemic, otherwise no epidemic would occur.

4.3.4 Stability of disease-free equilibrium point of SEIPR model

As mentioned in Section 2.3.1.1, the stability of the equilibrium can be determined by using Jacobian matrix. The disease-free equilibrium is stable when all the eigenvalues are negative. At disease-free equilibrium point, $E=I=P=R=0$. Next, we will show the Jacobian matrix from equations (4.2 – 4.5).

Let $A=\left(A_{ij}\right)$ the Jacobian matrix, where A is matrix A with entry A_{ij} at the intersection of the i^{th} row and j^{th} column, having the order of $m\times n$.

$$A=\begin{pmatrix} \frac{\partial}{\partial E}\left(\frac{dE}{dt}\right) & \frac{\partial}{\partial I}\left(\frac{dE}{dt}\right) & \frac{\partial}{\partial P}\left(\frac{dE}{dt}\right) & \frac{\partial}{\partial R}\left(\frac{dE}{dt}\right) \\ \frac{\partial}{\partial E}\left(\frac{dI}{dt}\right) & \frac{\partial}{\partial I}\left(\frac{dI}{dt}\right) & \frac{\partial}{\partial P}\left(\frac{dI}{dt}\right) & \frac{\partial}{\partial R}\left(\frac{dI}{dt}\right) \\ \frac{\partial}{\partial E}\left(\frac{dP}{dt}\right) & \frac{\partial}{\partial I}\left(\frac{dP}{dt}\right) & \frac{\partial}{\partial P}\left(\frac{dP}{dt}\right) & \frac{\partial}{\partial R}\left(\frac{dP}{dt}\right) \\ \frac{\partial}{\partial E}\left(\frac{dQ}{dt}\right) & \frac{\partial}{\partial I}\left(\frac{dQ}{dt}\right) & \frac{\partial}{\partial P}\left(\frac{dQ}{dt}\right) & \frac{\partial}{\partial R}\left(\frac{dQ}{dt}\right) \end{pmatrix} \qquad (4.31)$$

$$A=\begin{pmatrix} A_{11} & A_{12} & A_{13} & A_{14} \\ A_{21} & A_{22} & A_{23} & A_{24} \\ A_{31} & A_{32} & A_{33} & A_{34} \\ A_{41} & A_{42} & A_{43} & A_{44} \end{pmatrix}$$

Solving $\frac{\partial}{\partial R}\left(\frac{dE}{dt}\right)$, $\frac{\partial}{\partial P}\left(\frac{dI}{dt}\right)$, $\frac{\partial}{\partial R}\left(\frac{dI}{dt}\right)$, $\frac{\partial}{\partial E}\left(\frac{dP}{dt}\right)$, $\frac{\partial}{\partial R}\left(\frac{dP}{dt}\right)$, $\frac{\partial}{\partial E}\left(\frac{dQ}{dt}\right)$ and $\frac{\partial}{\partial I}\left(\frac{dQ}{dt}\right)$ will lead to zero. Hence, we obtain,

$$A=\begin{pmatrix} A_{11} & A_{12} & A_{13} & 0 \\ A_{21} & A_{22} & 0 & 0 \\ 0 & A_{32} & A_{33} & 0 \\ 0 & 0 & A_{43} & A_{44} \end{pmatrix} \qquad (4.32)$$

where

$$A_{11}=\beta_1 S-\beta_2-k_2$$

$$A_{12}=\beta_5 S$$

$$A_{13}=\beta_6 S$$

$$A_{21}=\beta_2$$

$$A_{22} = -\beta_3 - \left(k_2 + k_3\right)$$

$$A_{32} = \beta_3$$

$$A_{33} = -\beta_4 - k_2$$

$$A_{43} = \beta_4$$

$$A_{44} = -k_2 - \beta_7$$

The fourth column forms one eigenvalue as it contains only diagonal term, A_{44}. $A_{44} = -k_2 - \beta_7$ gives $A_{44} < 0$. With this, the equilibrium point is asymptomatically stable. Next, the fourth row and column are eliminated to form the matrix below:

$$A = \begin{pmatrix} A_{11} & A_{12} & A_{13} \\ A_{21} & A_{22} & 0 \\ 0 & A_{32} & A_{33} \end{pmatrix} \qquad (4.33)$$

The other three roots can be obtained from the eigenvalues from matrix A (4.33). The characteristic equation is defined by the following:

$$\det\left(AI - \lambda I\right) = 0$$

$$\det\left(AI - \lambda I\right) = \begin{vmatrix} A_{11} - \lambda & A_{12} & A_{13} \\ A_{21} & A_{22} - \lambda & 0 \\ 0 & A_{32} & A_{33} - \lambda \end{vmatrix}$$

$$= \left(A_{11} - \lambda\right)\left(A_{22} - \lambda\right)\left(A_{33} - \lambda\right) - A_{12}A_{21}\left(A_{33} - \lambda\right) + A_{13}A_{21}A_{32}$$

$$= A_{11}A_{22}A_{33} - A_{11}A_{22}\lambda - A_{11}A_{33}\lambda + A_{11}\lambda^2 - A_{22}A_{33}\lambda + A_{22}\lambda^2 + A_{33}\lambda^2 - \lambda^3 - A_{12}A_{21}A_{33} + A_{12}A_{21}\lambda + A_{13}A_{21}A_{32}$$

$$= -\lambda^3 + \left(A_{11} + A_{22} + A_{33}\right)\lambda^2 - \left(A_{11}A_{22} + A_{11}A_{33} + A_{22}A_{33} + A_{12}A_{21}\right)\lambda + A_{11}A_{22}A_{33} + A_{13}A_{21}A_{32} - A_{12}A_{21}A_{33}$$

$$\det\left(AI - \lambda I\right) = 0$$

$$\lambda^3 - \left(A_{11} + A_{22} + A_{33}\right)\lambda^2 + \left(A_{11}A_{22} + A_{11}A_{33} + A_{22}A_{33} + A_{12}A_{21}\right)\lambda - A_{11}A_{22}A_{33} - A_{13}A_{21}A_{32} + A_{12}A_{21}A_{33} = 0$$

To simplify the above, we let,

$$B_1 = -A_{11} = \beta_2 + k_2 - \beta_1 S$$

$$B_2 = A_{12} = \beta_5 S$$

$$B_3 = A_{13} = \beta_6 S$$

$$B_4 = A_{21} = \beta_2$$

$$B_5 = -A_{22} = \beta_3 + k_2 + k_3$$

$$B_6 = A_{32} = \beta_3$$

$$B_7 = -A_{33} = \beta_4 + k_2$$

So, the characteristic equation is

$$a_3\lambda^3 + a_2\lambda^2 + a_1\lambda + a_0 = 0 \qquad (4.34)$$

where,

$$a_3 = 1$$

$$a_2 = B_1 + B_5 + B_7$$

$$a_1 = B_1B_5 + B_1B_7 + B_5B_7 + B_2B_4$$

and

$$a_0 = B_1B_5B_7 - B_3B_4B_6 - B_2B_4B_7$$

As mentioned in Section 2.3.1.2, for a system to be stable, all the roots of the polynomial should have negative real parts and for this to happen, all coefficients of polynomial are positive.

The expression of a_0 can be written as

$$a_0 = \left(\beta_2 + k_2\right)\left(\beta_3 + k_2 + k_3\right)\left(\beta_4 + k_2\right)\left(1 - R_0\right), \text{ for } R_0 < 1, \text{ with this, } a_0 > 0.$$

The Routh Hurwitz criterion is adopted when $n = 3$. All the coefficients a_i in the characteristic equation (4.34) are not zero and are positive. This, the necessary condition in

the Routh Hurwitz criterion is fulfilled. Next, by using Routh Array, the number of the positive real roots is decided for which positive real roots are equivalent to the number of signs changing obtained from Routh Array.

Hence, we obtain the following:

$$\Delta_0 = a_3 = 1$$

$$\Delta_1 = a_2 = B_1 + B_5 + B_7$$

For $B_1 = \beta_2 + k_2 - \beta_1 S = \left(\beta_2 + k_2\right)\left(1 - R_1\right)$, for $R_1 < 1$, with this, $B_1 > 0$, thus, $\Delta_1 = a_2 > 0$.

$$\Delta_2 = \frac{a_2 a_1 - a_0 a_3}{a_2}$$

$$a_3 = 1$$

$$\Delta_2 = \frac{a_2 a_1 - a_0}{a_2}$$

$$a_2 a_1 - a_0 = \left(B_1 + B_5 + B_7\right)\left(B_1 B_5 + B_1 B_7 + B_5 B_7 + B_2 B_4\right) - B_1 B_5 B_7 + B_3 B_4 B_6 + B_2 B_4 B_7$$

$$= B_1^{\,2} B_5 + B_1^{\,2} B_7 + B_1 B_5^{\,2} + B_5^{\,2} B_7 + B_1 B_7^{\,2} + B_5 B_7^{\,2} + B_1 B_2 B_4 + B_2 B_4 B_5 + B_3 B_4 B_6 + 2B_1 B_5 B_7 + 2B_2 B_4 B_7 > 0$$

Thus, $\Delta_2 = \frac{a_2 a_1 - a_0 a_3}{a_2} > 0$ is the sum of positive terms.

$$\Delta_3 = a_0 > 0$$

With all the positive coefficient obtained from equation (4.34), thus, all roots of equation (4.34) have negative real parts, which means $R_0 < 1$. With this, by using the Routh Hurwitz criterion, it is proven that the disease-free equilibrium is stable when $R_0 < 1$.

4.3.5 Endemic equilibrium points for SEIPR model

Theorem 3.3.5 When R_0 >1, the disease-free equilibrium is unstable, and the endemic equilibrium exists.

Proof

We will analyze the model from equations (4.1 – 4.5)

$$\frac{dS}{dt} = k_1 N - \beta_1 SE - \beta_5 SI - \beta_6 SP - K_2 S + \beta_7 R$$
$$\frac{dE}{dt} = \beta_1 SE + \beta_5 SI + \beta_6 SP - \beta_2 E - k_2 E$$
$$\frac{dI}{dt} = \beta_2 E - \beta_3 I - \left(k_2 + k_3\right) I$$
$$\frac{dR}{dt} = \beta_3 I - \beta_4 P - k_2 P$$
$$\frac{dR}{dt} = \beta_4 P - k_2 R - \beta_7 R$$

To find the equilibrium point, we set the right hand side of the system above to zero. When $\frac{dI}{dt} = 0$, we obtain

$$E^* = \left(\frac{\beta_3 + k_2 + k_3}{\beta_2} \right) I^* \qquad (4.35)$$

$\frac{dE}{dt} = 0$, we obtain

$$\beta_5 S^* I^* + \beta_6 S^* P^* = \left(\beta_2 - \beta_1 S^* + k_2\right) E^* \qquad (4.36)$$

$\frac{dP}{dt} = 0$, we obtain

$$P^* = \left(\frac{\beta_3}{\beta_4 + k_2} \right) I^* \qquad (4.37)$$

To perform $\frac{(4.35)}{(4.36)}$:

$$\frac{E^*}{\left(\beta_2 - \beta_1 S^* + k_2\right) E^*} = \frac{\left(\frac{\beta_3 + k_2 + k_3}{\beta_2} \right) I^*}{\beta_5 S^* I^* + \beta_6 S^* \left(\frac{\beta_3}{\beta_4 + k_2} \right) I^*}$$

$$\frac{1}{\left(\beta_2 - \beta_1 S^* + k_2\right)} = \frac{\left(\frac{\beta_3 + k_2 + k_3}{\beta_2} \right)}{\beta_5 S^* + \beta_6 S^* \left(\frac{\beta_3}{\beta_4 + k_2} \right)}$$

$$\frac{1}{\left(\beta_2 - \beta_1 S^* + k_2\right)} = \frac{\beta_3 + k_2 + k_3}{\left(\beta_2\right) \left(\frac{\beta_5 S^* \left(\beta_4 + k_2\right) + \beta_3 \beta_6 S^*}{\beta_4 + k_2} \right)}$$

$$\beta_2 \left(\beta_5 S^* \left(\beta_4 + k_2 \right) + \beta_6 S^* \beta_3 \right) = \left(\beta_3 + k_2 + k_3 \right) \left(\beta_4 + k_2 \right) \left(\left(\beta_2 - \beta_1 S^* + k_2 \right) \right)$$

$$\begin{aligned} \left(\beta_2 \beta_5 \left(\beta_4 + k_2 \right) + \beta_2 \beta_6 \beta_3 \right) S^* = {} & \beta_2 \beta_3 \beta_4 + \beta_3 k_2 \beta_4 - \beta_1 \beta_3 \beta_4 S^* + \beta_2 k_2 \beta_4 + k_2^{\,2} \beta_4 - \beta_1 k_2 \beta_4 S^* \\ & + k_3 \beta_2 \beta_4 + k_2 k_3 \beta_4 - \beta_1 k_3 \beta_4 S^* + \beta_2 k_2 \beta_3 + \beta_3 k_2^{\,2} - \beta_1 \beta_3 k_2 S^* \\ & + \beta_2 k_2^{\,2} + k_2^{\,3} - \beta_1 k_2^{\,2} S^* + k_2 k_3 \beta_2 + k_2^{\,2} k_3 - \beta_1 k_2 k_3 S^* \end{aligned}$$

$$\left(\beta_2 \beta_5 \left(\beta_4 + k_2 \right) + \beta_2 \beta_6 \beta_3 + \beta_1 \beta_3 \beta_4 + \beta_1 k_2 \beta_4 + \beta_1 k_3 \beta_4 + \beta_1 \beta_3 k_2 + \beta_1 k_2^{\,2} + \beta_1 k_2 k_3 \right) S^* =$$
$$\beta_2 \beta_3 \beta_4 + \beta_3 k_2 \beta_4 + \beta_2 k_2 \beta_4 + k_2^{\,2} \beta_4 + k_3 \beta_2 \beta_4 + k_2 k_3 \beta_4 + \beta_2 k_2 \beta_3 + \beta_3 k_2^{\,2} + \beta_2 k_2^{\,2} + k_2^{\,3} + k_2 k_3 \beta_2 + k_2^{\,2} k_3$$

$$\left(\beta_2 \beta_5 \left(\beta_4 + k_2 \right) + \beta_2 \beta_6 \beta_3 + \beta_1 \beta_3 \beta_4 + \beta_1 k_2 \beta_4 + \beta_1 k_3 \beta_4 + \beta_1 \beta_3 k_2 + \beta_1 k_2^{\,2} + \beta_1 k_2 k_3 \right) S^* =$$
$$\left(\beta_2 \beta_3 + \beta_3 k_2 + \beta_2 k_2 + k_2^{\,2} + k_3 \beta_2 + k_2 k_3 + \beta_2 \beta_3 + \beta_3 k_2 + \beta_2 k_2 + k_2^{\,2} + k_3 \beta_2 + k_2 k_3 \right) \left(\beta_4 + k_2 \right)$$

$$\left(\beta_2 \beta_5 \left(\beta_4 + k_2 \right) + \beta_2 \beta_6 \beta_3 + \beta_1 \beta_3 \beta_4 + \beta_1 k_2 \beta_4 + \beta_1 k_3 \beta_4 + \beta_1 \beta_3 k_2 + \beta_1 k_2^{\,2} + \beta_1 k_2 k_3 \right) S^* =$$
$$\left(k_2 + \beta_2 \right) \left(\beta_3 + k_2 + k_3 \right) \left(\beta_4 + k_2 \right)$$

$$\left(\beta_2\beta_5\left(\beta_4+k_2\right)+\beta_2\beta_6\beta_3+\left(\beta_4\beta_1\right)\left(\beta_3+k_2+k_3\right)+\left(\beta_1k_2\right)\left(\beta_3+k_2+k_3\right)\right)S^*=$$
$$\left(k_2+\beta_2\right)\left(\beta_3+k_2+k_3\right)\left(\beta_4+k_2\right)$$
$$\left(\beta_2\beta_5\left(\beta_4+k_2\right)+\beta_2\beta_6\beta_3+\left(\beta_3+k_2+k_3\right)\left(\beta_4\beta_1+\beta_1k_2\right)\right)S^*=$$
$$\left(k_2+\beta_2\right)\left(\beta_3+k_2+k_3\right)\left(\beta_4+k_2\right)$$
$$\left(\beta_2\beta_5\left(\beta_4+k_2\right)+\beta_2\beta_6\beta_3+\left(\beta_3+k_2+k_3\right)\left(\beta_4+k_2\right)\beta_1\right)S^*=$$
$$\left(k_2+\beta_2\right)\left(\beta_3+k_2+k_3\right)\left(\beta_4+k_2\right)$$

$$S^*=\frac{\left(k_2+\beta_2\right)\left(\beta_3+k_2+k_3\right)\left(\beta_4+k_2\right)}{\left(\beta_2\beta_5\left(\beta_4+k_2\right)+\beta_2\beta_6\beta_3+\left(\beta_3+k_2+k_3\right)\left(\beta_4+k_2\right)\beta_1\right)}$$

$$\frac{1}{S^*}=\frac{\left(\beta_2\beta_5\left(\beta_4+k_2\right)+\beta_2\beta_6\beta_3+\left(\beta_3+k_2+k_3\right)\left(\beta_4+k_2\right)\beta_1\right)}{\left(k_2+\beta_2\right)\left(\beta_3+k_2+k_3\right)\left(\beta_4+k_2\right)}$$

$$=\frac{\beta_1}{\left(k_2+\beta_2\right)}+\frac{\beta_2\beta_5}{\left(k_2+\beta_2\right)\left(\beta_3+k_2+k_3\right)}+\frac{\beta_2\beta_6\beta_3}{\left(k_2+\beta_2\right)\left(\beta_3+k_2+k_3\right)\left(\beta_4+k_2\right)}$$

$$\frac{1}{S^*}=\frac{R_0}{S_0}$$

$$S^*=\frac{S_0}{R_0} \qquad (4.38)$$

When $\frac{dS}{dt}=0$, we obtain,

$$\beta_1S^*E^*+\beta_5S^*I^*+\beta_6S^*P^*+k_2S^*=k_1N-\beta_7R^*$$

$$\beta_1S^*E^*+\beta_5S^*I^*+\beta_6S^*P^*+k_2S^*=k_1N-\left(\beta_1S^*E^*+\beta_5S^*I^*+\beta_6S^*P^*+k_2S^*-k_1N\right)$$
$$\beta_1S^*E^*+\beta_5S^*I^*+\beta_6S^*P^*+k_2S^*=k_1N+k_1N-\beta_1S^*E^*-\beta_5S^*I^*-\beta_6S^*P^*-k_2S^*$$

$$2\left(\beta_1S^*E^*+\beta_5S^*I^*+\beta_6S^*P^*+k_2S^*\right)=2k_1N$$
$$\beta_1S^*E^*+\beta_5S^*I^*+\beta_6S^*P^*+k_2S^*=k_1N$$
$$\beta_1\left(\frac{\beta_3+k_2+k_3}{\beta_2}\right)I^*+\beta_5I^*+\beta_6\left(\frac{\beta_3I^*}{\beta_4+k_2}\right)+k_2=\frac{k_1N}{S^*}$$

$$\beta_1\left(\frac{\beta_3+k_2+k_3}{\beta_2}\right)I^*+\beta_5 I^*+\beta_6\left(\frac{\beta_3 I^*}{\beta_4+k_2}\right)=\frac{k_1N}{S^*}-k_2$$

$$\beta_1\left(\frac{\beta_3+k_2+k_3}{\beta_2}\right)+\beta_5+\beta_6\left(\frac{\beta_3}{\beta_4+k_2}\right)\left(I^*\right)=\frac{k_1N}{S^*}-k_2$$

$$\frac{\beta_1\left(\beta_3+k_2+k_3\right)\left(\beta_4+k_2\right)+\beta_5\beta_2\left(\beta_4+k_2\right)+\beta_2\beta_3\beta_6}{\beta_2\left(\beta_4+k_2\right)}\left(I^*\right)=\frac{k_1N}{S^*}-k_2$$

$$I^*=\frac{\beta_2\left(\beta_4+k_2\right)}{\beta_1\left(\beta_3+k_2+k_3\right)\left(\beta_4+k_2\right)+\beta_5\beta_2\left(\beta_4+k_2\right)+\beta_2\beta_3\beta_6}\left(\frac{k_1N}{S^*}-k_2\right)$$

$$\text{Let } m=\frac{\beta_2\left(\beta_4+k_2\right)}{\beta_1\left(\beta_3+k_2+k_3\right)\left(\beta_4+k_2\right)+\beta_5\beta_2\left(\beta_4+k_2\right)+\beta_2\beta_3\beta_6}$$

$$I^*=m\left(\frac{k_1N}{S^*}-k_2\right)$$

From equation (4.38),

$$I^*=m\left(\frac{k_1N}{\frac{S_0}{R_0}}-k_2\right)$$

$$I^*=m\left(\frac{R_0k_1N}{S_0}-k_2\right)$$

From equation (4.13),

$$N=\frac{k_2N^*}{k_1}=\frac{k_2S_0}{k_1}$$

$$I^*=m\left(R_0k_2-k_2\right)$$

Hence, we obtain,

$$I^*=mk_2\left(R_0-1\right) \qquad (4.39)$$

From (4.35),

$$E^* = \left(\frac{\beta_3 + k_2 + k_3}{\beta_2} \right) I^*$$

$$E^* = \left(\frac{\beta_3 + k_2 + k_3}{\beta_2} \right) mk_2 \left(R_0 - 1 \right) \qquad (4.40)$$

From (4.37),

$$P^* = \left(\frac{\beta_3}{\beta_4 + k_2} \right) I^*$$

$$P^* = \left(\frac{\beta_3}{\beta_4 + k_2} \right) mk_2 \left(R_0 - 1 \right) \qquad (4.41)$$

Hence, the endemic equilibrium point, $E_e = \left(S^*, E^*, I^*, P^*, R^* \right)$, is as follow:

$$E_e = \left(\frac{S_0}{R_0}, \left(\frac{\beta_3 + k_2 + k_3}{\beta_2} \right) mk_2 \left(R_0 - 1 \right), mk_2 \left(R_0 - 1 \right), \left(\frac{\beta_3}{\beta_4 + k_2} \right) mk_2 \left(R_0 - 1 \right), N - S^* - E^* - I^* - P^* \right) \qquad (4.42)$$

The disease is to prevail in the population when $I^* > 0$. Thus, when R_0>1, the endemic equilibrium point exist meaning that the disease remains in the population. When R_0=1, it is given us the disease-free equilibrium point. Also, if R_0=1, it means that there will be approximately the same number of infected cases all the time, which the endemic occurs (Heffernan et al., 2005).

4.4 Numerical results for SEIPR model

The ordinary differential equations in (4.1 – 4.5) are in the form of

$$\begin{aligned}
\frac{dy_1}{dt} &= f\left(y_1, y_2, \ldots, y_n, t\right), \\
\frac{dy_2}{dt} &= f\left(y_1, y_2, \ldots, y_n, t\right), \\
&\vdots \\
\frac{dy_n}{dt} &= f\left(y_1, y_2, \ldots, y_n, t\right).
\end{aligned}$$

Here, $y_1 = S, y_2 = E, y_3 = I, y_4 = P$ and $y_5 = R$. The system is to be solved numerically. The method used is based on fourth-order Runge Kutta method in MatLab program. The time span used for our simulation is $t_0 = p$ to $t = q$ where p is initial value and q is the terminal value. Initial conditions and parameter values are to be determined to simulate the SEIPR model. Table 4.1 shows the description of parameters values for SEIPR model.

Table 4.1: Parameters values of SEIPR model description.

Parameter	Definitions (unit)	References
β_1	Transmission coefficient of susceptible individuals getting infected by incubation period individual for SEIPR model (per time)	fitting
β_2	The rate at which an asymptomatic patient developing symptoms for SEIPR model (per time)	fitting
β_3	The rate at which an infectious individual clinically recovered for SEIPR model (per time)	fixed
β_4	The rate at which a clinically recovered individual fully recovered for SEIPR model (per time)	fixed

Table 4.1 continued

β_5	Transmission coefficient of susceptible individuals getting infected by infectious individual for SEIPR model (per time)	fitting
β_6	Transmission coefficient of susceptible individuals getting infected by clinically recovered individual for SEIPR model (per time)	fitting
β_7	The rate at which a recovered individual loses its immunity for SEIPR model (per time)	fixed
k_1	Natural birth rate (per time)	actual data
k_2	Natural death rate (per time)	actual data
k_3	Death rate which is caused by disease (per time)	actual data
E	Number of infected individual during incubation period at time t	fitting
I	Number of infectious individual at time t	actual data
N	Total population	fitting
P	Number of clinically recovered individual (post-infectious virus shedding period) at time t	actual data
R	Number of fully recovered individual at time t	fixed
S	Number of susceptible at time t	fixed

From table 4.1, k_1 and k_2 are actual data obtained from Department of Statistic Malaysia. k_3 together with the initial conditions for I and P are actual data taken from the

actual cases reported from Sarawak Health Department. I is number of HFMD cases of the first week of the year and P is the number of HFMD of the last week from previous year. Values of P in years 2006 and 2010 are made based on the assumption, as we have no information for the number of HFMD cases during the last weeks of 2005 and 2009.

Next, we will discuss the fixed parameters values, β_3, β_4, β_7, R, S and N. β_3 is the rate at which an infectious individual clinically recovered per unit time. In other words, β_3 is the rate of time a symptomatic patient has symptoms subsided. From literature review, the most contagious period of HFMD spreading is the first week during the infectious period when symptoms appear and the symptoms normally will resolve in 7 to 10 days (CDC, 2015; Mandal, 2017; Ministry of Health, 2014; Podin et al., 2006; Roy & Halder, 2010). We then decide that the time taken for symptoms subsided is seven days. Besides that, we found out the best simulation results obtained for our study when the infectious individual to reach clinically recovered stage is set to be one week as well.

On the other hand, β_4 is the rate at which a clinically recovered individual fully recovered per unit time. Clinically recovered individual is having the transition process from symptomatic infectious individual to asymptomatic post-infectious individual. Before a clinically recovered patient reaches fully recovered stage, the patient can still carry the post-infectious virus shedding. As mentioned in 2.2, most of the clinically recovered cases will carry the post-infectious virus shedding for at least one week and for some cases, post-infectious virus shedding can persist in stool and throat for several weeks. (Han et al., 2010; Li et al., 2013; Podin et al., 2006; Teng et al., 2013). Based on the best simulation results from sensitivity tests in Section 4.4.1 and trial running for other years (2010-2014)

of HFMD outbreaks simulation, we decide to fix the time taken for clinically recovered individual fully recovered as seven days.

β_7 is the rate recovered individual loses its immunity and it was predicted that the period of losing immunity is 100 days after a few simulation ran by (Tiing & Labadin, 2008). We decide to use the same value as our study area taken is same with (Tiing & Labadin, 2008). Whereas, for R, fully recovered cases, we fix the value as zero because no infected patient is recovered at the initial condition. Meanwhile, S and N, susceptible and total population are fixed as 10000 after the sensitivity tests and discussion made in Section 4.4.1 below.

Besides, the initial condition for E, incubation period cases, is fitting value decided based on the I and P taken together with the consideration of the best simulation results. While β_2, the rate at which asymptomatic patient developing symptoms per unit time is fitting value based on the best simulation results and literature review. Incubation period can last for one day and up to two weeks (CDC, 2015; Lai et al., 2016; Mandal, 2017; Ministry of Health, 2014; Podin et al., 2006). In our study, we fix the incubation period as 1.27 day for all the years taken except in year 2014, the incubation period taken is 3.9 days. Besides, β_1, β_5 and β_6 are fitting values based on the best results after many time of running the simulations.

For the next section, sensitivity analysis for SEIPR model's parameters will be discussed. The numerical results then will be verified by using root square mean error (RMSE).

4.4.1 Sensitivity analysis for SEIPR model's parameters

The sensitivity analysis for SEIPR model's parameters is used to determine the best initial values for parameters. Sensitivity test is laborious task as it took a lot of trials attempting to search for the best fit between the predicted results and actual data results. We have done countless simulation tests in order to give the reasonable parameters values to be used. Table 4.2 summarizes the closer range of parameters values to reach the best fit for sensitivity analysis.

Table 4.2: Parameters values of SEIPR model for sensitivity analysis.

Parame-ters Values	**Trial tests for sensitivity analysis**					
	First trial	**Second trial**	**Third trial**	**Fourth trial**	**Fifth trial**	**Sixth trial**
k_1	2.923×10^{-4}	2.923×10^{-4}	2.923×10^{-4}	2.923×10^{-4}	2.923×10^{-4}	2.923×10^{-4}
k_2	1.077×10^{-4}	1.077×10^{-4}	1.077×10^{-4}	1.077×10^{-4}	1.077×10^{-4}	1.077×10^{-4}
k_3	1.731×10^{-5}	1.73×10^{-5}	1.731×10^{-5}	1.731×10^{-5}	1.731×10^{-5}	1.731×10^{-5}
β_1	9×10^{-5}	3.5×10^{-5}	3×10^{-5}	5.3×10^{-5}	6×10^{-6}	1.4×10^{-5}
β_2	5.5	5.5	5.5	5.5	5.5	5.5
β_3	1	1	1	1	1	1
β_4	1	1	1	1	1	1
β_5	5.5×10^{-4}	2.5×10^{-4}	1.5×10^{-4}	1×10^{-4}	1.5×10^{-4}	1×10^{-4}
β_6	9×10^{-5}	3×10^{-5}	6×10^{-5}	5.4×10^{-5}	2×10^{-6}	1.2×10^{-5}
β_7	0.07	0.07	0.07	0.07	0.07	0.07
E	4	4	4	4	4	4
I	4	4	4	4	4	4

Table 4.2 continued

N	5,000	8,000	10,000	12,000	12,000	15,000
P	4	4	4	4	4	4
R	0	0	0	0	0	0
S	5,000	8,000	10,000	12,000	12,000	15,000

From table 4.2, parameters values of SEIPR model for sensitivity analysis are tested by running the simulation based on the actual HFMD cases in 2006. Fixed parameter values are β_2, β_3, β_4, β_7 and R. As mentioned in Section 4.4, fixed parameter values have been taken after the thorough study of biological factors whereas, k_1, k_2, k_3 and I are actual data values. Fitting values, which are β_1, β_5 and β_6 are recorded after the simulation, which showed the relevant best match with the actual HFMD cases in 2006. On the other hand, fitting values for E, P and N are based on the assumption. For the value S, before the fixed value is determined, some values are selected to run the sensitivity tests based on the reference taken from (Tiing & Labadin, 2008) because the study area taken for their works are similar as our study. The following are the numerical results for the sensitivity analysis.

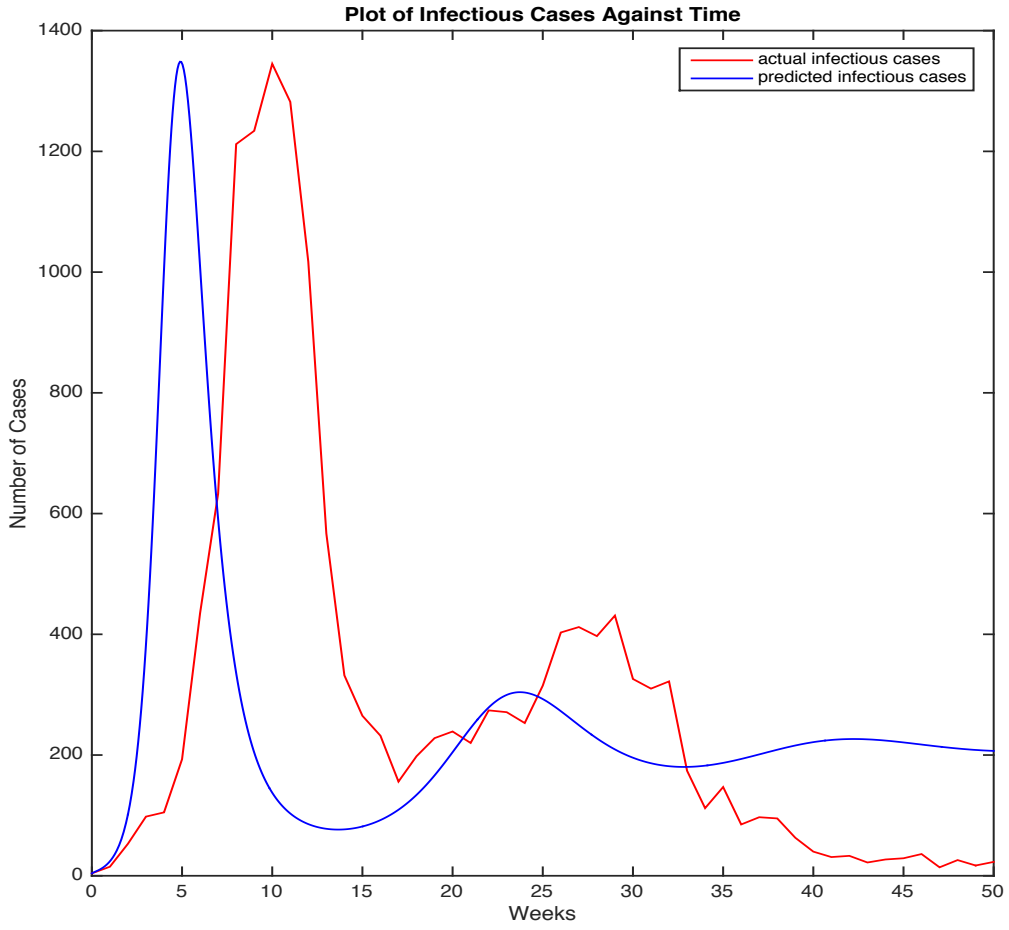

Figure 4.8: Comparison of the actual infectious cases and predicted infectious cases, first trial.

From Figure 4.8, the SEIPR model predicts the HFMD cases with a rapid spreading and reached the peak a lot earlier than the real cases by visual inspection. This is because the susceptible used is too small that is 5000 in which resulted the β_5 is too high in order to reach the same peak with the real cases. With high β_5, the predicted graph shifts too fast, thus the timing predicted is not accurate and not suitable compare to the actual data. Next, we will increase the number of susceptible to 8000 for second trial test and the numerical result is shown in Figure 4.9.

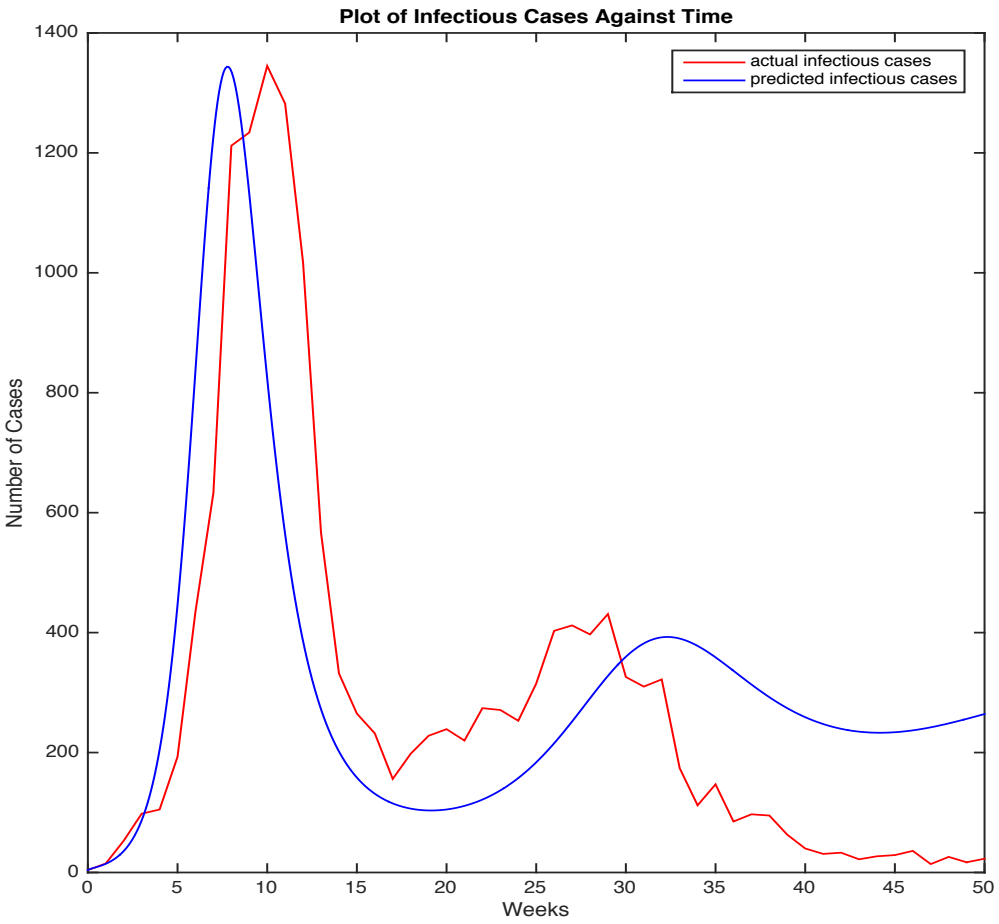

Figure 4.9: Comparison of the actual infectious cases and predicted infectious cases, second trial.

As shown in Figure 4.9, SEIPR model predicts the HFMD cases with fast spreading and reached the peak earlier than the real cases as well. This may due to the susceptible used is still too small and the β_5 is still too high in order to reach the same peak with the real cases. The timing predicted is still not accurate and not suitable compare to the actual data. We then increase the number of susceptible to 10000 for third trial test and the numerical result is shown in Figure 4.10.

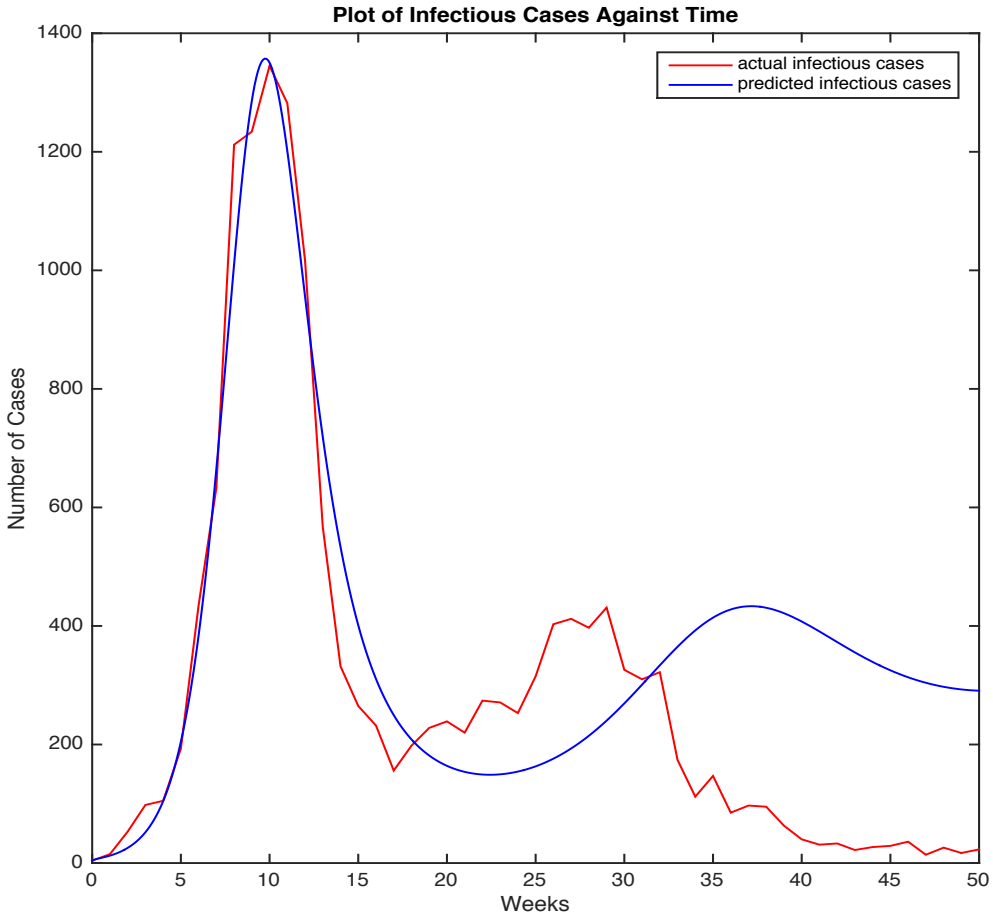

Figure 4.10: Comparison of the actual infectious cases and predicted infectious cases, third trial.

Figure 4.10 shows the fitting between predicted infectious cases and actual infectious cases during the first wave of the outbreak is well matched from visual inspection. The predicted infectious cases able to the peak almost the same time as the real infectious cases. Thus, the timing predicted is suitable compare to the actual data for the first wave. In order to have more supporting reasons to decide the value of *S*, again, we continue to increase the number of susceptible to 12000 for fourth trial test and the numerical result is shown in Figure 4.11.

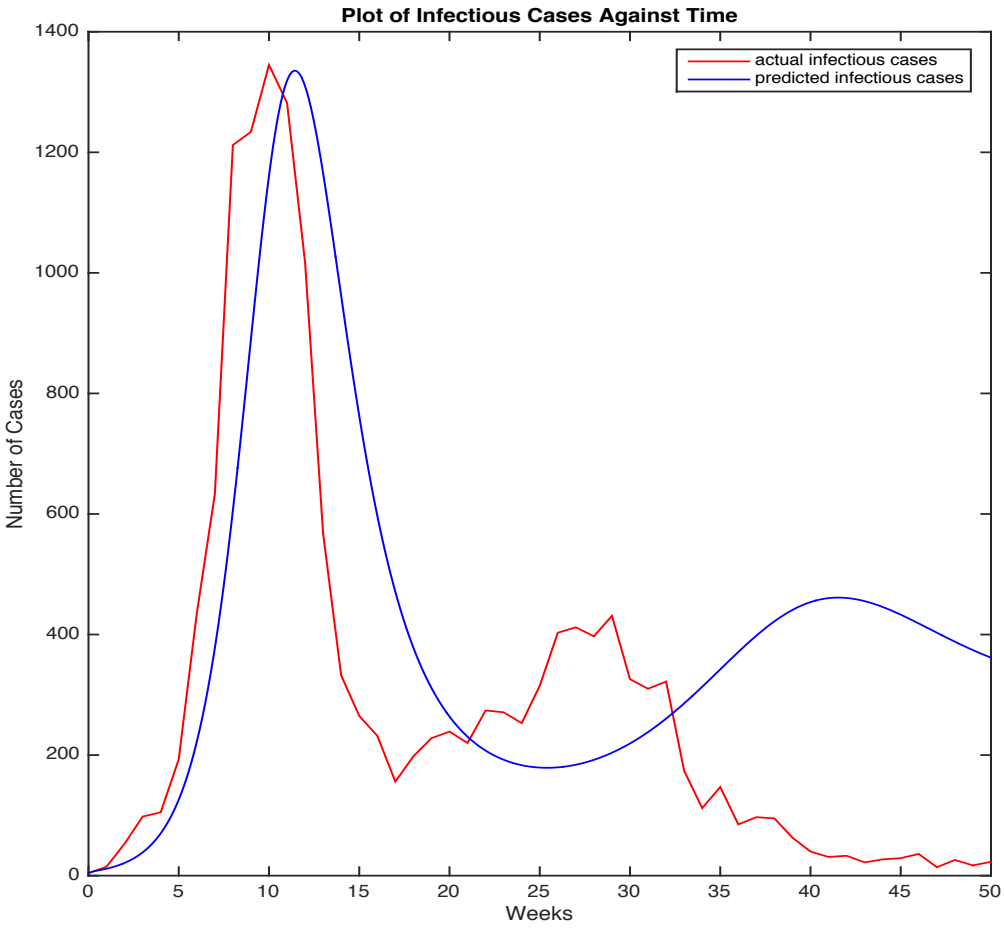

Figure 4.11: Comparison of the actual infectious cases and predicted infectious cases, fourth trial.

As shown in Figure 4.11, SEIPR model predicts the HFMD cases with slower spreading and reached the peak slower than the real cases. This may due to the susceptible used is big and the β_5 cannot fit to have the result to reach the peak same with the real cases. With this the timing predicted is not accurate and not suitable compare to the actual data. Next step, we will use the same number of susceptible for fifth trial test but trying to change the other fitting values as shown in Table 4.2 and the numerical result is shown in Figure 4.12.

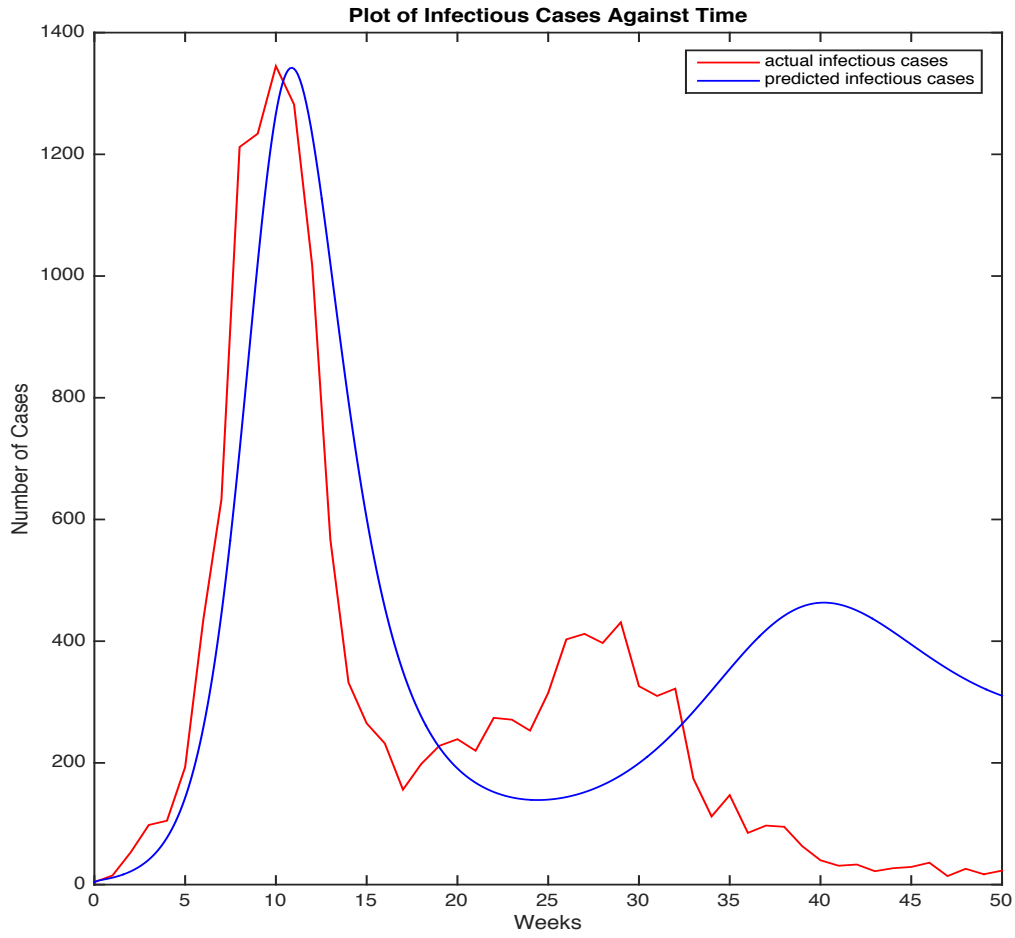

Figure 4.12: Comparison of the actual infectious cases and predicted infectious cases, fifth trial.

From Figure 4.12, SEIPR model predicts the HFMD cases with slightly slower spreading. The timing predicted again is not suitable compare to the actual data. To have more significant reason to choose a suitable value for *S*, we increase the number of susceptible again to 15000 for sixth trial test and the numerical result is shown in Figure 4.13.

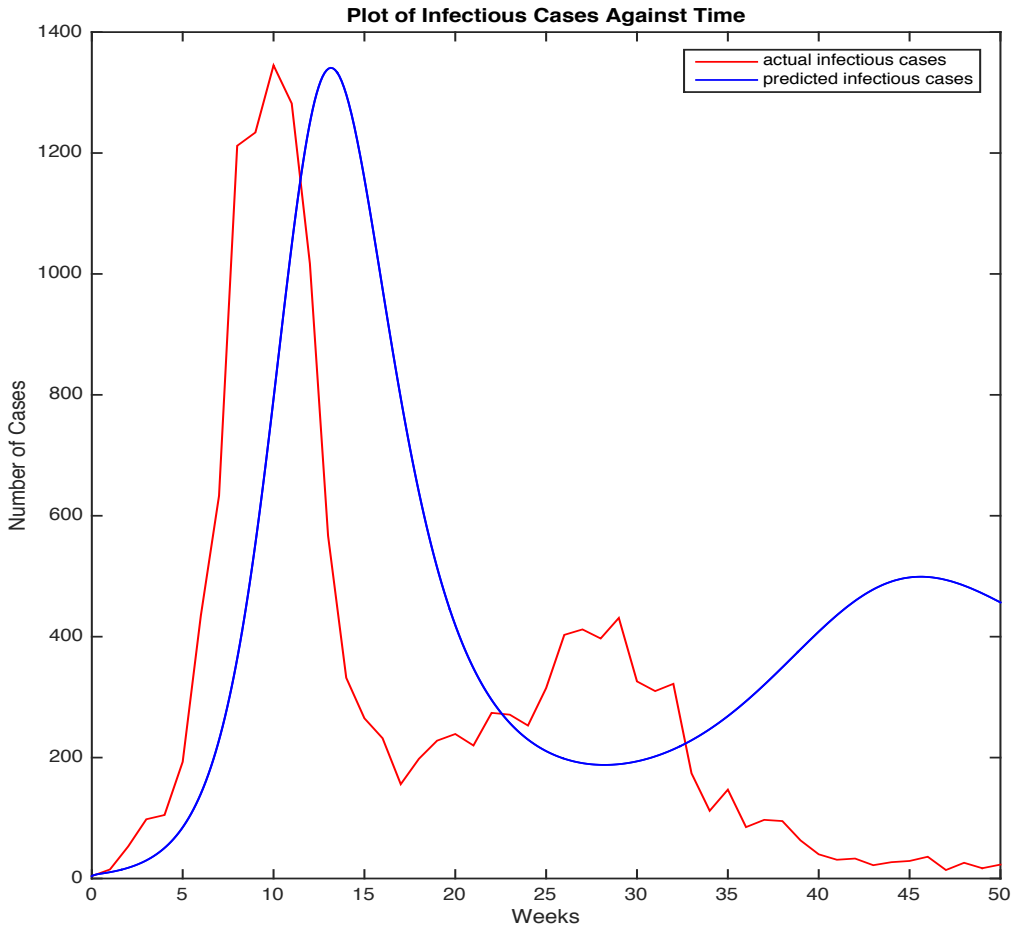

Figure 4.13: Comparison of the actual infectious cases and predicted infectious cases, sixth trial.

From Figure 4.13, SEIPR model predicts the HFMD cases with slower spreading than the actual cases. With higher value of *S*, β_5 chosen has to be smaller so that the over rapid spreading can be avoided. After the simulation, Figure 4.13 shows that the timing predicted again is not suitable compare to the actual data. Thus, the value of *S,* 15000 is not suitable.

After running so many sensitivity tests, we found out the suitable value for *S* that can be chosen is 10000 for HFMD cases in year 2006 by using SEIPR model. To ensure

that the value of S is 10000, we calculate the RMSE by using the predicted results and actual results.

As mentioned in Section 2.3.5, RMSE calculates the prediction error. The closer the predicted results to the actual results, the smaller the RMSE and indicates better prediction. Since, our model able to predict the first wave of the HFMD cases more accurately at third trial sensitivity test based on the numerical results as seen in Figure 4.10, thus we choose the first thirteen weeks duration by estimation for the first wave to test the RMSE by using the RMSE program in MatLab.

Table 4.3: Results of the actual infectious cases in 2006 and predicted infectious cases of sensitivity analysis by using SEIPR model for first until sixth trial.

Weeks	**Actual infectious cases**	**Predicted infectious cases of sensitivity analysis**					
		First trial	**Second trial**	**Third trial**	**Fourth trial**	**Fifth trial**	**Sixth trial**
0	4	4	4	4	4	4	4
1	15	23	23	16	16	12	14
2	53	102	54	46	291	22	24
3	98	374	136	96	53	42	41
4	105	1001	311	104	95	77	67
5	193	1348	609	192	166	139	110
6	435	997	1045	433	290	262	191
7	633	579	1341	635	490	441	300
8	1212	333	1250	1218	749	706	455
9	1234	207	966	1280	1050	1031	691
10	1345	137	686	1349	1275	1264	934
11	1282	103	457	1194	1340	1341	1180
12	1017	86	322	1021	1251	1224	1321
13	567	77	236	563	1064	1027	1344
RMSE values		530.3	455.7	28.67	231.1	220.4	363.3

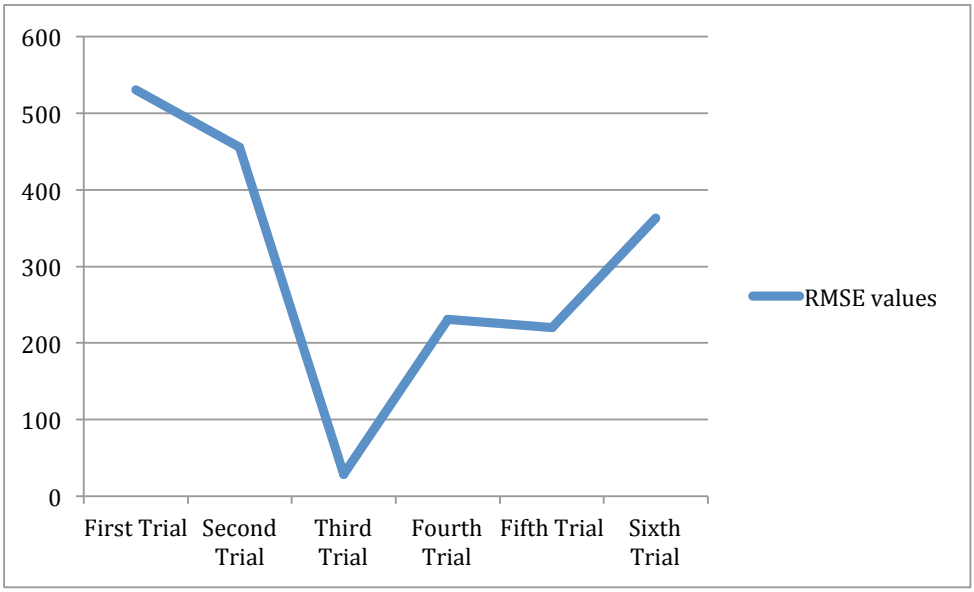

Figure 4.14: Plot of RMSE values for first trial until sixth trial.

Table 4.3 shows the actual data for HFMD cases in 2006, predicted data and RMSE values for sensitivity analysis from first trial until sixth trial. Figure 4.14 shows the plot of RMSE values obtained by comparing the actual data and predicted data. From Figure 4.14, it is noticed that the lowest prediction error happens at the third trial sensitivity analysis test. Thus, the parameters used are more suitable for the prediction and the S value, which is 10000 will be chosen as benchmark for our study. Since our study will include other years of HFMD outbreaks, which are 2010, 2011, 2012, 2013 and 2014, thus, before we select the suitable value of S, we compare the actual number of HFMD cases on those years with the number of susceptible taken from Department of Statistic Malaysia and the data is shown in Table 4.4.

Table 4.4: Total population of children under age 9 and number of HFMD cases, year 2006, 2010, 2011, 2012, 2013 and 2014.

Years	Total population of children under age 9	Number of HFMD cases
2006	550700	14875
2010	466853	5010
2011	464000	2944
2012	456100	13388
2013	455100	8568
2014	444300	9452

Table 4.4 shows the total population of children under age 9 taken from Department of Statistic Malaysia and number of HFMD cases taken from Sarawak Health Department in years 2006, 2010, 2011, 2012, 2013 and 2014. The data is taken in consideration for choosing the value of *S* in order to run the simulation of SEIPR model in predicting the HFMD cases on those years. The comparison result is shown in Figure 4.15 below.

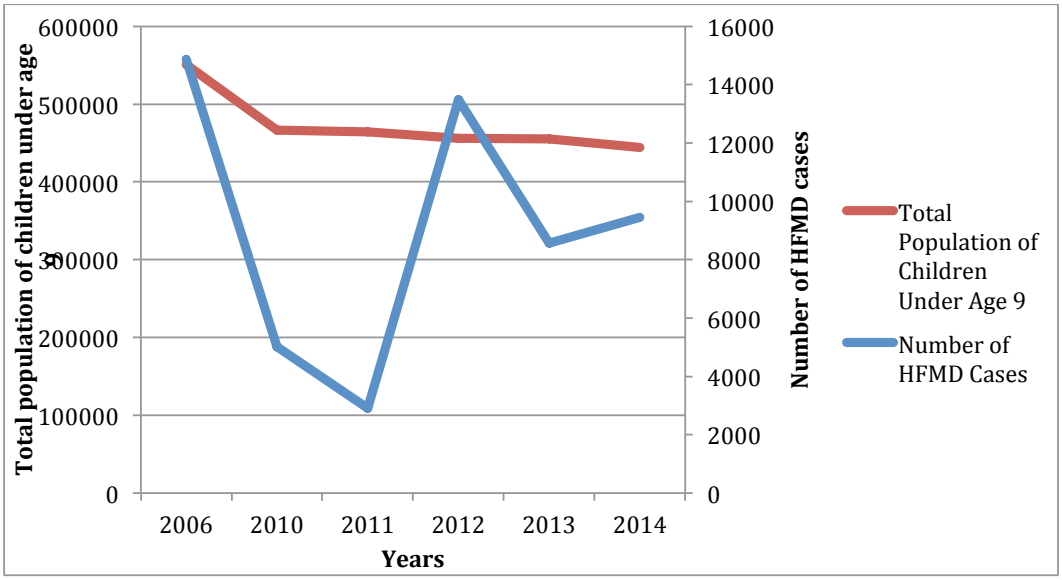

Figure 4.15: Comparison between the total population of children under age 9 and number of HFMD cases.

From Figure 4.15, the curve for number of HFMD cases is fluctuating. Over the years since 2010, the total population of children under age 9 is decreasing slightly. The total population of children under age 9 is used as susceptible benchmark in Sarawak as the total population by age provided from Department of Statistic Malaysia is grouped from year 0-4, 5-9, 10-14 and so on. Thus, we choose children below age 9 as susceptible benchmark (Chan et al., 2000; Lu et al., 2013; Podin et al., 2006; Solomon et al., 2010).

However, the total population of children under age 9 does not change dramatically and has insignificant role in affecting the fluctuating HFMD cases over the years. Even clearly as seen in year 2012, while the total population of children under age 9 was decreasing, the HFMD cases had sharply increased. With this, we ensure that the spreading of HFMD cases is not merely affected by the number of susceptible but it is mainly caused by the contact rate when there is a cohort of children having a close contact to each other met the HFMD viruses (Podin et al., 2006; Roy & Halder, 2010).

Further more, since Sarawak is a big state with an area of 123,449 km^2 where the population is dispersed throughout the country and quite majority of the children were staying in the rural area (Tiing & Labadin, 2008). Since the model mode is using mass action principle in which force of infection is to be applied, we need to consider the chances of susceptible to meet with the infectious individual (Keeling & Rohani, 2008). In the rural area, the chances of close contact between susceptible and infectious are lower compare to towns and cities area. The disease is showing the trend to spread among school going children in nurseries, kindergartens and primary schools (Tiing & Labadin, 2008). Therefore, after consider all the factors discussed and the results of sensitivity tests above, the initial condition used for susceptible was lower down and fixed as 10000 for our research study. At the same time, we estimate the value of N as 10000 to have relevant

total population involved by taking the ratio of population same as the number of susceptible.

For the next section, numerical results for SEIPR model for the years of 2006, 2010, 2011, 2012, 2013 and 2014 will be shown and analyzed by using threshold value, basic reproductive number, goodness of fit test and lastly the results will be summarized

4.4.2 Numerical results for SEIPR model, year 2006

From Section 4.4.1, sensitivity analysis tests by using the actual data in year 2006 show the best simulation result is the third trial sensitivity test. This can be seen at Figure 4.10 of which by visual inspection, the graphs are best fit during the first wave of the outbreak. The data is analyzed and in Table 4.3, it is shown that the third trial sensitivity test shows the least RMSE. Thus, we will use the third trial parameters to discuss the analytical analysis of threshold value and basic reproductive number for numerical results of 2006 and hence, verified the SEIPR model by comparing the results to the SIR model discussed in Chapter 3. Initial conditions and parameter values are $S=10000,\ E=4,\ I=4,\ P=4,$ $R=0,\quad k_1=0.0002923,\quad k_2=0.0001077,\quad k_3=0.00001731,\quad \beta_1=0.00003,\quad \beta_2=5.5,$ $\beta_3=1,\ \beta_4=1,\ \beta_5=0.00015,\ \beta_6=0.00006,\ \beta_7=0.07.$ The SEIPR model plot is shown at Figure 4.16.

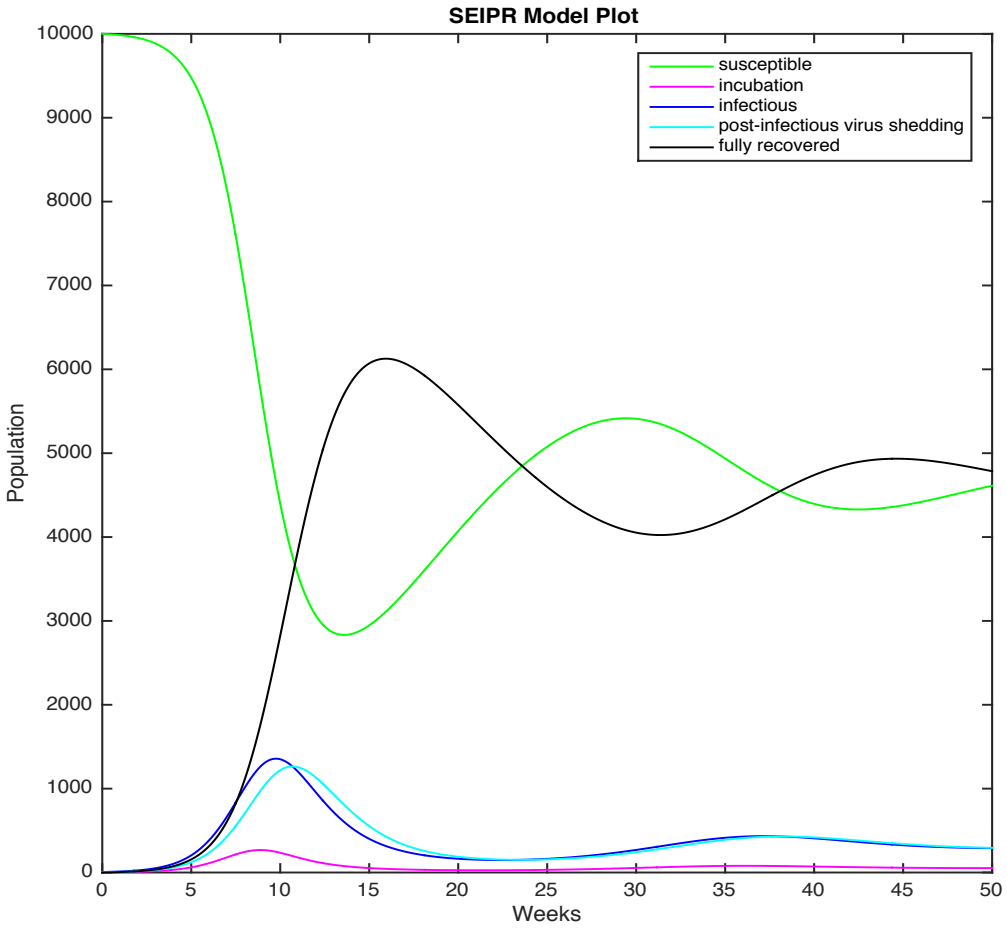

Figure 4.16: The predicted cases of the SEIPR model for susceptible, incubation period, infectious, post-infectious virus shedding and fully recovered over time, year 2006.

From Figure 4.16, the susceptible curve drops sharply when infectious cases increasing rapidly. After about ten weeks, the infectious cases start to decrease, susceptible graph is bouncing back and fully recovered individual are increasing a lot. Post-infectious virus shedding graph shows similar wave with infectious graph but slower cycle as post-infectious virus shedding cases only happens after the infectious period. Graph of incubation period increases slowly shows that the incubation period patients played a small role in contributing to the virus spreading. We will have two comparisons of the actual

infectious cases of year 2006 by using SEIPR model and SIR model in Figure 4.17 and 4.18.

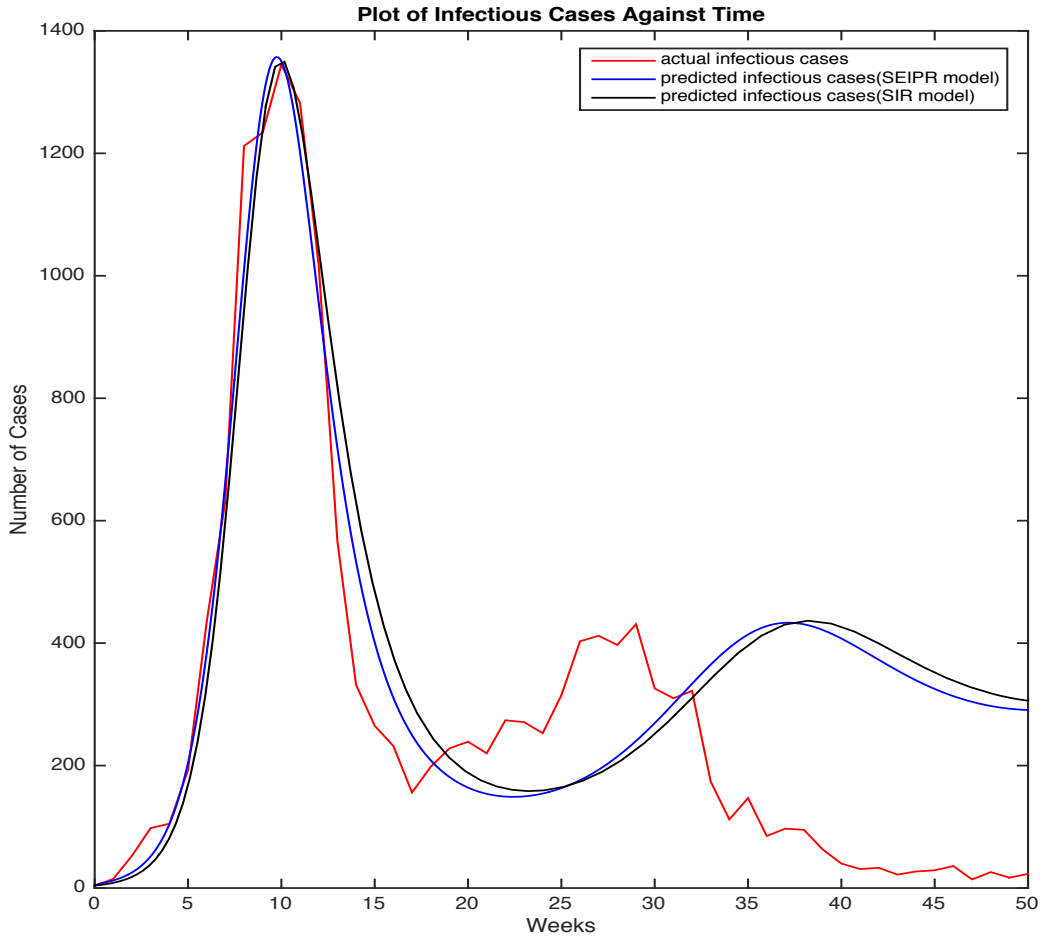

Figure 4.17: Comparison of the best fit between SEIPR and SIR models. Parameters for SEIPR model are $S=10000$, $E=4$, $I=4$, $P=4$, $R=0$, $k_1=0.0002923$, $k_2=0.0001077$, $k_3=0.00001731$, $\beta_1=0.00003$, $\beta_2=5.5$, $\beta_3=1$, $\beta_4=1$, $\beta_5=0.00015$, $\beta_6=0.00006$ and $\beta_7=0.07$. Parameters for SIR model are $S=9000$, $I=4$, $R=0$, $k_1=0.0002923$, $k_2=0.0001077$, $k_3=0.00001731$, $\alpha_1=0.0001771$, $\alpha_2=0.07$ and $\alpha_3=0.8325$.

Figure 4.17 is the comparison of the best fit for both SEIPR and SIR model. However, for the best fit by using the SIR model, the initial value of S is 9000 as mentioned in Section 3.4 which is different with SEIPR model, the initial S value is 10000. Both models with the best simulation show the best fit during the first wave of the HFMD outbreak. The RMSE calculated is slightly different with SEIPR model is approximately 28.67 and SIR model is approximately 44.65.

On the other hand, Figure 4.18 shows the comparison of the actual infectious cases and predicted infectious cases by using SEIPR model and SIR model when the initial value of S is same, S =10000. The predicted cases for SEIPR model still same as Figure 4.17, but the predicted cases for SIR model is different with Figure 4.17 as the parameters changed. Figure 4.18 shows that the prediction by using SEIPR model is well matched compare to the prediction by using SIR model with the real data at the first wave of the disease spreading. The predicted infectious cases able to shift faster and reach the peak almost the same time as the real infectious cases for SEIPR model. However, the prediction timing for infectious cases by using the SIR model has a slower cycle running.

This may due to SEIPR includes both the incubation period and post-infectious virus shedding period as parts of the compartments have shown their abilities to contribute to the disease spreading help to speed up the virus spreading and hence, the prediction infectious cases can shift faster compare to SIR model. The RMSE calculated for SIR model is approximately 194.4. Thus, both comparison results verified that the SEIPR model is able to predict the first wave of the HFMD outbreaks as well with smaller RMSE.

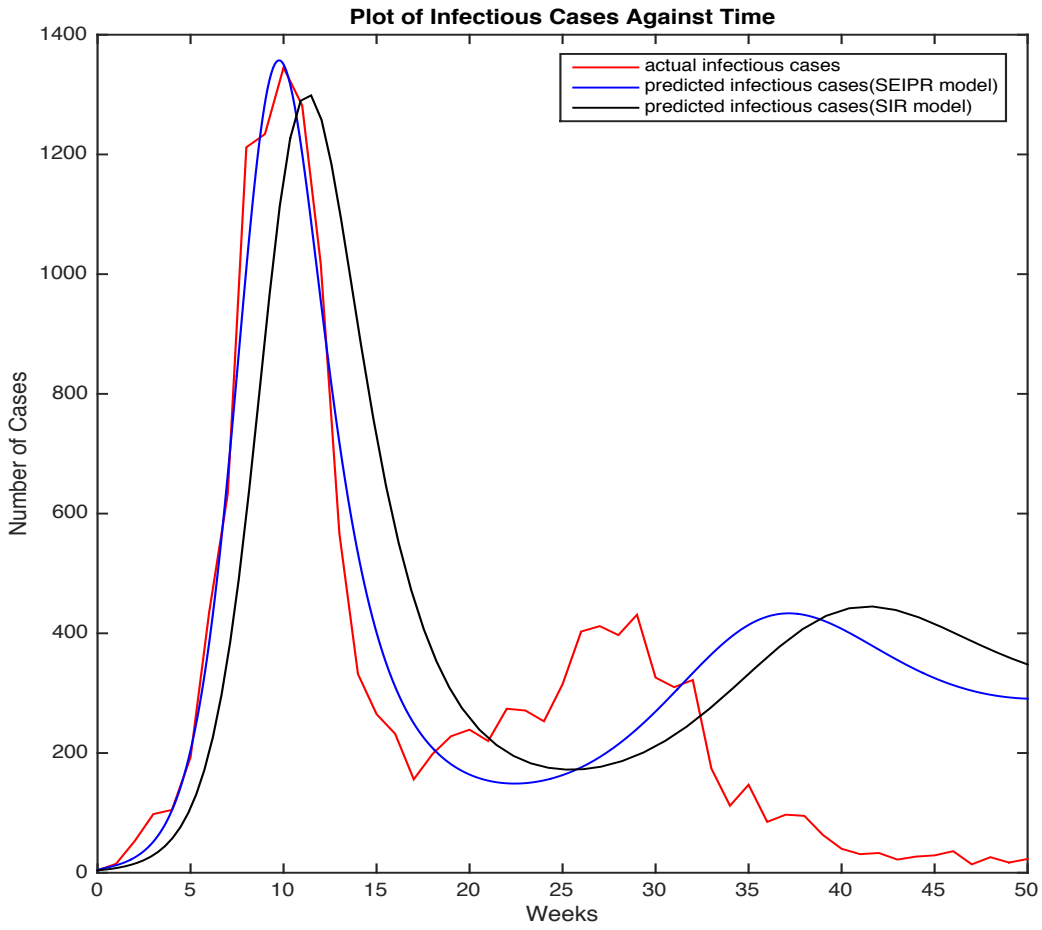

Figure 4.18: Comparison of the best fit between SEIPR and SIR models with value of initial S is 10000. Parameters for SEIPR model are $S=10000$, $E=4$, $I=4$, $P=4$, $R=0$, $k_1=0.0002923$, $k_2=0.0001077$, $k_3=0.00001731$, $\beta_1=0.00003$, $\beta_2=5.5$, $\beta_3=1$, $\beta_4=1$, $\beta_5=0.00015$, $\beta_6=0.00006$ and $\beta_7=0.07$. Parameters for SIR model are $S=10000$, $I=4$, $R=0$, $k_1=0.0002923$, $k_2=0.0001077$, $k_3=0.00001731$, $\alpha_1=0.00015$, $\alpha_2=0.07$ and $\alpha_3=0.8325$.

Although SIR model in Figure 4.17 has the best fit almost same as SEIPR model when the value of S is reduced to 9000, however, SIR model only provides the limited ability where only the infectious period is giving the transmission role. As mentioned in Section 3.5, a lot of studies have mentioned incubation period and post-infectious virus shedding period together with the infectious period contribute to the disease transmission (Chadsuthi & Wichapeng, 2018; Phutthichayanon & Naowarat, 2015; Podin et al., 2006; Shi et al., 2018; Teng et al., 2013). Therefore, we cannot ignore some of the known biological factors while studying the HFMD behaviors. With this, we present our SEIPR model by adding in the complete biological factors with the aim to provide a more suitable framework to deliberate the HFMD behaviors.

Next, we will look at the threshold value. As mentioned in Section 2.3.3, threshold value is minimum proportion of the population in which creates the liability of disease spreading. Threshold value formulated is shown at equation (4.30). Figure 4.19 shows the real infectious cases and predicted infectious cases are having a good match at the first wave by visual inspection. The calculated threshold value benchmark is 4642, which means the outbreak occurs when the susceptible exceeds this value for the first wave of outbreak in 2006.

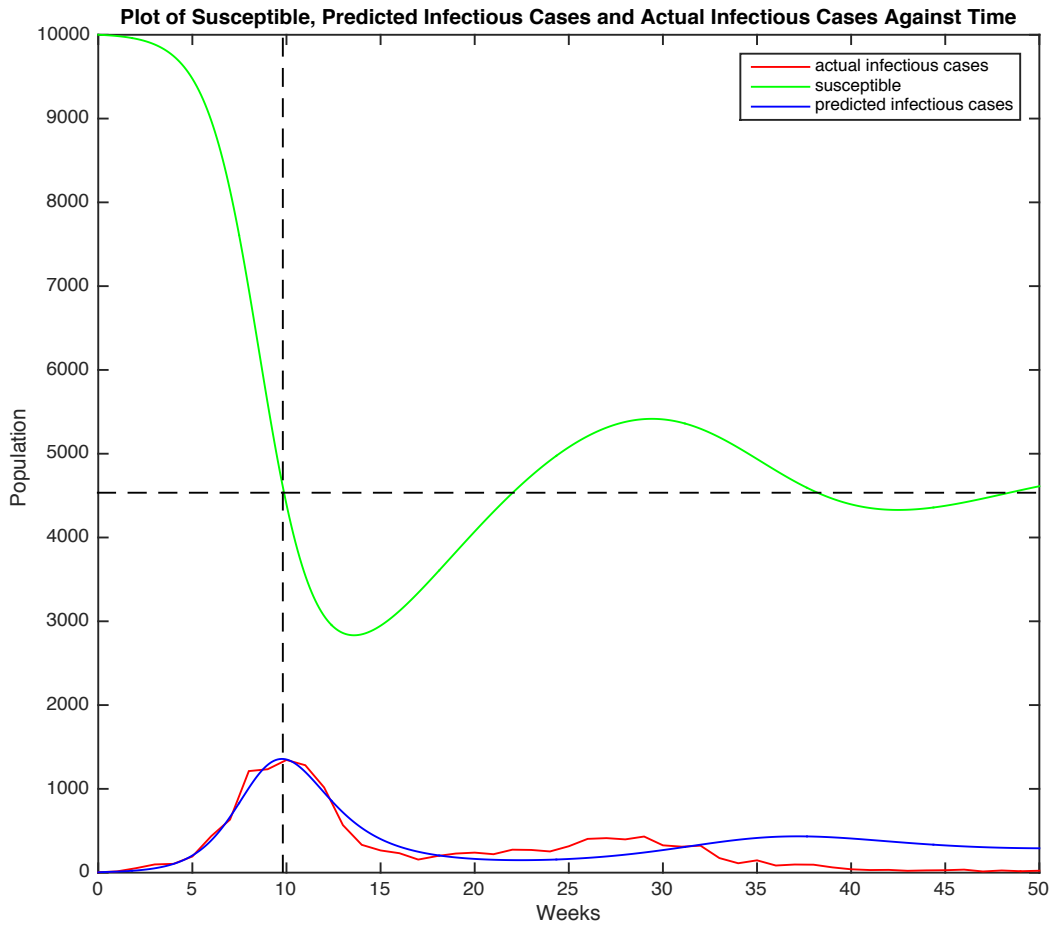

Figure 4.19: Susceptible, predicted infectious cases and actual infectious cases based on SEIPR model, year 2006. Dashed line indicated threshold value.

Basic reproductive number, R_0, on the other hand, is the average number of secondary infections produced by an infectious case in a complete susceptible population. The equation (4.26) allows the R_0 to be found. The R_0 consists of three terms, which are R_1, R_2 and R_3. After calculation, we found that R_0 is 2.15 where the R_1 is 0.05, R_2 is 1.5 and R_3 is 0.6, indicating that the disease invaded the susceptible rapidly and outbreak occurred. The R_0 of 2.15 means that every infectious child would infect almost two to

three children over the course of his or her entire infectious period. The first term, R_1 is 0.05, showing that the incubation group was mildly infectious but still had the capability to transmit the disease even the infected individual had not shown any symptom. In the meantime, the second term, R_2 is 1.5, which means the infectious individual was the most contagious during the infectious period. During this time, the patients had shown the HFMD symptoms, thus, the patients would be advised to stay isolation and avoid having close contact with others. Meanwhile, $R_3 = 0.6$, saying that after the symptoms subsided, the HFMD viruses continued to shed and still could cause the virus transmission and contributed to the number of infected cases. After this, regression analysis is done by using linear regression equation, correlation coefficient and residuals plot. As discussed in Section 2.3.4, regression analysis is a goodness of fit method to test the best match between the observed data and predicted data. The linear regression plot, linear regression equation, correlation coefficient, r^2 and residuals plot are done by using the built-in regression analysis programs in the Matlab. We will use the regression analysis to test the goodness of fit for the predicted data and actual data up to 13 weeks for year 2006 outbreak.

Table 4.5: Results of the observed values and predicted values by using SEIPR model, year 2006.

Outbreak in 2006		
Weeks	**Actual infectious cases**	**Predicted infectious cases**
0	4	4
1	15	16
2	53	46
3	98	96
4	105	104
5	193	192
6	435	433
7	633	635
8	1212	1218
9	1234	1280
10	1345	1349
11	1282	1194
12	1017	1021
13	567	563

Based on the results in Table 4.5, the predicted infectious data and observed infectious data are plotted and shown in Figure 4.20. The best fitting straight line as mentioned in Section 2.3.4.2 is found. The best fitting line or called as linear regression equation is $y = x + 1.783$. Furthermore, as mentioned in Section 2.3.4.3, we will get the r-square, r^2, or being called as correlation coefficient in which is used to read the respond of the variability between the actual data and the predicted data around its mean. The higher the value of the r^2 means that the variability of the actual and predicted data had higher responds around its mean and indicating a better fit. From the built-in program in Matlab, we get $r^2 = 0.9973$.

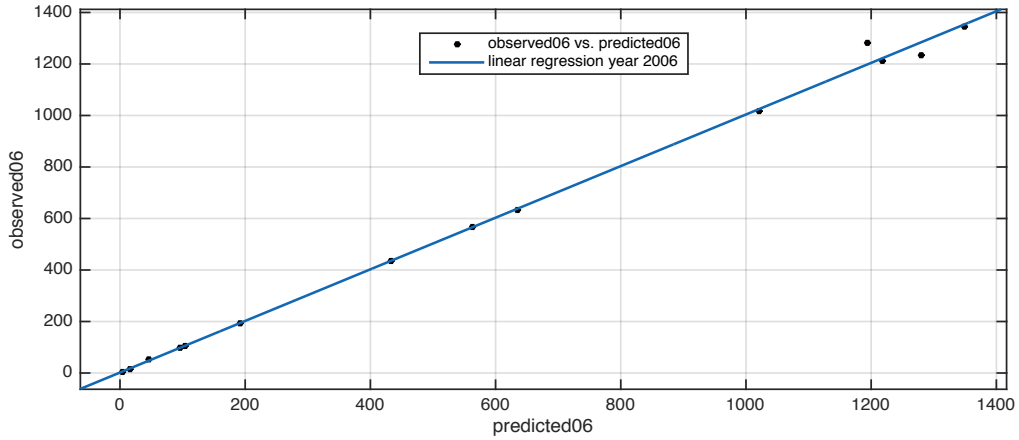

Figure 4.20: Simple linear regressions plot, year 2006.

Then, in order to make the goodness of fit more reliable, we continue the testing by residuals plot. In Section 2.3.4.4, it mentioned that the residuals plot is a graph that all the residuals are plotted on the y-axis and predicted values are plotted on the x-axis. If the points in a residual plot are dispersed randomly around the horizontal line, thus the linear regression model is appropriate for the data. Hence, the validation of the mathematical model is convincing.

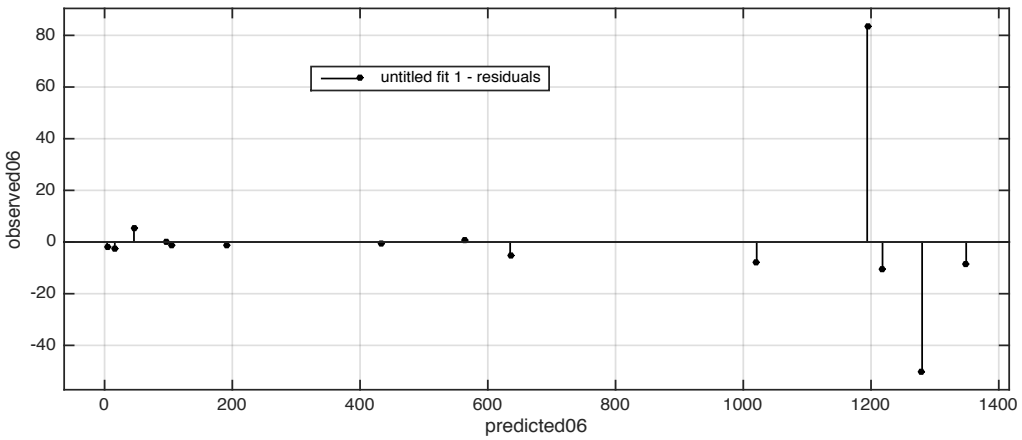

Figure 4.21: Residuals plot, year 2006.

In Figure 4.21, the residuals plot shows that most of the residuals are dispersed near the horizontal line. Meanwhile, the correlation coefficient, r^2 equals to 0.9973, means that 99.73% of the variability of the data used from SEIPR prediction cases and the actual infectious cases for the year 2006 has the respond around its mean. With this, we conclude that the SEIPR model is stable for the prediction infectious cases for the first 13 weeks, year 2006.

From Figure 4.19, we can see clearly the model can help to predict the second wave of the virus spreading, however, the prediction shows that the spreading of the disease is slightly advance compare to the real data. This may due to the changing transmission parameters (Lai et al., 2016) as after the peak infectious cases, public health personnel had taken the preventions and precautions into the account to educate the public to raise the awareness in order to curb the virus spreading. The changing of the contact pattern altered the transmission coefficient resulted the second wave of the outbreak had a different transmission compare with the first wave.

As a result, the force of infection plays an important role in disease spreading. The outbreak can only occur when a cohort of children who have not been exposed to the disease encounter the viruses. Other transmission parameters that are β_1, β_5 and β_6 play the significant role in virus spreading as well because the transmission parameters take into account the close contact and transmission probability. When there are infectious individuals being introduced to the group and multiply with the transmission parameters, force of infection produces the newly infected individual.

Finally, after the simulation and goodness of fit test, we conclude that the close contact between the susceptible and transmission parameters play the significant roles for causing the infectious dynamic wave. The validation of the SEIPR model is reliable and

stable to predict the infectious cases for the first wave of outbreak. For next sections, we will discuss the simulation done by using the clinical data for the years 2010, 2011, 2012, 2013 and 2014 obtained from Sarawak Health Department.

4.4.3 Numerical results for SEIPR model, year 2010

As mentioned in Section 4.4.1, fixed parameter values taken to run the simulation are $R=0,\ S=10000,\ \beta_3=1,\ \beta_4=1$ and $\beta_7=0.07$. Fitting values are $E=50,\ \beta_1=0.00001,$ $\beta_2=5.5,\ \beta_5=0.00009$ and $\beta_6=0.00003$. Actual values are $I=121,\ P=100,$ $k_1=0.0003212,\ k_2=0.000005192$ and $k_3=0$.

The above k_1 and k_2 were calculated by using the following formulae steps:

$$k_1=\frac{\frac{crude\ birth\ \ rate}{1000}\times 100}{52}=\frac{\frac{16.2}{1000}\times 100}{52}=0.03212\%\ \ per\ week$$

$$k_2=\frac{\frac{crude\ death\ \ rate}{1000}\times 100}{52}=\frac{\frac{0.27}{1000}\times 100}{52}=0.0005192\%\ per\ week$$

The numerical result for SEIPR model, year 2010 is shown at Figure 4.22. The result shown is validated by the HFMD clinical data, year 2010.

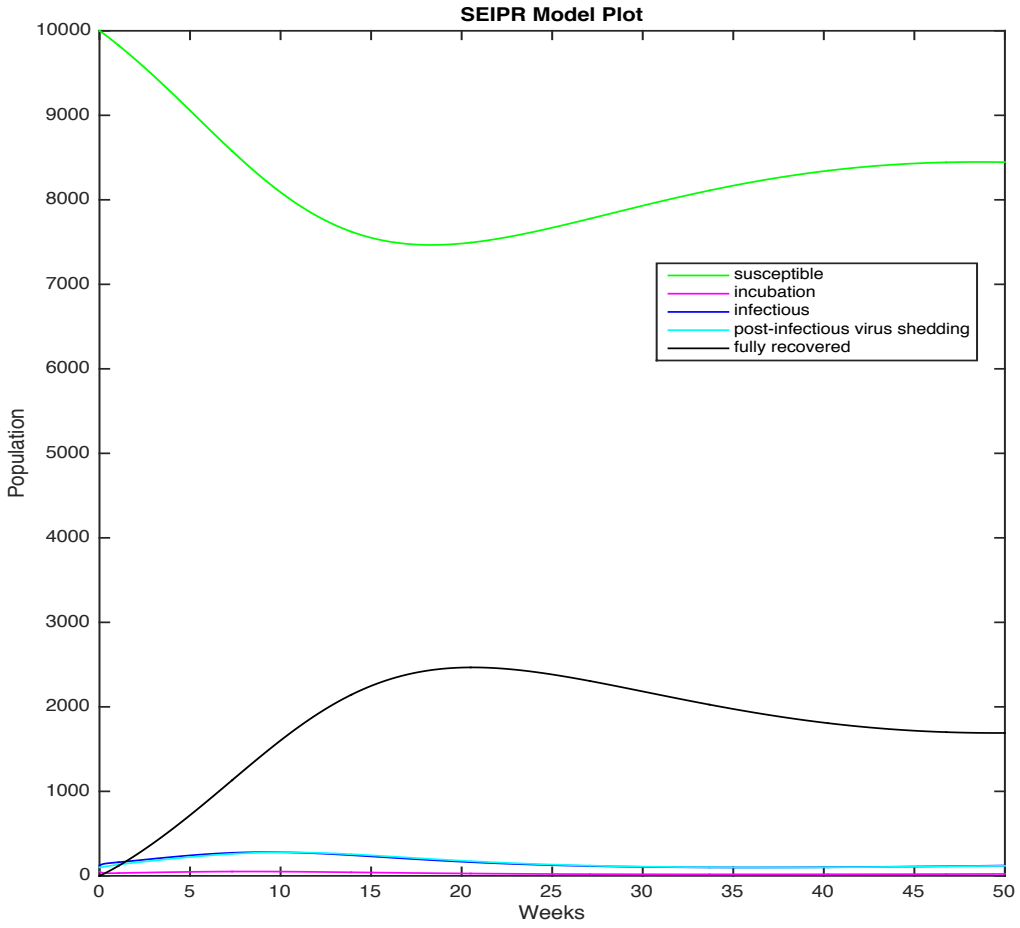

Figure 4.22: The predicted cases of the SEIPR model for susceptible, incubation period, infectious, post-infectious virus shedding and fully recovered over the time, year 2010.

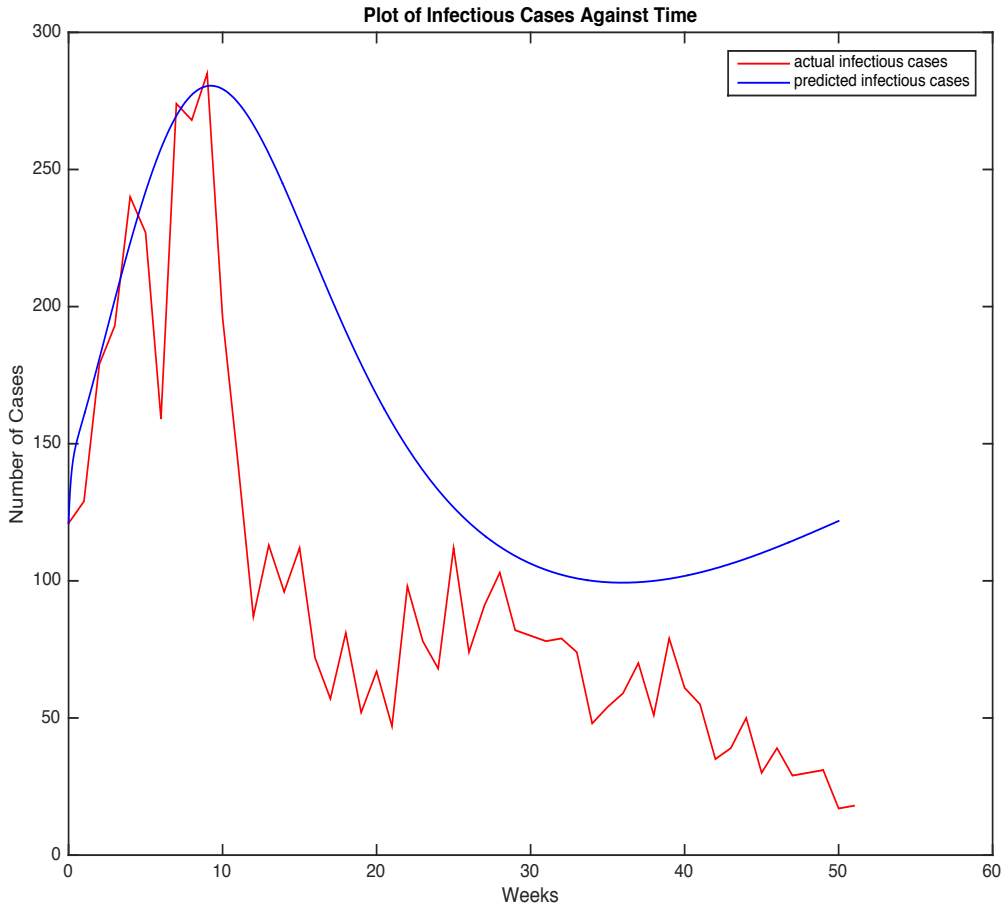

Figure 4.23: Comparison of the actual infectious cases and predicted infectious cases, year 2010.

From Figure 4.23, by visual inspection, the comparison of the actual infectious cases and predicted infectious cases shows the best fit at the first wave for ten weeks. Since the predicted data and actual data reach the peak at the same time, next, we will look at the threshold value. By using the equation (4.30), the threshold value calculated is 8209. It can be seen from Figure 4.24.

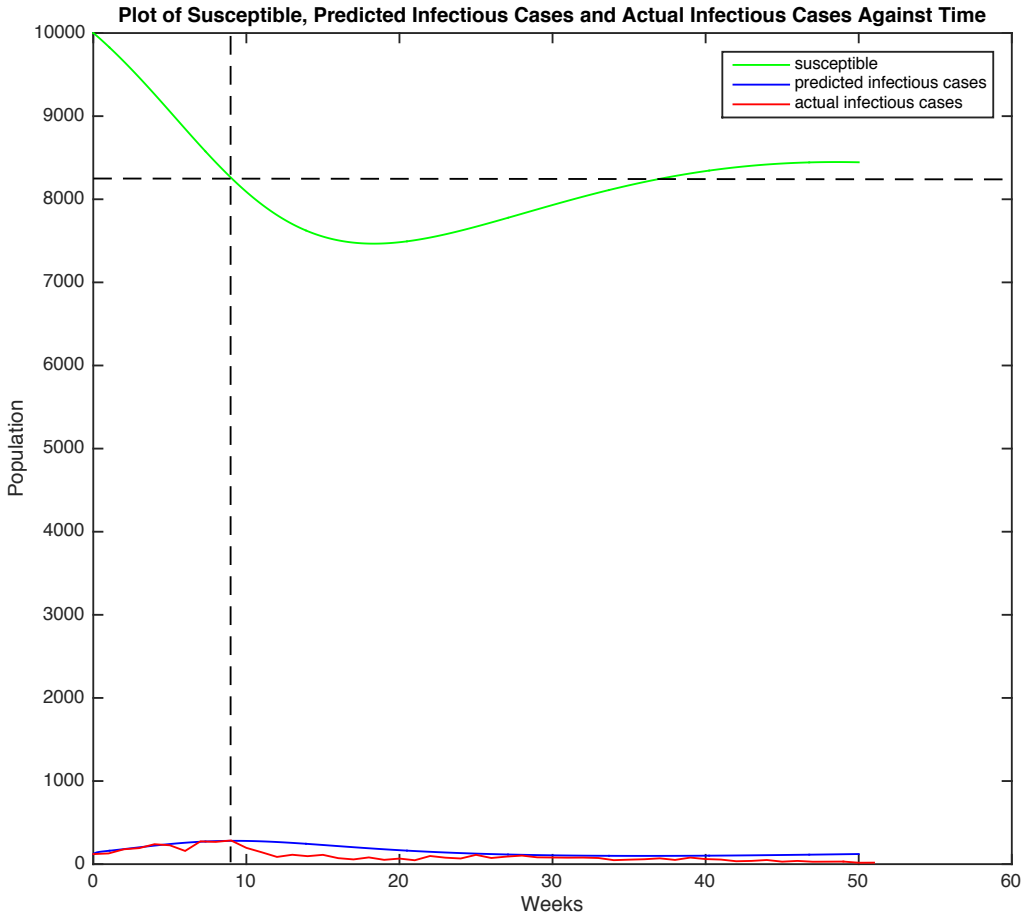

Figure 4.24: Susceptible, predicted infectious cases and actual infectious cases based on SEIPR model, year 2010. Dashed line indicated threshold value.

By comparing the threshold value to year 2006, threshold value in year 2010 is higher and transmission coefficients for β_1, β_5 and β_6 are lower, this explains that the outbreak in 2010 had a smaller number of the infectious cases than year 2006.

On the other hand, the basic reproductive number, R_0, is 1.22. Based on the formula from equation (4.26), $R_1 = 0.018$, $R_2 = 0.9$ and $R_3 = 0.3$. From the result, incubation group was mildly infectious, followed by post-infectious group and the

infectious group was the most contagious. As mentioned earlier in Section 2.3.2, R_0>1 indicates the outbreak occurs. In year 2010, based on the analysis, the outbreak was mainly contributed by infectious individuals but also was caused by post-infectious patients as R_2 itself could not reach value of one. Next, we will use the regression analysis to test the goodness of fit for the predicted data and actual data up to 10 weeks.

Table 4.6: Results of the observed values and predicted values, year 2010.

Outbreak in 2010		
Weeks	**Actual infectious cases**	**Predicted infectious cases**
0	121	121
1	129	136
2	179	182
3	193	203
4	240	241
5	227	243
6	159	259
7	274	274
8	268	277
9	285	280
10	196	275

The predicted infectious data and observed infectious data in Table 4.6 are plotted and shown in Figure 4.25. The best linear regression equation is $y = 0.8038x + 24.43$ and $r^2 = 0.6609$.

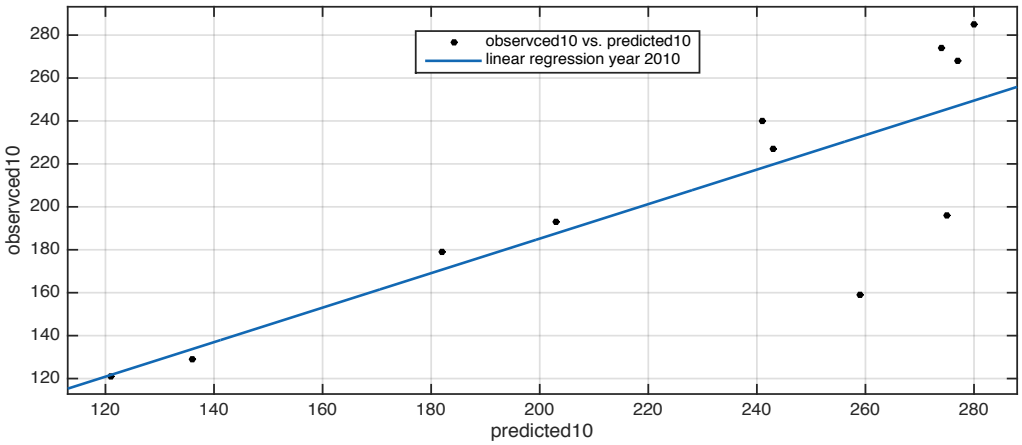

Figure 4.25: Simple linear regressions plot, year 2010.

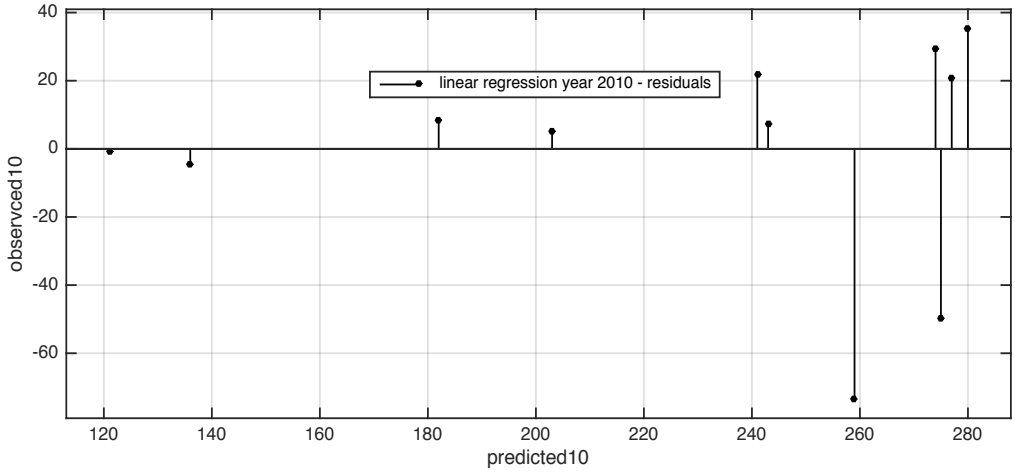

Figure 4.26: Residuals plot, year 2010.

In Figure 4.26, the residuals plot shows that most of the residuals are randomly dispersed near the horizontal line although there are a few outliers that are dispersed far from the observed data (actual data). Next, the correlation coefficient, r^2 equals to 0.6609, means that 66.09% of the variability of the data used from SEIPR prediction cases and the actual infectious cases for the year 2010 has the respond around its mean. The outliers do not bring big impact to the data as we can see in Figure 4.23, the predicted data and real

data have shown the same spreading duration for the first wave to reach the peak and thus we conclude that the SEIPR model is stable for the prediction infectious cases for the first 10 weeks, year 2010.

4.4.4 Numerical results for SEIPR model, year 2011

Based on the actual infectious cases in year 2011 (Figure 4.28), we decide to consider two waves in doing the simulation because the first wave is not an outbreak. From our verification done in Section 4.4.1, our model able to predict the first wave of the outbreak each year. So, since the outbreak starts nearly after week 21 in 2011, we separate the study case to two parts, which are first dynamic wave from zero week to week 21 and second dynamic wave from week 21 to week 50. 21 week as the cut-off point taken from the middle point by estimation between the endemic and first fluctuating outbreak points. In 2011, initial conditions and parameter values taken to run the simulation are as follows:

A First dynamic waves of the HFMD, from zero week to week 21

Fixed parameter values taken to run the simulation are $R=0$, $S=10000$, $\beta_3=1$, $\beta_4=1$ and $\beta_7=0.07$. Fitting values are $E=10$, $\beta_1=0$, $\beta_2=5.5$, $\beta_5=0.0001$ and $\beta_6=0$. Actual values are $I=33$, $P=10$, $k_1=0.0003308$, $k_2=0.000005154$ and $k_3=0$.

B Second dynamic waves of the HFMD, from week 21 to week 50

Fixed parameter values taken to run the simulation are $\beta_3 = 1,\ \beta_4 = 1$ and $\beta_7 = 0.07.$ Fitting values for $I = 25,\ R = 350$ and $S = 9700$ are taken based on the estimation from the graphs after 21st week by visual inspection and best fit of the simulation, whereas $P = 10$ and $E = 10$ are fitting values taken same as first wave while $\beta_1 = 0.000025,$ $\beta_2 = 5.5,\ \beta_5 = 0.00008$ and $\beta_6 = 0.000032$ are fitting values of the best fit Actual values are $k_1 = 0.0003308,\ k_2 = 0.000005154$ and $k_3 = 0$.

The numerical result for SEIPR model, year 2011 is shown at Figure 4.27. The result shown is validated by the HFMD clinical data, year 2011. Figure 4.27 shows the dynamic characteristic of the SEIPR model. The dashed line separates the dynamic waves to two parts, first dynamic wave with total of 21 weeks and second dynamic wave is shown after week 21. The predicted cases in Figure 4.27 is enlarged in Figure 4.28.

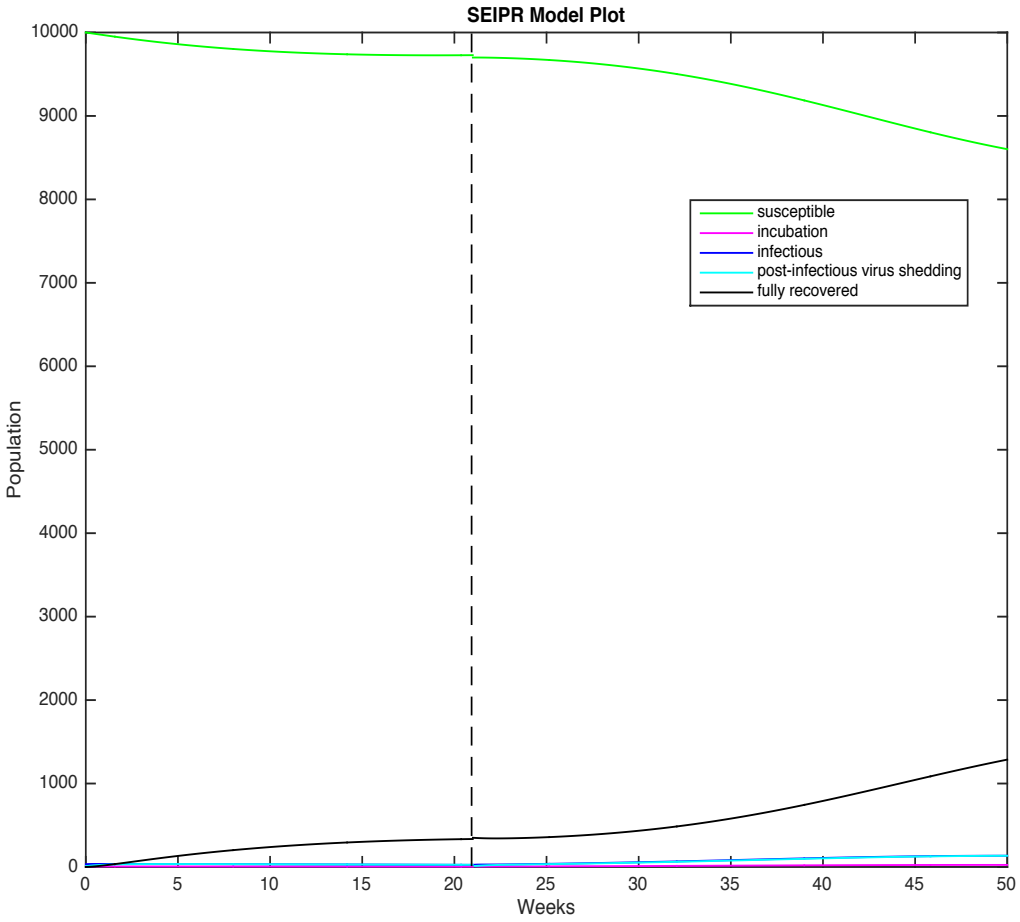

Figure 4.27: The predicted cases of the SEIPR model for susceptible, incubation period, infectious, post-infectious virus shedding and fully recovered over the time, year 2011. Dashed line separated the dynamic waves to two parts, first 21 weeks and after 21 weeks.

Whereas, from the Figure 4.28, the best fit between the predicted data and the observed data is lasted for 45 weeks by visual inspection. By looking at the infected behavior curve from the first dynamic wave, there was no outbreak occur. However after about 21 week, outbreak occurred. Next, we proceed to the threshold value and R_0.

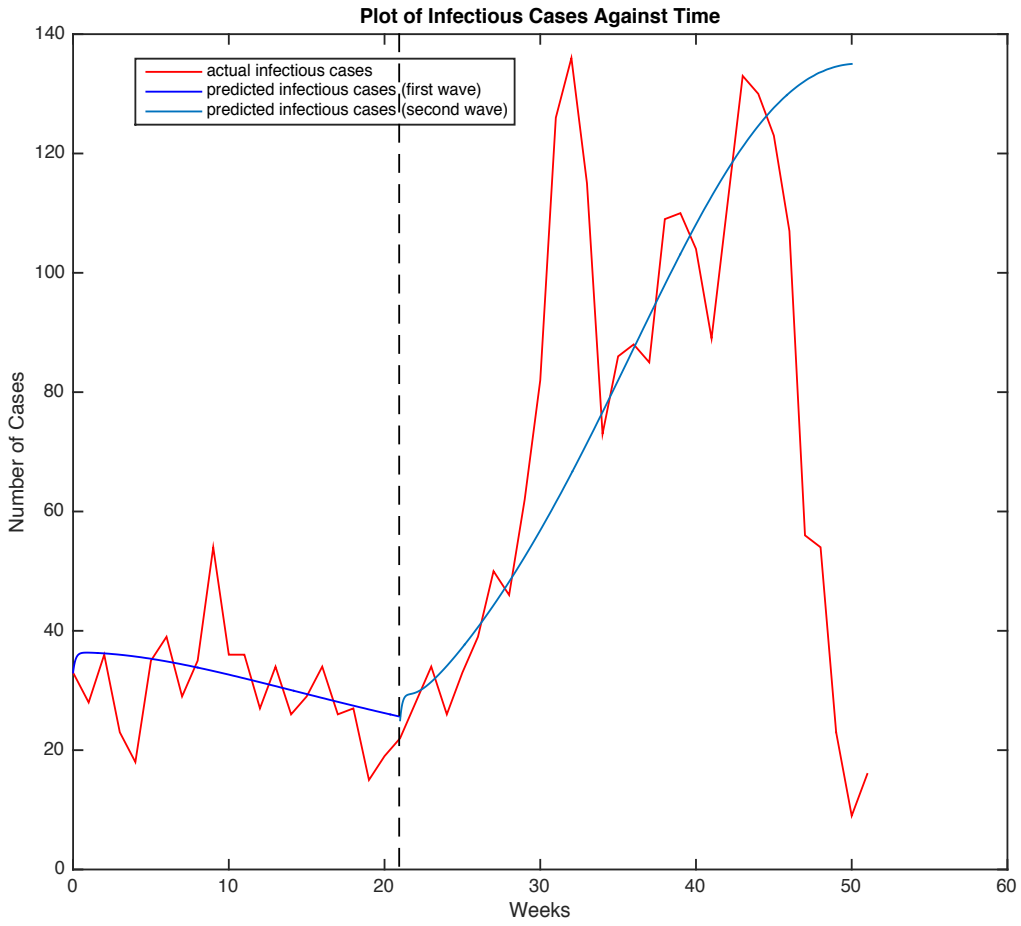

Figure 4.28: Comparison of the actual infectious cases and predicted infectious cases, year 2011. Dashed line separated the dynamic waves to two parts, first 21 weeks and after 21 weeks.

As mentioned in Section 4.3.5, when R_0 =1, it is given us the disease-free equilibrium point and also if R_0 =1, it means that there will be approximately the same number of infected cases all the time, which the endemic occur. Virulence during the first wave do not have the ability to attack the susceptible, thus, there is no benchmark to decide the minimum proportion of the population to create the liability of disease spreading. However, by looking at Figure 4.27, there is slightly dropping of the susceptible curve and

slightly increasing at the recovery curve at the first wave. This explains that when $R_0 = 1$, there were still infected cases but the number of infected cases are approximately same all the time and hence, no outbreak occurs.

For second wave, the threshold value is 8580 and R_0 is 1.13. The scenario explains that after 21 weeks, the virus meets the cohort and outbreak occurs. From the calculation, R_0 is obtained from incubation period patients with $R_1 = 0.044$, infectious patients, $R_2 = 0.78$ and post-infectious patients, $R_3 = 0.31$. The outbreak occurs due to the increasing transmission coefficients from β_1 and β_6. The incubation period patients and post-infectious patients together with the infectious patients play the role to transmit the disease and cause the outbreak around the middle of the year. This may due to the remaining disease in the population at the beginning of the year caused the outbreak when the viruses met the cohort.

On the other hand, from Figure 4.29, for the outbreak to reach the peak, the predicted threshold value calculated is 8580. Figure 4.30 is enlarged figure for predicted infectious cases and actual infectious cases which appeared too small at the bottom of Figure 4.29. Since the timing for actual and predicted infectious cases to reach peak number are different, we can see from the Figure 4.30, the actual infectious reached the peak faster (dotted line) compare to the predicted data (dashed line). Thus the threshold value for year 2011 is recommended for reference only. The actual threshold value was higher than 8580. By comparing with year 2010, the threshold value is higher and the R_0 is lower in year 2011, means that less people were infected in year 2011 compare to 2010. Next, the goodness of fit test is done by using regression analysis for the predicted data and actual data up to 45 weeks.

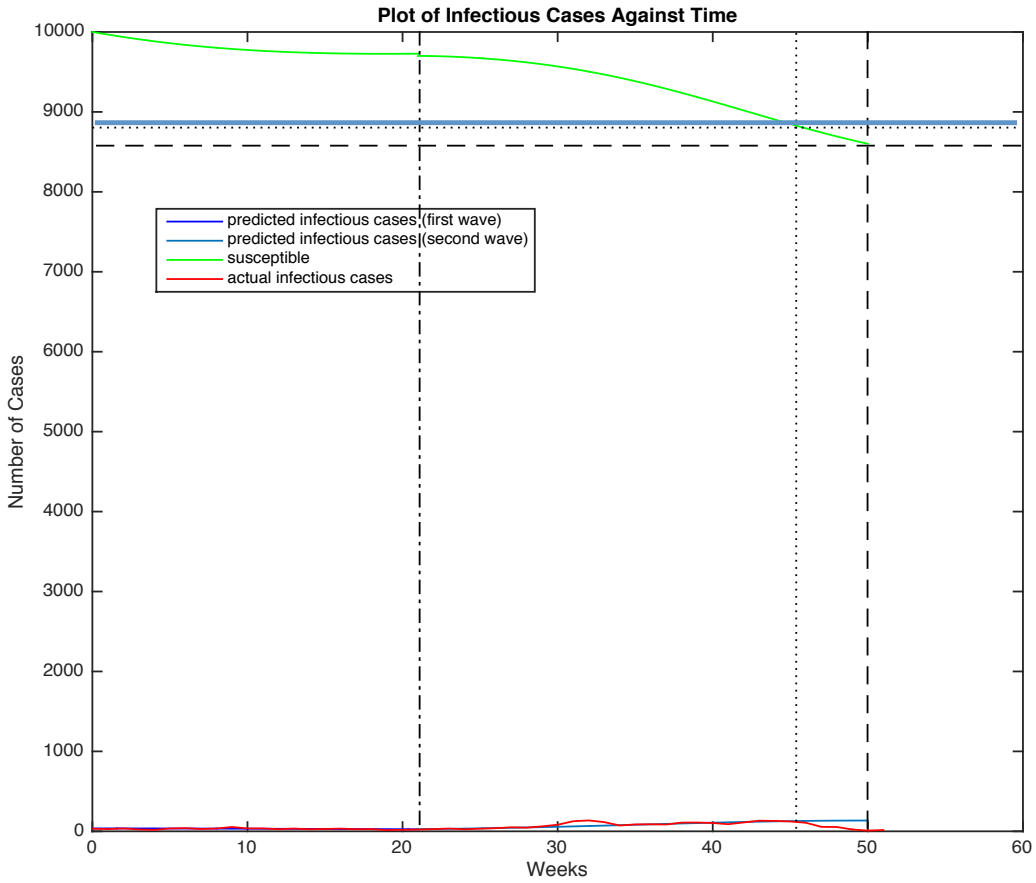

Figure 4.29: Susceptible, predicted infectious cases and actual infectious cases based on SEIPR model, year 2011. Dashed line indicated threshold value of predicted data. Dotted line indicated threshold value of real data. Dashed-dotted line separated the dynamic waves to two parts, first 21 weeks and after 21 weeks.

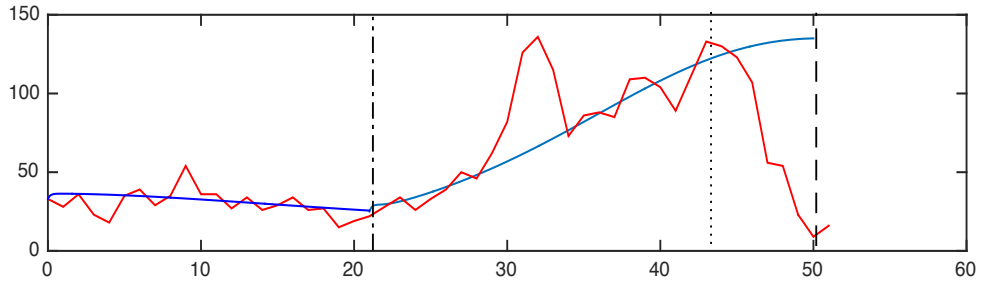

Figure 4.30: Enlarge figure for predicted infectious cases and actual infectious cases from Figure 4.29.

Table 4.7 shows the predicted and actual data. Figure 4.31 shows the best fitting straight line. Linear regression equation obtained as $y = 1.031x + 0.874$. Furthermore, correlation coefficient, r^2 found is 0.8201, means that 82.01% of the variability of the data used from SEIPR prediction and the actual infectious cases for the year 2011 has the respond around its mean.

Table 4.7: Results of the observed values and predicted values, year 2011.

Outbreak in 2011		
Weeks	**Actual infectious cases**	**Predicted infectious cases**
0	33	33
1	28	36
2	36	36
3	23	35
4	18	35
5	35	35
6	39	34
7	29	33
8	35	33
9	54	32
10	36	32
11	36	31
12	27	30
13	34	30
14	26	29
15	29	29
16	34	28
17	26	27
18	27	27
19	15	26
20	19	25
21	22	25
22	28	29
23	34	33
24	26	34
25	33	37
26	39	41
27	50	48
28	46	51
29	62	56

Table 4.7 continued

30	82	61
31	126	64
32	136	71
33	115	76
34	73	79
35	86	86
36	88	90
37	85	93
38	109	107
39	110	107
40	104	108
41	89	113
42	111	117
43	133	124
44	130	127
45	123	128

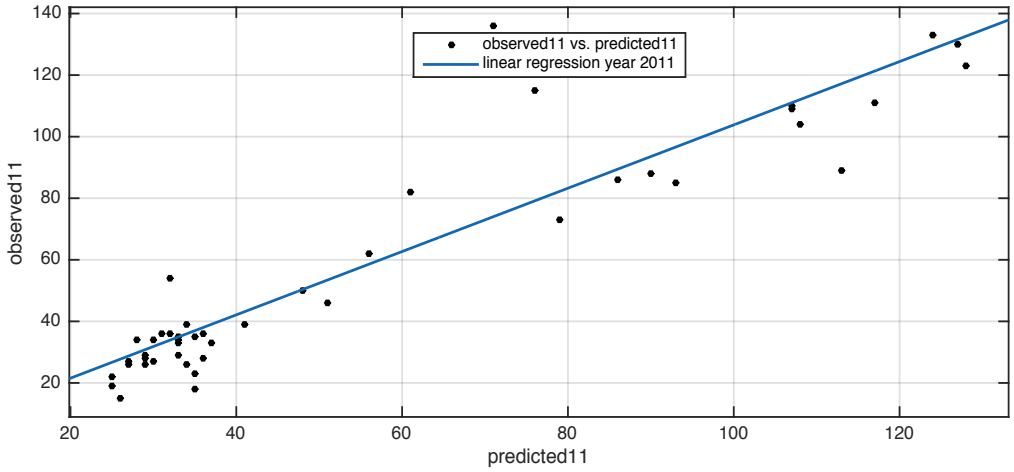

Figure 4.31: Simple linear regressions plot, year 2011.

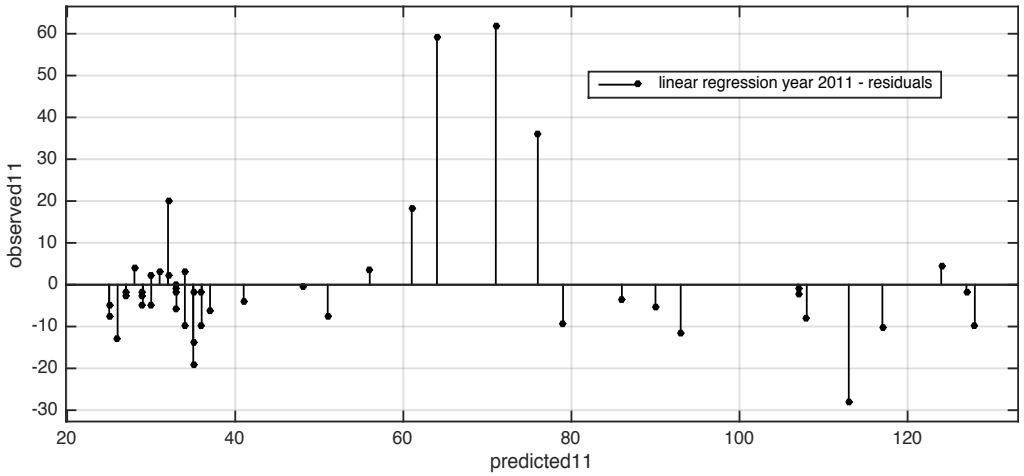

Figure 4.32: Residuals plot, year 2011.

Meanwhile from residuals plot (Figure 4.32), most of the residuals are randomly dispersed near the x-axis. With this, we conclude that the SEIPR model is stable for the prediction infectious cases for the year 2011 up to 45 weeks.

4.4.5 Numerical results for SEIPR model, year 2012

Fixed parameter values taken are $R=0$, $S=10000$, $\beta_3=1$, $\beta_4=1$ and $\beta_7=0.07$. Fitting values are $E=16$, $\beta_1=0.00001$, $\beta_2=5.5$, and $\beta_5=0.000142$ and $\beta_6=0.00001$. Actual values are $I=62$, $P=16$, $k_1=0.0003212$, $k_2=0.000004923$ and $k_3=0$. The numerical result for SEIPR model, year 2012 is shown at Figure 4.33. The result shown is validated by the HFMD clinical data, year 2012.

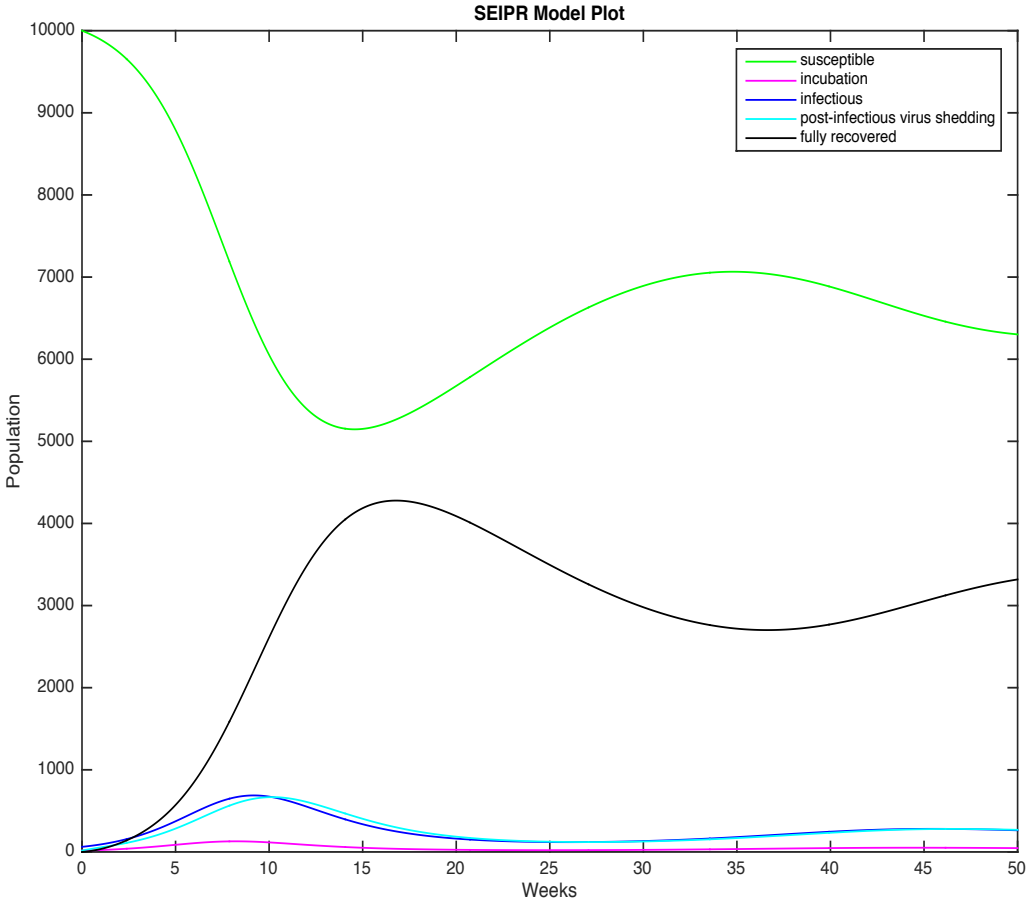

Figure 4.33: The predicted cases of the SEIPR model for susceptible, incubation period, infectious, post-infectious virus shedding and fully recovered over the time, year 2012.

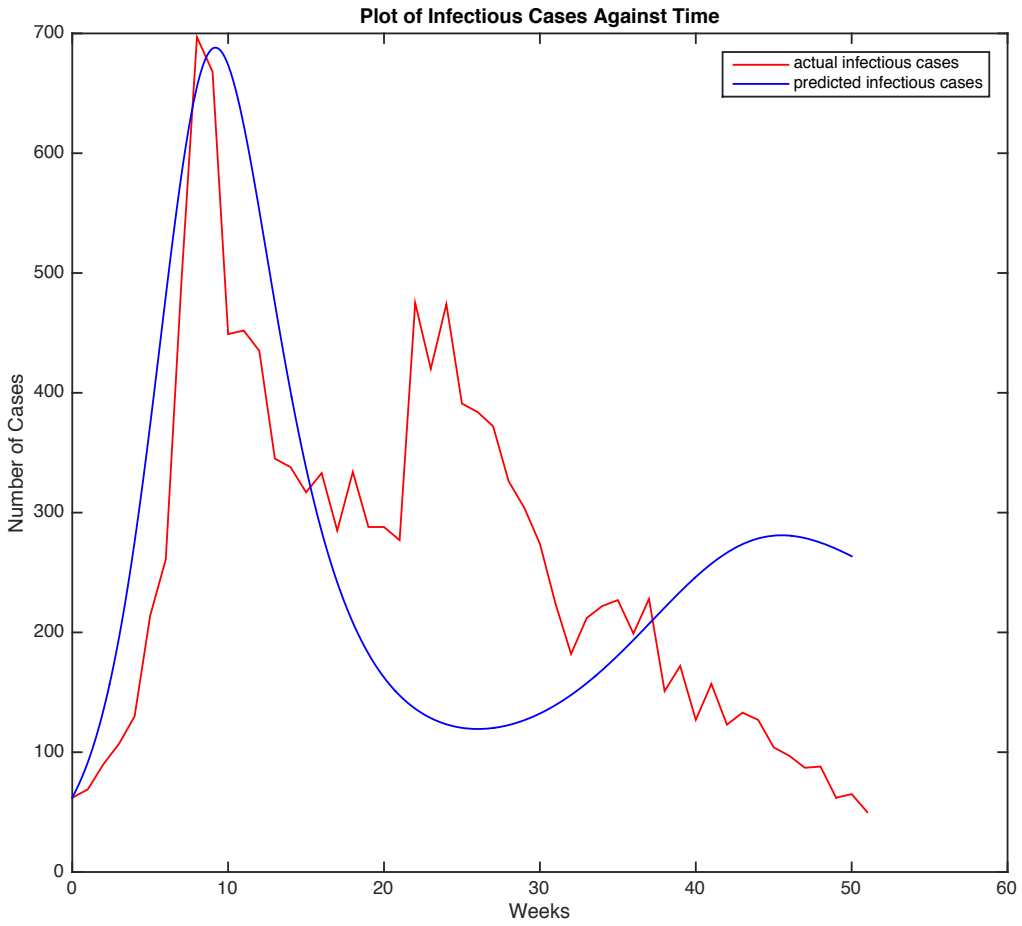

Figure 4.34: Comparison of the actual infectious cases and predicted infectious cases, year 2012.

From Figure 4.34, by visual inspection, the best fit between the predicted data and the observed data is at the first wave for first 15 weeks. Threshold value found (Figure 4.35) is 6501 and R_0 is 1.54, where $R_0 = R_1 + R_2 + R_3 =$ 0.018+1.42+0.1, thus outbreak occurred. By comparing to the year 2011, the threshold value is lower and R_0 is higher, indicating the infected cases were a lot more compare to the year 2011. The fast spreading was helped by the transmission contributed from infectious patients. Higher value of β_5

leads to $R_2 = 1.42$. Figure 4.34 shows the actual infectious cases for second wave happen faster than predicted cases. This may due to the changing of the transmission coefficients. Thus, based on our study in this case, we hope that the public health personnel can take the intervention right after the first outbreak to control the next spreading cycle.

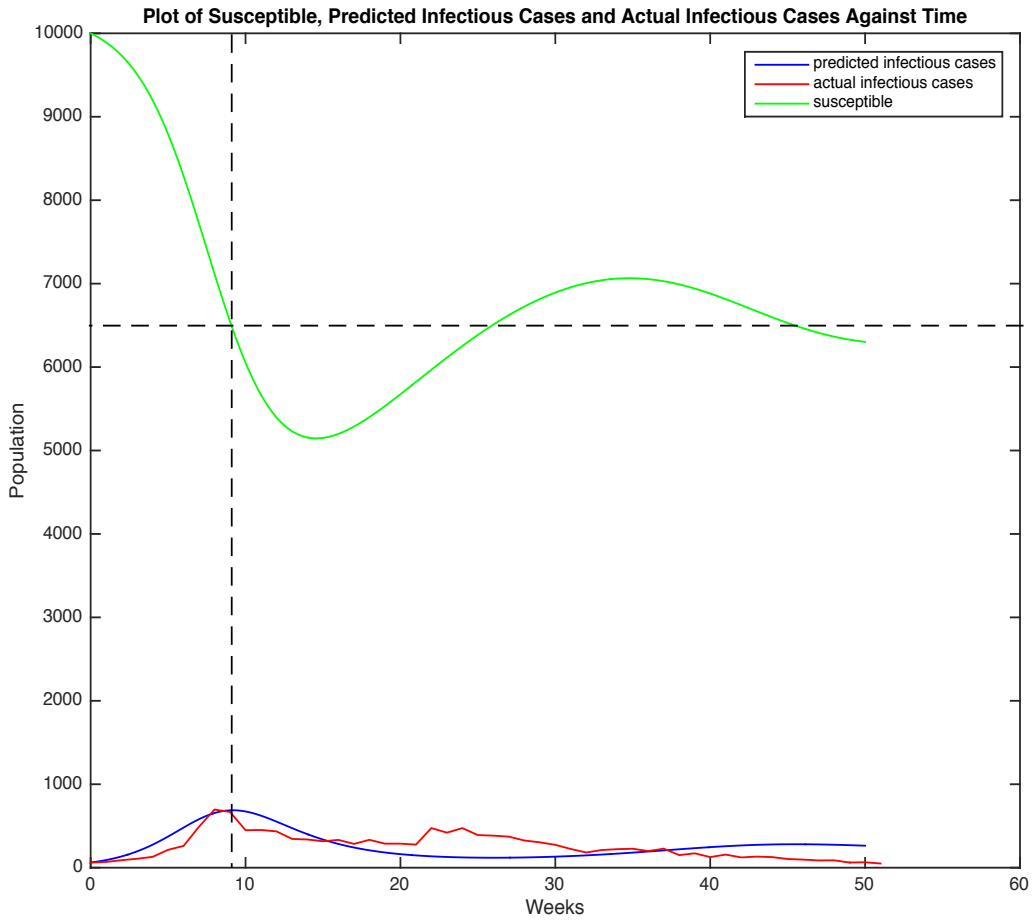

Figure 4.35: Susceptible, predicted infectious cases and actual infectious cases based on SEIPR model, year 2012. Dashed line indicated threshold value.

Table 4.8 shows the results of the observed values and predicted values. Next, we will discuss the regression analysis based on Table 4.8, Figure 4.36 and Figure 4.37.

Table 4.8: Results of the observed values and predicted values, year 2012.

Outbreak in 2012		
Weeks	**Actual infectious cases**	**Predicted infectious cases**
0	62	62
1	69	93
2	90	135
3	107	195
4	130	285
5	214	375
6	261	480
7	492	590
8	697	661
9	668	668
10	449	630
11	452	563
12	435	484
13	345	406
14	338	346
15	317	315

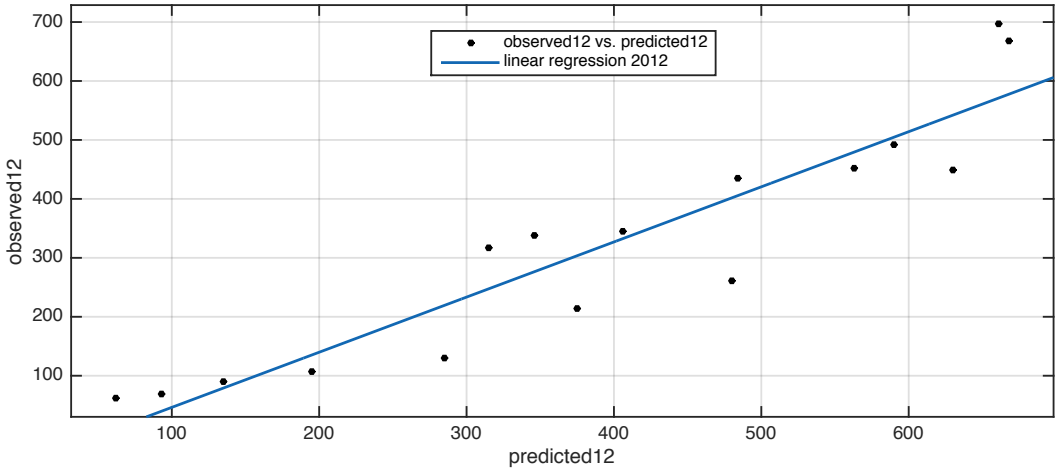

Figure 4.36: Simple linear regressions plot, year 2012.

Simple linear regression plot can be seen in Figure 4.36, and linear regression equation found is $y = 0.9353x - 47.21$. The correlation coefficient, r^2 is 0.8557, means that 85.57 % of the variability of the data used from SEIPR prediction and the actual infectious cases for the year 2012 has the respond around its mean.

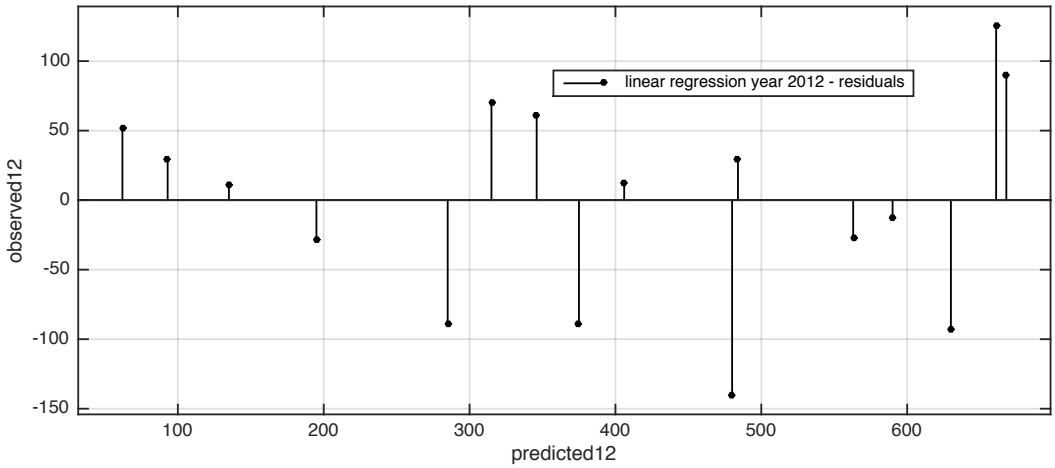

Figure 4.37: Residuals plot, year 2012.

Meanwhile from Figure 4.37, the residuals plot, we can see that most of the residuals were randomly dispersed near the x-axis. With this, we conclude that the SEIPR model is stable and able for the prediction infectious cases for the first 15 weeks, year 2012.

4.4.6 Numerical results for SEIPR model, year 2013

Fixed parameter values taken are $R=0$, $S=10000$, $\beta_3=1$, $\beta_4=1$ and $\beta_7=0.07$. Fitting values are $E=50$, $\beta_1=0.000038$, $\beta_2=5.5$, and $\beta_5=0.0001$ and $\beta_6=0.00003$. Actual values are $I=143$, $P=50$, $k_1=0.0002904$, $k_2=0.000004313$ and $k_3=0$. The numerical result for SEIPR model, year 2013 is shown at Figure 4.38. The result shown is validated by the HFMD clinical data, year 2013.

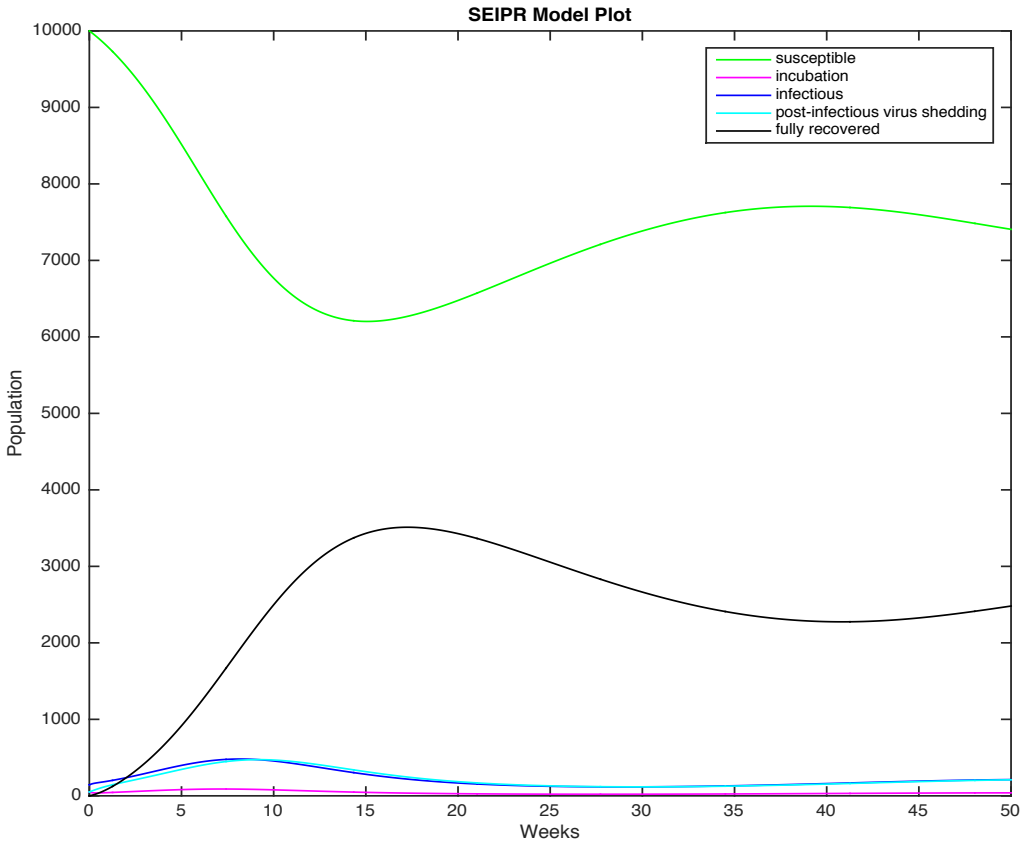

Figure 4.38: The predicted cases of the SEIPR model for susceptible, incubation period, infectious, post-infectious virus shedding and fully recovered over the time, year 2013.

From Figure 4.39, we can see that the best fit between the actual infectious data and predicted infectious data is at the first twenty-two weeks of the first wave outbreak. The threshold value found is 7304 (Figure 4.40). While R_0=1.37 indicating outbreak occurred. The outbreak was mostly contributed by infectious patients which the $R_2 = 1$. However the incubation period patient and post-infectious patients also contributed the transmission as both had $R_1 = 0.069$ and $R_3 = 0.3$. The threshold value is higher and the R_0 is lower than year 2012. Thus, the infected cases were lower than 2012. However, if compare to the years 2010 and 2011, the threshold value is lower and R_0 is higher, means that the infected cases in year 2013 were more compare with the years 2010 and 2011.

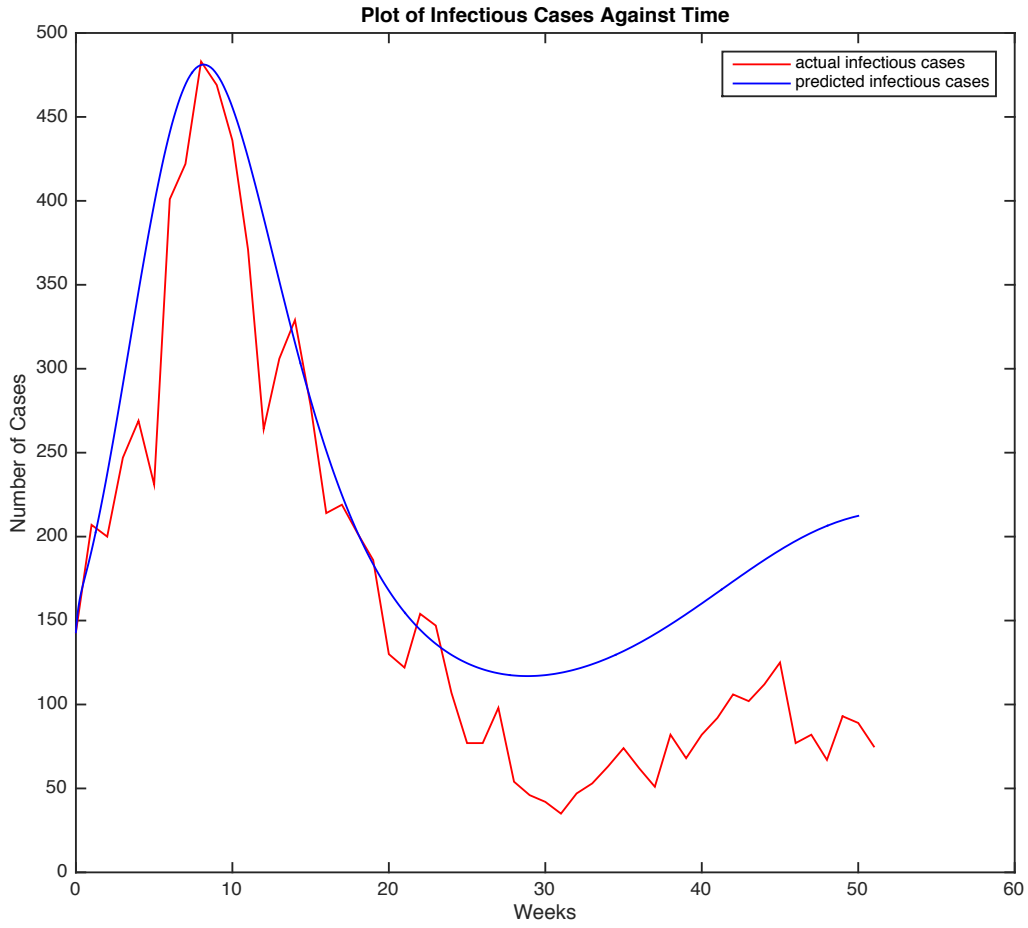

Figure 4.39: Comparison of the actual infectious cases and predicted infectious cases, year 2013.

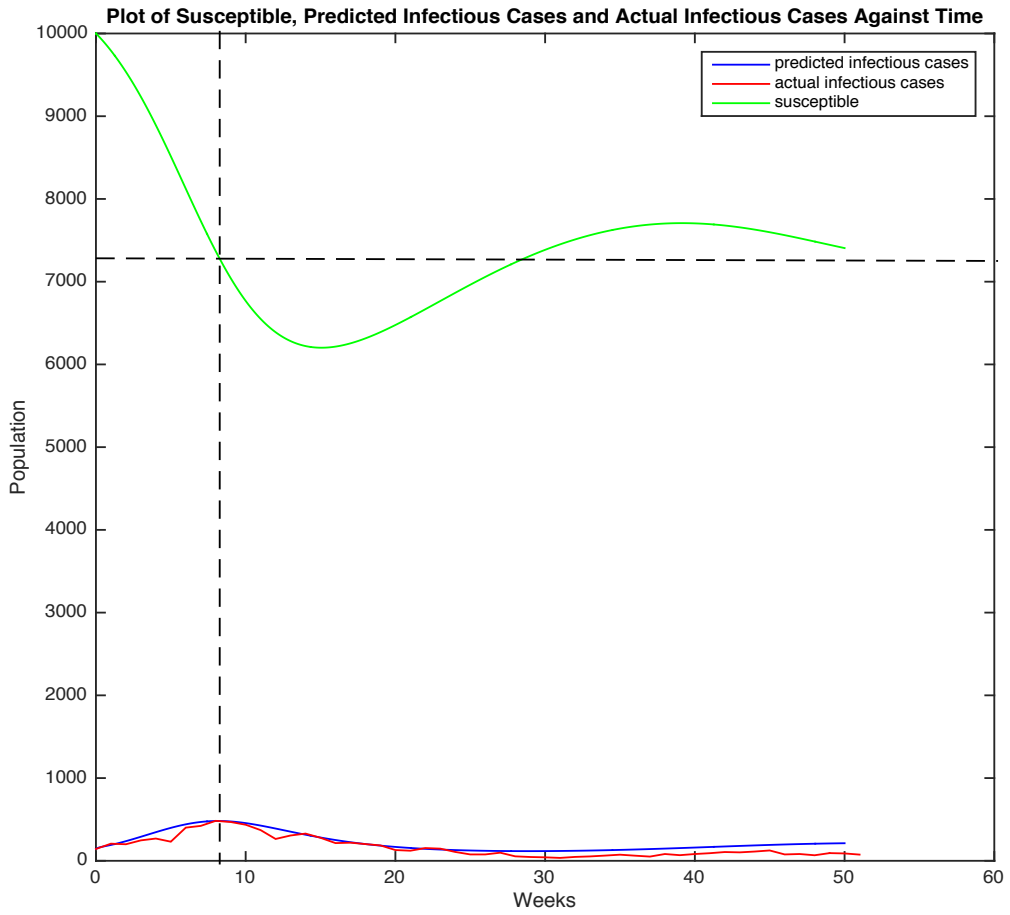

Figure 4.40: Susceptible, predicted infectious cases and actual infectious cases based on SEIPR model, year 2013. Dashed line indicated threshold value.

Next, like previous years, regression analysis is done for 2013 based on Table 4.9, Figure 4.41 and Figure 4.42. Linear regression equation in Figure 4.41 obtained is. $y = 0.8908x + 7.797$. The correlation coefficient, r^2, found is 0.8653, means that 86.53 % of the variability of the data used from SEIPR prediction and the actual infectious cases has the respond around its mean.

Table 4.9: Results of the observed values and predicted values, year 2013.

Outbreak in 2013		
Week	**Actual infectious cases**	**Predicted infectious cases**
0	143	143
1	207	207
2	200	241
3	247	290
4	269	347
5	231	398
6	401	441
7	422	470
8	483	482
9	469	468
10	436	434
11	371	393
12	264	354
13	306	318
14	329	313
15	278	276
16	214	226
17	219	220
18	202	202
19	186	183
20	130	157
21	122	145
22	154	144

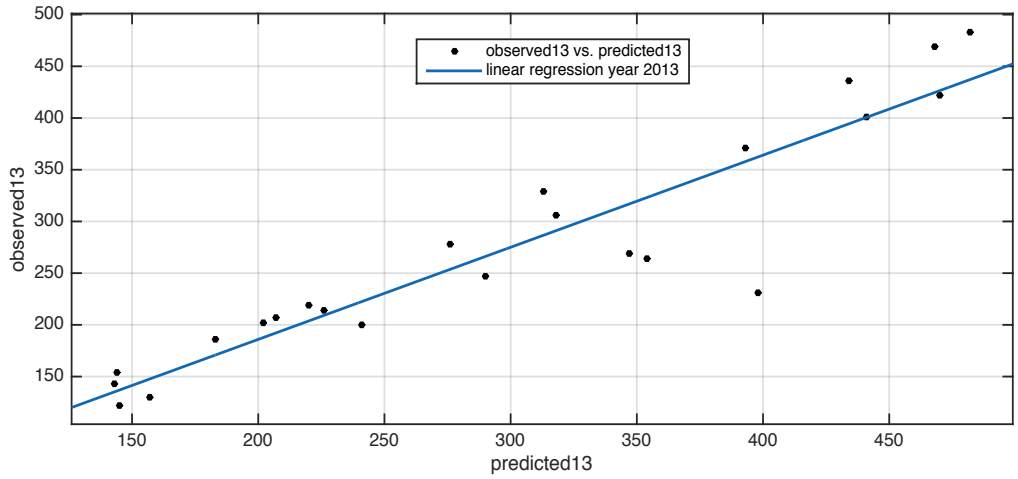

Figure 4.41: Simple linear regressions plot, year 2013.

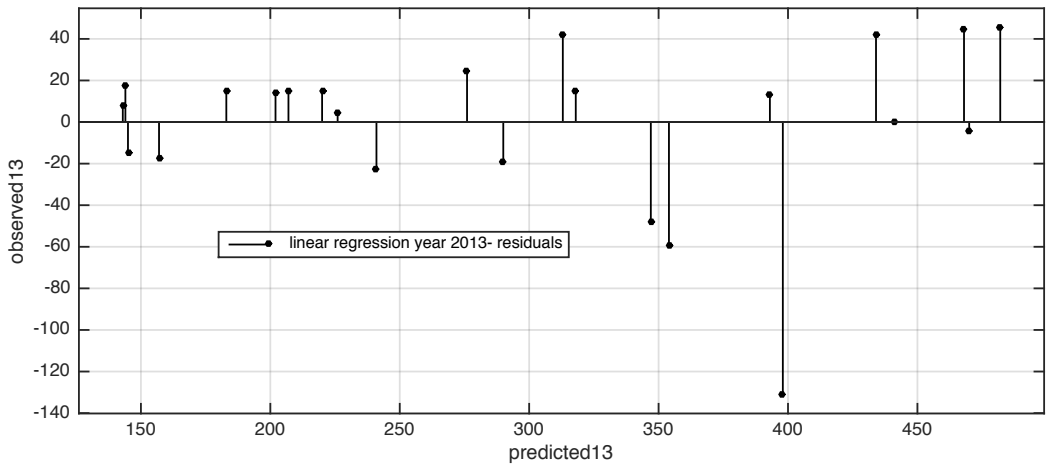

Figure 4.42: Residuals plot, year 2013.

Residuals plot (Figure 4.42) shows that most of the residuals are randomly dispersed near the x-axis. With this, we conclude that the SEIPR model is stable and able for the prediction infectious cases for the first twenty-two weeks, year 2013.

4.4.7 Numerical results for SEIPR model, year 2014

Fixed parameter values taken are $R=0,\ S=10000,\ \beta_3=1,\ \beta_4=1$ and $\beta_7=0.07.$ Fitting values are $E=10,\ \beta_1=0.000011,\ \beta_2=1.8,$ and $\beta_5=0.00011$ and $\beta_6=0.00002$. Actual values are $I=68,\ P=75,\ k_1=0.0002904,\ k_2=0.000004313$ and $k_3=0$. The numerical

result for SEIPR model, year 2014 is shown at Figure 4.43. The result shown is validated by the HFMD clinical data, year 2014.

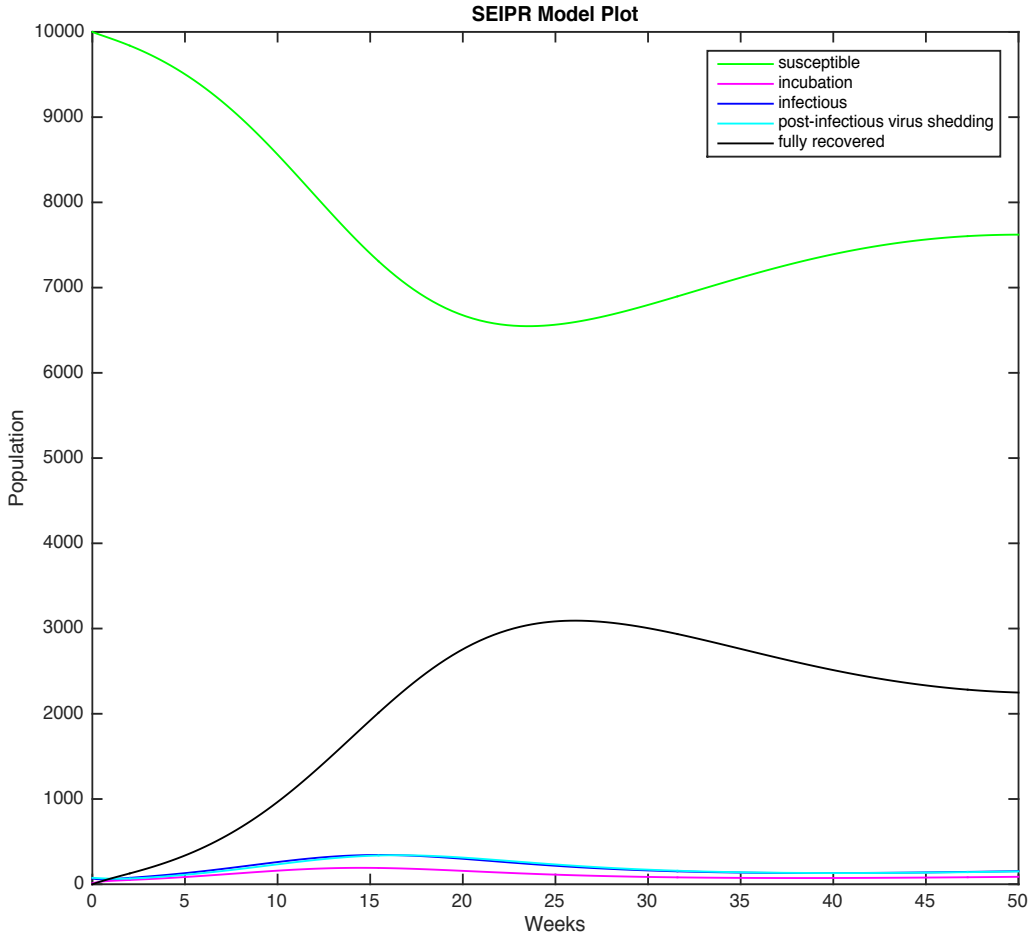

Figure 4.43: The predicted cases of the SEIPR model for susceptible, incubation period, infectious, post-infectious virus shedding and fully recovered over the time, year 2014.

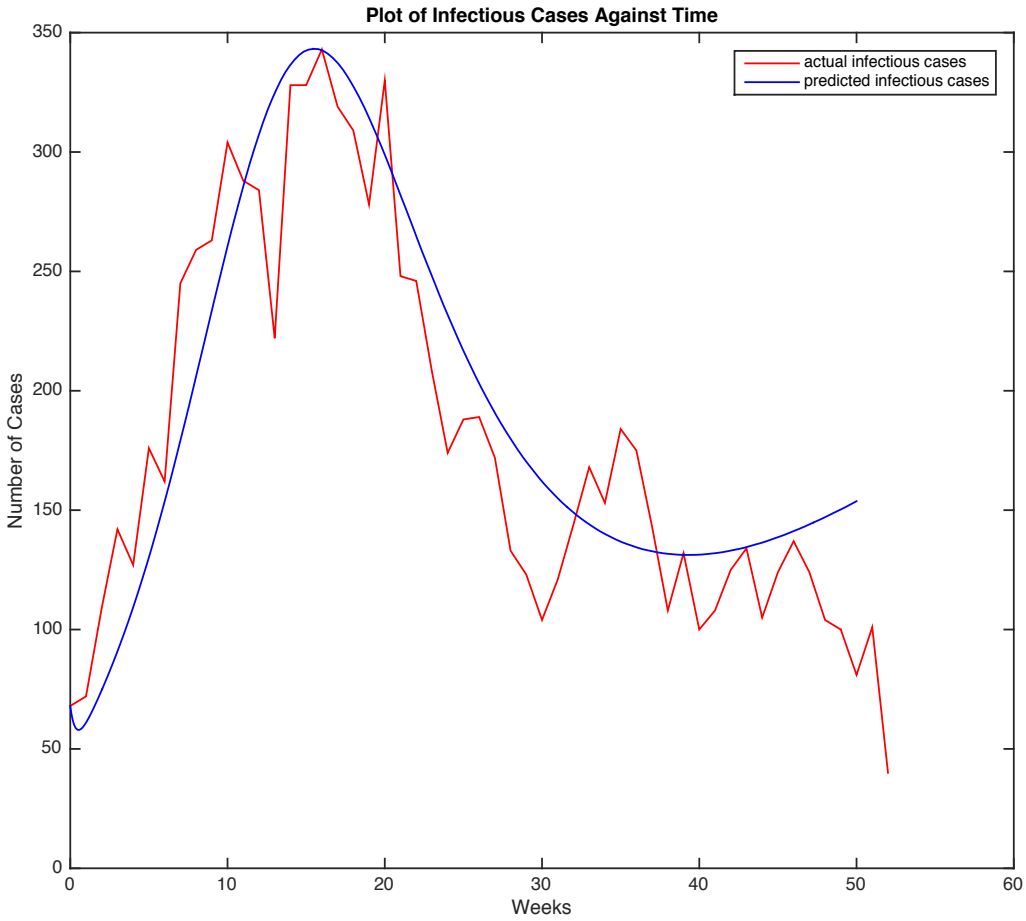

Figure 4.44: Comparison of the actual infectious cases and predicted infectious cases, year 2014.

By visual inspection, Figure 4.44 shows the best fit between the actual infectious data and predicted infectious data is at the first thirty weeks of the first wave outbreak. Threshold value calculated is 7347 and R_0 calculated is 1.36.

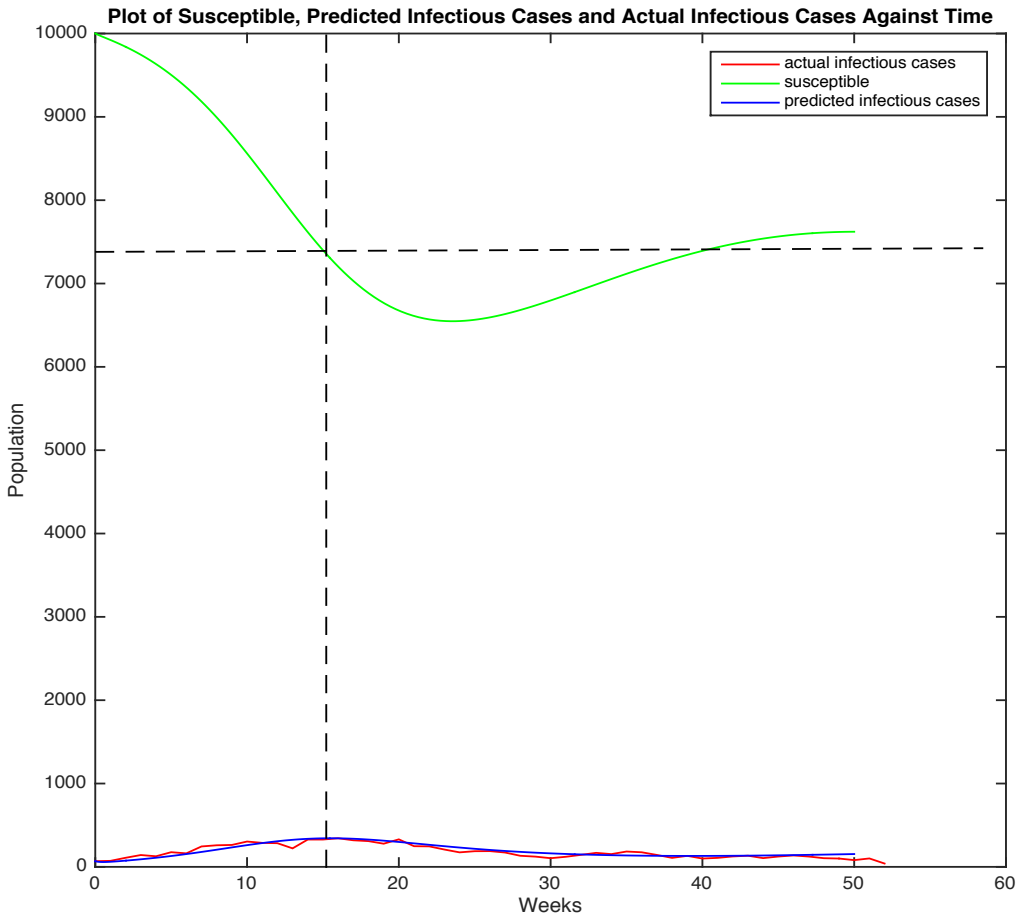

Figure 4.45: Susceptible, predicted infectious cases and actual infectious cases based on SEIPR model, year 2014. Dashed line indicated threshold value.

From Figure 4.45, threshold value shown is 7347. While $R_0 = 1.36$ indicating outbreak occurred. The outbreak was mostly contributed by infectious patients which the $R_2 = 1.1$. However $R_1 = 0.06$ and $R_3 = 0.2$ show mild infectious characteristic and also contributed to the transmission. On the other hand, Table 4.10, Figure 4.46 and Figure 4.47 are used for regression analysis.

Table 4.10: Results of the observed values and predicted values, year 2014.

Outbreak in 2014		
Weeks	**Actual infectious cases**	**Predicted infectious cases**
0	68	68
1	72	70
2	109	89
3	142	108
4	127	126
5	176	148
6	162	156
7	245	200
8	259	229
9	263	260
10	304	281
11	288	288
12	284	312
13	222	226
14	328	338
15	328	343
16	343	342
17	319	331
18	309	319
19	278	302
20	330	297
21	248	271
22	246	253
23	208	242
24	174	218
25	188	206
26	189	195
27	172	183
28	133	173
29	123	164
30	104	158

Table 4.10 shows the observed values and predicted values. The linear regression plot in Figure 4.46 has the equation $y = 0.909x + 19.06$ and the correlation coefficient,

r^2 shows that 85.15% of the variability of the data used from SEIPR prediction and the actual infectious cases for the year 2014 has the respond around its mean

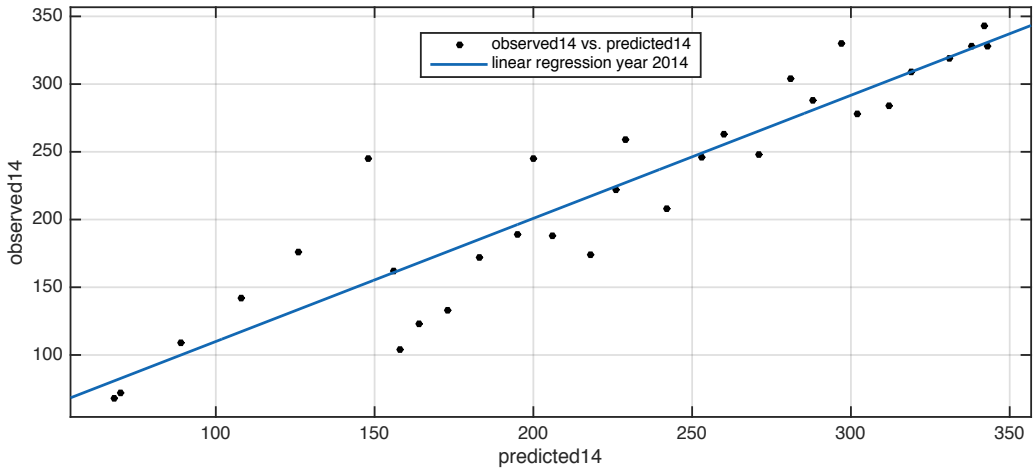

Figure 4.46: Simple linear regression plot, year 2014.

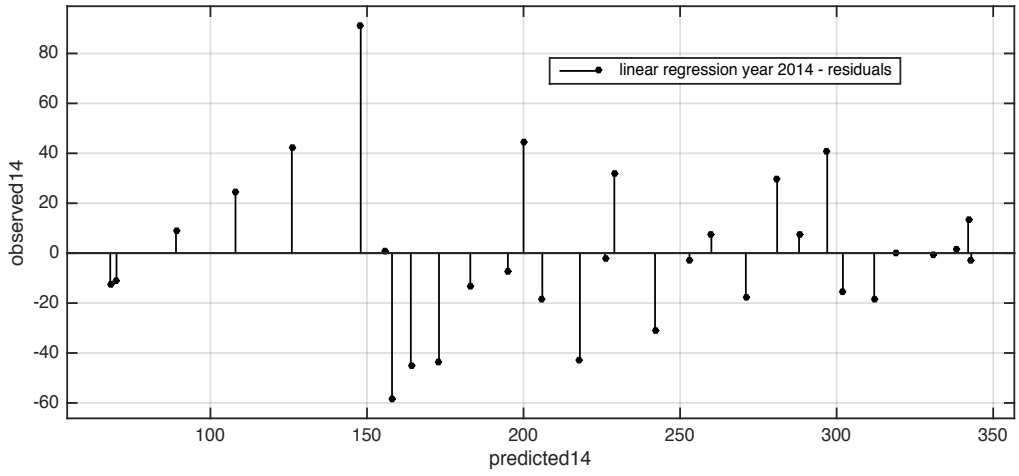

Figure 4.47: Simple linear regression plot, year 2014.

.Residuals plot in Figure 4.47 has most residuals randomly dispersed near the x-axis. Hence, we conclude that the SEIPR model is stable and able for the prediction infectious cases for the first thirty weeks, year 2014.

4.5 Comparison of theoretical analysis and numerical results for the year 2006, 2010, 2011, 2012, 2013 and 2014

SEIPR model had been used to analyze the transmission dynamics of HFMD for year 2006, 2010, 2011, 2012, 2013 and 2014. The comparison results between the predicted data from SEIPR model and actual clinical data throughout the study years verified that SEIPR model is stable to predict the infectious cases especially for the first wave of the outbreak. Regression analysis is used to test the goodness of fit between the actual infectious data and predicted infectious data for our study. The summarized results are shown in the Table 4.11 and Table 4.12.

Table 4.11: The initial and parameters values.

Initial and Parame-ters Values	**Outbreak**						
	2006	**2010**	**2011**		**2012**	**2013**	**2014**
			First Wave	**Second Wave**			
S	**10,000**	**10,000**	**10,000**	**9700**	**10,000**	**10,000**	**10,000**
E	4	50	10	10	16	50	10
I	4	121	33	25	62	143	68
P	4	100	10	10	16	50	75
R	0	0	0	350	0	0	0

Table 4.11 continued

k_1	2.923 $\times10^{-4}$	3.212 $\times10^{-4}$	3.308 $\times10^{-4}$	3.308 $\times10^{-4}$	3.212 $\times10^{-4}$	2.904 $\times10^{-4}$	2.904 $\times10^{-4}$
k_2	1.077 $\times10^{-4}$	5.192 $\times10^{-6}$	5.154 $\times10^{-6}$	5.154 $\times10^{-6}$	4.923 $\times10^{-6}$	4.313 $\times10^{-6}$	4.313 $\times10^{-6}$
k_3	1.731 $\times10^{-5}$	0	0	0	0	0	0
β_1	3 $\times10^{-5}$	1 $\times10^{-5}$	0	2.5 $\times10^{-5}$	1 $\times10^{-5}$	3.8 $\times10^{-5}$	1.1 $\times10^{-5}$
β_2	5.5	5.5	5.5	5.5	5.5	5.5	1.8
β_3	1	1	1	1	1	1	1
β_4	1	1	1	1	1	1	1
β_5	1.5 $\times10^{-4}$	9 $\times10^{-5}$	1 $\times10^{-4}$	8 $\times10^{-5}$	1.42 $\times10^{-4}$	1 $\times10^{-4}$	1.1 $\times10^{-4}$
β_6	6 $\times10^{-5}$	3 $\times10^{-5}$	0	3.2×10^{-5}	1 $\times10^{-5}$	3 $\times10^{-5}$	2 $\times10^{-5}$
β_7	0.07	0.07	0.07	0.07	0.07	0.07	0.07

Table 4.12: Threshold values, basic reproductive numbers (R_0) and correlation coefficient (r^2)

Values	**Outbreak**						
	2006	**2010**	**2011**		**2012**	**2013**	**2014**
			First Wave	**Second Wave**			
Threshold Values	**4642**	**8209**	**10,000**	**8580-9000**	**6501**	**7304**	**7347**
$R_0 = R_1 + R_2 + R_2$	2.15= 0.05 +1.5 +0.6	1.22= 0.018 +0.9 +0.3	1= 0 +1 +0	1.13= 0.044 +0.78 +0.31	1.54= 0.018 +1.42 +0.1	1.37= 0.069 +1 +0.3	1.36= 0.06 +1.1 +0.2
Correlation Coefficient, r^2	0.9973	0.6609	0.8201		0.8557	0.8653	0.8515

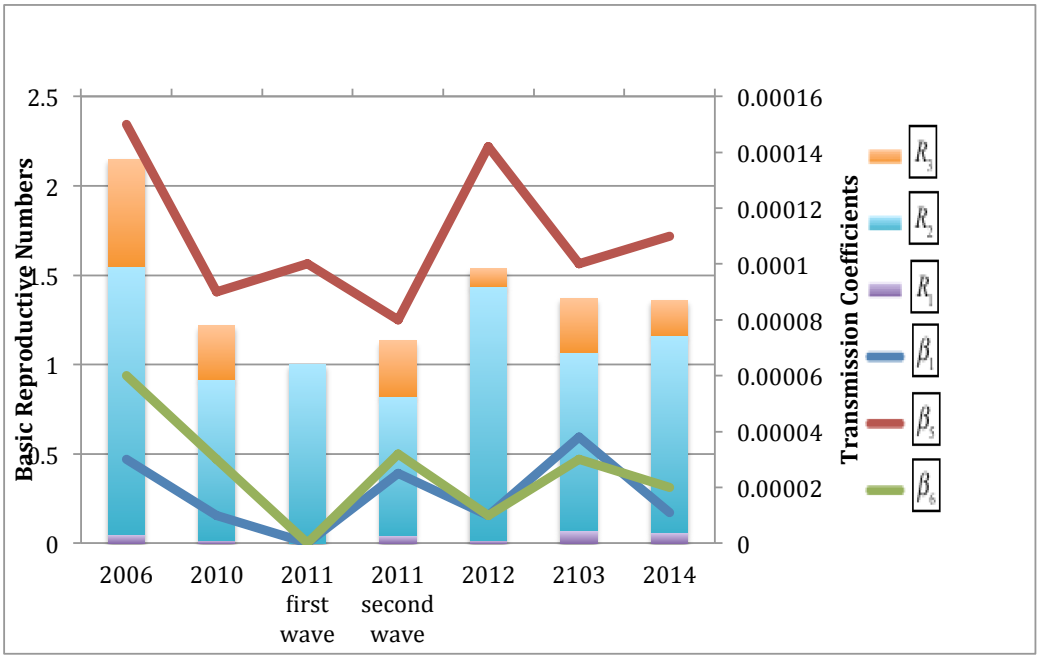

Figure 4.48: Comparison between the transmission coefficients and basic reproductive numbers.

From Figure 4.48, it is notice that β_5, the transmission coefficient from infectious individual to susceptible played the main role to spread the disease throughout the years. However, β_1 and β_6 cannot be ignored as both transmission coefficients gained from incubation period patients and post-infectious patients changed the dynamic behaviors of HFMD. We learned that from the simulation done by SEIPR model, the parameters β_1 and β_6 help to speed up the transmission process by shifting the infectious cases curve to reach the peak of the curve within shorter duration. This means, the viruses can invade the susceptible rapidly when they met the cohort. Throughout this research study, the β_5 is recorded at the range between 0.8×10^{-4} to 1.5×10^{-4}, β_1 is recorded at the range between 0.1×10^{-4} to 0.38×10^{-4} and β_6 is recorded at the range between 0.1×10^{-4} to 0.6×10^{-4}.

On the other hand, basic reproductive numbers, R_0, if more than one, then it is indicating that the outbreak occurs. As seen in Table 4.12, infectious patients contribute to the R_2 are the most contagious as they are the main role to infect more people during their infectious time. This is followed by post-infectious patients, R_3 and incubation period patients, R_1. Interestingly, in year 2011 during the first wave of the infection, the R_0 calculated is one, this means the disease free equilibrium point is achieved and endemic occurred. We can see that during the disease free duration, β_1 and β_6 do not play any role in the transmission and R_1 and R_3 are zero, this may due to the threshold condition of reaching the number of cohort was not met. Also from Table 4.12, the basic reproductive numbers, R_0 recorded are between 1.13 and 2.15 during the outbreaks. R_1 is recorded at the range between 0.018 to 0.069, R_2 is recorded at the range between 0.78 to 1.5 and R_3 is recorded at the range between 0.1 to 0.6. From the records, the R_2 has not exceeded one in year 2010, 2011 and 2013. Thus, the outbreaks to be occurred were helped by incubation period and post-infectious patients.

As mention in Section 2.3.3, threshold value is the minimum proportion of the population in which creates the liability of disease spreading. From Figure 4.49, we notice that when the value of R_0 is higher, the threshold value is smaller. Meanwhile, from Figure 4.48, when R_0 is higher, the transmission coefficient also higher. The results shown are what is expected because when threshold value is small, the transmission coefficient is high, which means the average number of contacts any person in the population is higher and virus is easily spreading within the cohort. As a consequence, the transmission is aggressive and more people being infected, so R_0 becomes higher.

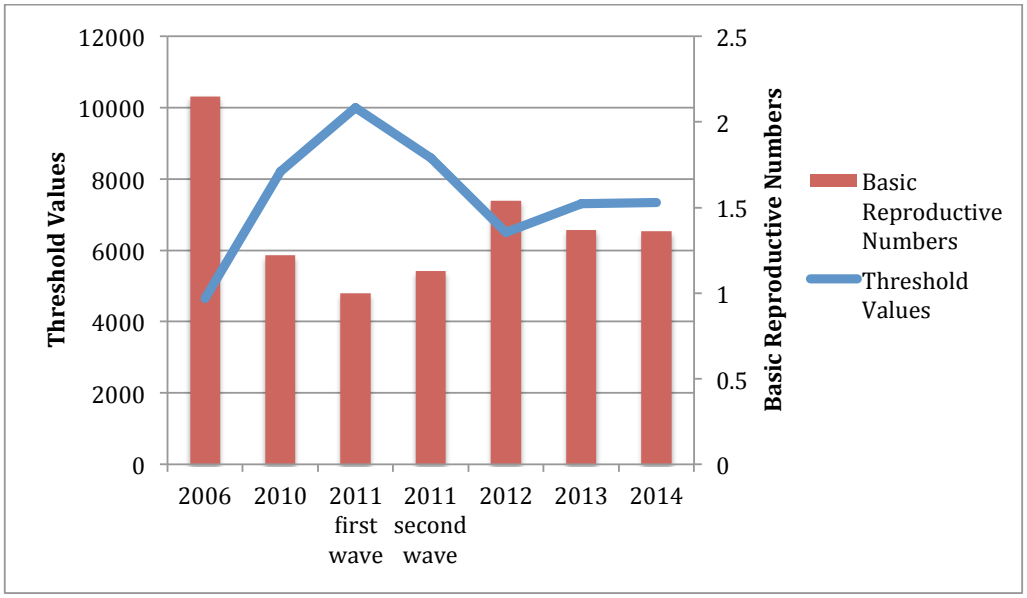

Figure 4.49: Comparison between the threshold values and basic reproductive numbers.

The goodness of fit tests chosen to validate the data is regression analysis. Correlation coefficient, r^2 and residuals plot are used. As mentioned in Section 2.3.4.3, the higher the value of the r^2 means that the variability of the actual and predicted data has higher respond around its mean and indicating a better fit. In year 2010, r^2 is 0.6609, means that 66.09 % of the predicted infectious and actual infectious data have the variability responds around its mean. Whereas in year 2006, and from year 2011 until year 2014, the variabilities of the actual infectious and predicted infectious data have higher respond around its mean, range between 82% to 99%, indicating a good fit between the predicted and actual data.

From the entire finding discussed, we conclude that the parameters that play the significant roles in disease spreading are close contact between the susceptible and

transmission coefficients. The model validation done by using the predicted infectious data and actual infectious data is reliable as those data are in the best matched. Hence, SEIPR model is stable and able to predict the HFMD cases especially during the first wave of the outbreaks.

4.6 Summary

In Chapter 4, a formulation of SEIPR model has been discussed. The inclusion of the post-infectious virus shedding period into the infected compartments formed the SEIPR model. The numerical results in Section 4.4 is gained from the simulation ran by SEIPR model by using fourth-order Runge Kutta method, the built-in function in MatLab and had been tested for validation by using goodness of fit test based on the predicted infectious data and actual infectious data. The goodness of fit test showed that there were good fit between the predicted infectious data and actual infectious data within the periods chosen. Hence, by using the parameters obtained from the simulation, we calculated the threshold values and basic reproductive numbers, R_0 for years 2006, 2010, 2011, 2012, 2013 and 2014. The threshold value for each year is 4642 people in 2006, 8209 people in 2010, 10000 people in first wave of the outbreak in 2011, 8580-9000 people in second wave of the outbreak in 2011, 6501 people in 2012, 7304 people in 2013 and 7347 people in 2014. Whereas the R_0 acted correspondingly where when the value of R_0 is higher, the threshold value is smaller. R_0 in year 2006 is 2.15, 1.22 in year 2010, 1.00 in first wave of the outbreak in year 2011, 1.13 in second wave of the outbreak in year 2011, 1.54 in year 2012, 1.37 in year 2013 and

1.36 in year 2014. On the other hand, it is observed that the transmission coefficient gained from the simulation ran by SEIPR model is higher when R_0 is higher. With this, we conclude that the transmission coefficients play an important role in controlling the HFMD outbreak. Hence, in order to control the outbreaks, the transmission coefficient needs to be reduced which means the number of any contact person within the infected region needs to be controlled.

CHAPTER 5

CONCLUSION AND RECOMMENDATIONS

5.1 Introduction

SEIPR model was formulated to satisfy the first objective of this thesis of which the aim of the model was to incorporate the virus biological factors namely the incubation, infectious and post infectious periods in order predict the infectious cases. As shown in Chapter 3 and Chapter 4, analysis of the models have been done, numerical results are obtained and being analyzed, methods of goodness of fit test are used to validate the results and also results obtained are discussed and summarized. In this chapter, contribution of the research works, limitation and future work will be discussed.

5.2 Contribution

The SEIPR model in this thesis has incorporating the biological factors of the viruses during the incubation period, infectious period and post-infectious virus shedding period (CDC, 2015; Han et al., 2010; Li et al., 2013; Mandal, 2017; Ministry of Health, 2014; Podin et al., 2006; Roy & Halder, 2010; Teng et al., 2013) that make a more reliable predicting method of the disease outbreak. The transmission coefficients used are based on the best results after simulation of the model implied the average number of contacts any

person in the population creates the chance of disease spreading when they meet an infected individual that is introduced to the population. The higher the transmission coefficients, the higher R_0 will be produced and the faster the disease is spreading. At the same time, from the R_0 calculating, there are R_1 and R_3 besides R_2 which are contributed by incubation period and post-infectious patients, help to speed up the transmission process. R_1 shows that the transmission happens even the patients have shown no symptoms and this is the blind spot for disease prevention. In the other hand, R_3 is contributed by the post-infectious patients (clinically recovered) who are post-infectious virus shedding carrier with the disease symptoms have subsided.

To date, it was reported that vaccine EV71 has started being used for infants and children in China. The vaccine EV71 does not provide life long immunity to the vaccinated individuals. At the same time, the vaccinated individuals still can be infected by other HFMD viruses besides virus EV71 (Shi et al., 2018; Tan & Cao, 2018). Meanwhile, in other countries, there is no vaccine and specific treatment applied to protect against the virus (Ministry of Health, 2014; SHD, 2018). Thus, to implement the intervention, we suggest that all children who are diagnosed as HFMD patients should be quarantined to at least another one more week after symptoms subside, as the clinically recovered patients are still being able to transmit the disease. And, for incubation period patients, are hardly to be diagnosed by visual inspection, thus, all the susceptible should avoid to go nearer to those who have close contact with the infectious patients as they may have been infected but no symptoms shown.

Besides, threshold value found is to predict the minimum proportion of population that creates the liability of the disease outbreak. By comparing the threshold values and

transmission coefficients results throughout the years, when the cohort condition met and the average number of contact any person in the population is high, once an infected individual is introduced to the group, the disease can spread rapidly with a smaller threshold value indicating more people will be infected.

As a conclusion, SEIPR shares a comprehensive description of the HFMD transmission dynamics. Since the HFMD is very contagious, thus, with all the reliable results obtained from our research, we hope that more effective control interventions can be planned by public health personnel to reduce the effect of the future outbreaks.

5.3 Limitation

The SEIPR model discussed in this thesis did not study much about the second wave of the outbreaks. The reason we did not focus on the second wave is that after the first wave of the outbreaks, the public health personnel would take the preventive actions in order to control the disease. Once the public is acknowledging with the outbreaks, people will start to avoid close contact with the infected patients, prevent to go to the crowded area and aware with the hygiene implementation. With this prevention acts, the number of actively susceptible provided for the virulence has been reduced causing the contact rate is low which means the force of infection is not aggressive and resulted that transmission coefficients are lower compare to the first wave of outbreak. Thus, the prediction based on the model would not be accurate, as the transmission coefficients have changed (Lai et al., 2016).

Also, the number of susceptible and incubation patients are from the best assumption as real number of the susceptible and incubation patients are unable to be found accurately. Besides, parameter β_2, the rate at which an asymptomatic patient develops the symptoms is the best result after the simulation running. Since β_2 can be from one day to two weeks (CDC, 2015; Lai et al., 2016; Mandal, 2017; Ministry of Health, 2014; Podin et al., 2006), we can only get the rate by testing the simulation within the correct range.

On the other hand, parameter β_4, the rate at which a clinically recovered individual fully recovered is also the best result after running. Although for most of the cases, the virus will continue to shed for at least one week after symptoms gone, however, for some cases, the post-infectious virus still can continue to shed for another few more weeks as mentioned in Section 2.2.

5.4 Future work

The SEIPR model has helped to predict the HFMD based on the biological factors of HFMD. The model can predict the infectious cases with a good match with the actual infectious data during the first waves of the outbreaks. However, most of the second waves of the outbreaks are not accurate based on the simulation. This may due to transmission coefficients have changed (Lai et al., 2016). Thus, some refinements can still be carried out to improve the performance of the model by allowing the transmission parameters changing and also may include the prevention factor as part of the compartments in order

to improve the HFMD second wave transmission dynamics. With more compartments added in, the parameter values can have more sensitivity analysis and the prediction results can be more reliable.

REFERENCES

Abramson, G. (2001). Mathematical modeling of the spread of infectious diseases. *A series of lectures given at PANDA, UNM*.

Anderson, R. M., & May, R. M. (1992). *Infectious diseases of humans: dynamics and control*. London, LDN: Oxford University Press.

Benesty, J., Chen, J., Huang, Y., & Cohen, I. (2009). Pearson correlation coefficient. In *Noise Reduction in Speech Processing* (pp. 1-4). Germany, DE: Springer.

Bhattacharya, P., Paul, S., & Biswas, P. (2015). Mathematical Modeling of Treatment SIR Model with Respect to Variable Contact Rate. *International Proceedings of Economics Development and Research, 83*, 34.

Cardosa, M. J., Krishnan, S., Tio, P. H., Perera, D., & Wong, S. C. (1999). Isolation of subgenus B adenovirus during a fatal outbreak of enterovirus 71-associated hand, foot, and mouth disease in Sibu, Sarawak. *The Lancet, 354*(9183), 987-991.

CDC. (2015). *Hand foot and mouth disease.* Retrieved from http://www.cdc.gov/hand-foot-mouth/about/transmission.html

Chadsuthi, S., & Wichapeng, S. (2018). The modelling of hand, foot, and mouth disease in contaminated environments in Bangkok, Thailand. *Computational and Mathematical Methods in Medicine, 2018*. https://doi.org/10.1155/2018/5168931

Chan, L., Parashar, U. D., Lye, M., Ong, F., Zaki, S. R., Alexander, J. P., Ho, K., Han, L. L., Pallansch, M. A., & Suleiman, A. B. (2000). Deaths of children during an outbreak of hand, foot, and mouth disease in Sarawak, Malaysia: clinical and pathological characteristics of the disease. *Clinical Infectious Diseases, 31*(3), 678-683.

Chuo, F. S. T. (2008). *Mathematical modeling on the spread of hand, foot and mouth disease. (HFMD) in Sarawak.* Retrieved from http://ir.unimas.my/id/eprint/1710

Giesecke, J. (2017). *Modern infectious disease epidemiology*. United States of America, USA: CRC Press.

Han, J., Ma, X.-J., Wan, J.-F., Liu, Y.-H., Han, Y.-L., Chen, C., Tian, C., Gao, C., Wang, M., & Dong, X.-P. (2010). Long persistence of EV71 specific nucleotides in respiratory and feces samples of the patients with hand-foot-mouth disease after recovery. *BioMed Central Infectious Diseases, 10*(1), 178. https://doi.org/10.1186/147-2334-10-178

Heffernan, J., Smith, R., & Wahl, L. (2005). Perspectives on the basic reproductive ratio. *Journal of the Royal Society Interface, 2*(4), 281-293.

Hethcote, H. W. (2000). The mathematics of infectious diseases. *SIAM review, 42*(4), 599-653.

Hii, Y. L., Rocklöv, J., & Ng, N. (2011). Short term effects of weather on hand, foot and mouth disease. *PLoS One, 6*(2), e16796.

Hirsch, M. W., Smale, S., & Devaney, R. L. (2012). *Differential equations, dynamical systems, and an introduction to chaos*. United States of America, USA: Academic press.

Huang, S.-W., Hsu, Y.-W., Smith, D. J., Kiang, D., Tsai, H.-P., Lin, K.-H., Wang, S.-M., Liu, C.-C., Su, I.-J., & Wang, J.-R. (2009). Reemergence of enterovirus 71 in 2008 in taiwan: dynamics of genetic and antigenic evolution from 1998 to 2008. *Journal of Clinical Microbiology, 47*(11), 3653-3662.

Johnston, M. D., Edwards, C. M., Bodmer, W. F., Maini, P. K., & Chapman, S. J. (2007). Examples of mathematical modeling. *National Center for Biotechnology Information, 6*(17), 2106-2112.

Keeling, M. J., & Rohani, P. (2008). *Modeling infectious diseases in humans and animals*. United States of America, USA: Princeton University Press.

Keeping, E. S. (1962). *Introduction to statistical inference*. Princeton, New Jersey, NJ: D. Van Nostrand Company.

Lai, C.-C., Jiang, D.-S., Wu, H.-M., & Chen, H.-H. (2016). A dynamic model for the outbreaks of hand, foot, and mouth disease in Taiwan. *Epidemiology and Infection, 144*(07), 1500-1511.

Li, J., Lin, C., Qu, M., Li, X., Gao, Z., Zhang, X., Liu, Y., Huang, Y., Wang, X., & Jia, L. (2013). Excretion of enterovirus 71 in persons infected with hand, foot and mouth disease. *Virology Journal, 10*(31). http://doi.org/10.1186/1743-422X-10-31

Li, X., Zhang, X., Ding, J., Xu, Y., Wei, D., Tian, Y., Chen, W., Huang, J., Wen, T., & Li, S. (2014). Comparison between Chinese herbal medicines and conventional therapy in the treatment of severe hand, foot, and mouth disease: a randomized controlled trial. *Evidence-Based Complementary and Alternative Medicine, 2014*. doi:10.1155/2014/140764

Li, Y., Zhang, J., & Zhang, X. (2014). Modeling and Preventive Measures of Hand, Foot and Mouth Disease (HFMD) in China. *International Journal of Environmental Research and Public Health, 11*(3), 3108-3117.

Lu, C., Liu, X., Ding, X., Chen, X., Fan, H., Liu, Y., Xie, N., Tan, Y., Ko, J., & Zhang, W. (2013). A metabolomics profiling study in hand-foot-and-mouth disease and modulated pathways of clinical intervention using liquid chromatography/quadrupole time-of-flight mass spectrometry. *Evidence-Based Complementary and Alternative Medicine, 2013*. doi:10.1155/2013/647452

Mandal, D. A. (2017, 3 Aug 2017). Hand, foot and mouth disease – What is HFMD? Retrieved from http://www.news-medical.net/health/Hand-foot-and-mouth-disease-e28093-What-is-HFMD.aspx

McMinn, P. C. (2002). An overview of the evolution of enterovirus 71 and its clinical and public health significance. *Federation of European Microbiological Societies Microbiology Reviews, 26*(1), 91-107.

Ministry of Health, S. (2014). Hand, Foot & Mouth Disease. Retrieved from https://www.moh.gov.sg/content/moh_web/home/diseases_and_conditions/h/hfmd.html

Mondaini, L. (2002). Obtaining a new representation for the golden ratio by solving a biquadratic equation. *arXiv preprint math/0208210*.

Phutthichayanon, T., & Naowarat, S. (2015). Effects of hand washing campaign on dynamical model of hand foot mouth disease. *International Journal of Modeling and Optimization, 5*(2), 104.

Podin, Y., Gias, E. L., Ong, F., Leong, Y.-W., Yee, S.-F., Yusof, M. A., Perera, D., Teo, B., Wee, T.-Y., & Yao, S.-C. (2006). Sentinel surveillance for human enterovirus 71 in Sarawak, Malaysia: lessons from the first 7 years. *BioMed Central Public Health, 6*(1), 180. http://doi/10.1186/1471-2458-6-180

Roy, N. (2012). Mathematical modeling of hand-foot-mouth disease: quarantine as a control measure. *International Journal of Advanced Scientific Engineering and Technological Research, 1*(2), 34-44.

Roy, N., & Halder, N. (2010). Compartmental modeling of hand, foot and mouth infectious disease (HFMD). *Research Journal of Applied Sciences, 5*(3), 177-182.

Samanta, G. (2014). Analysis of a delayed hand–foot–mouth disease epidemic model with pulse vaccination. *Systems Science & Control Engineering: An Open Access Journal, 2*(1), 61-73.

Roy, N., & Halder, N. (2010). Compartmental modeling of hand, foot and mouth infectious disease (HFMD). *Research Journal of Applied Sciences, 5*(3), 177-182.

Samanta, G. (2014). Analysis of a delayed hand–foot–mouth disease epidemic model with pulse vaccination. *Systems Science & Control Engineering: An Open Access Journal, 2*(1), 61-73.

SHD. (2006a). Sarawak Health Department - Sihat Sepanjang Hayat. Retrieved from http://jknsarawak.moh.gov.my/en/modules/profile/user.php?xoops_redirect=/en/modules/wfdownloads/viewcat.php?cid=31&PHPSESSID=9c3740556068ffbda0b58a20ace1fd0e

SHD. (2006b). Sarawak Health Department - Sihat Sepanjang Hayat. Retrieved from http://www.moh.gov.my/images/gallery/Garispanduan?GuidelinesHFMD2007. pdf

SHD. (2015). Sarawak Health Department - Sihat Sepanjang Hayat. Retrieved from http://jknsarawak.moh.gov.my/en/modules/mastop_publish/?tac=147

SHD. (2018, 8 March 2018). Sarawak Health Department - Sihat Sepanjang Hayat. Retrieved from http://jknsarawak.moh.gov.my/en/modules/mastop_publish/?tac=122

Shi, L., Zhao, H., & Wu, D. (2018). Modelling and analysis of HFMD with the effects of vaccination, contaminated environments and quarantine in mainland China. *Mathematical Biosciences and Engineering, 16*(1), 474-500.

Solomon, T., Lewthwaite, P., Perera, D., Cardosa, M. J., McMinn, P., & Ooi, M. H. (2010). Virology, epidemiology, pathogenesis, and control of enterovirus 71. *The Lancet Infectious Diseases, 10*(11), 778-790.

Tan, H., & Cao, H. (2018). The Dynamics and Optimal Control of a Hand-Foot-Mouth Disease Model. *Computational and Mathematical Methods in Medicine, 2018*. https://doi.org/10.1155/2018/9254794

Teng, S., Zhao, S., Wei, Y., Shao, Q., Jiang, M., Cui, D., & Xie, G. (2013). Observation on virus shedding periods of enterovirus-71 and coxsackievirus A 16 monitored by nucleic acids determination in stool samples of children with hand, foot and mouth disease. *Zhonghua Er Ke Za Zhi= Chinese Journal of Pediatrics, 51*(10), 787-792.

Thomas, J. C., & Weber, D. J. (2001). *Epidemiologic methods for the study of infectious diseases*. London, LDN: Oxford University Press.

Tiing, F. C. S., & Labadin, J. (2008). A simple deterministic model for the spread of hand, foot and mouth disease (HFMD) in Sarawak. *2008 Second Asia International Conference on Modelling & Simulation*. doi**:** 10.1109/AMS.2008.139

Trottier, H., & Philippe, P. (2001). Deterministic modeling of infectious diseases: theory and methods. *The Internet Journal of Infectious Diseases, 1*(2), 3. ISPUB.com/IJID/1/2/12783

Ugwa, K. A., & Agwu, I. (2013). Mathematical analysis of the endemic equilibrium of the transmission dynamics of tuberculosis. *International Journal of Scientific & Technology Research, 2*(12), 263-269.

van den Driessche, P. (2017). Reproduction numbers of infectious disease models. *Infectious Disease Modelling, 2*(3), 288-303. doi:https://doi.org/10.1016/j.idm.2017.06.002

van den Driessche, P., & Watmough, J. (2008). Further notes on the basic reproduction number. In *Mathematical Epidemiology* (pp. 159-178). Germany, DE: Springer.

Weisstein, E. W. (2002). Least squares fitting. Retrieved from http://mathworld.wolfram.com/LeastSquareFitting/html

Wu, C. (2017). Analysis of a Hand-Foot-Mouth Disease Model with Standard Incidence Rate and Estimation for Basic Reproduction Number. *Mathematical and Computational Applications, 22*(2), 29. doi:https://doi.org/10.3390/mca22020029

Zhao, Y., Xu, Q., Chen, Y., Tsui, K. L. (2018). Using Baidu index to nowcast hand-foot-mouth disease in China: a meta learning approach. *BioMed Central Infectious Diseases, 18*(1), 398.

Zhu, Y., Xu, B., Lian, X., Lin, W., Zhou, Z., & Wang, W. (2014). A hand-foot-and-mouth disease model with periodic transmission rate in Wenzhou, China. *Abstract and Applied Analysis, 2014*. http://doi.org/10.1155/2014/234509

APPENDIX

List of Publication

Chan, S. J., Labadin, J., & Podin, Y. (2017). A Dynamic SEIPR Model for The Spread of Hand, Foot and Mouth Disease in Sarawak. *Journal of Telecommunication, Electronic and Computer Engineering, 9*(3-10), 125-129.